

**Regulation of the Ran GTPase System and
Nucleocytoplasmic Transport**

Mandovi Chatterjee

Kolkata, India

B.S. Zoology, University of Calcutta, Kolkata, India – 2004

M.S. Zoology, Presidency University, Kolkata, India – 2006

A dissertation presented to the Graduate Faculty
of the University of Virginia in Candidacy for the
Degree of Doctor of Philosophy

Department of Cell Biology

University of Virginia

December 2014

ABSTRACT

Hutchinson-Gilford Progeria Syndrome (HGPS) is a premature aging syndrome in children that is caused by an accumulation of a mutant form of lamin A, Progerin, in the nuclear lamina. This results in the alteration of nuclear morphology, and several other cellular phenotypes, including reduction in heterochromatin marks, a large-scale change in gene expression, Ran gradient disruption and nucleocytoplasmic transport defect. Given a number of tissues that are affected in Progeria, it is likely that the accumulation of Progerin in the nuclear lamina disrupts fundamental features of nuclear function that have cell-wide consequences. Gene expression is thought as one such phenomenon that is altered by Progerin expression. We propose that nucleocytoplasmic transport is another critical process in cells, which when affected can impair the basic cellular operation. In this dissertation, I sought to study the regulation of the Ran GTPase system, which drives the process of nucleocytoplasmic transport. In the first part, I demonstrate a mechanism by which the Ran GTPase system is affected in the presence of oxidative stress, one of the factors implicated in age-associated diseases. I showed that oxidative stress inhibits the nucleotide exchange factor for Ran (RanGEF), RCC1, to disrupt the Ran gradient in cells. The second part shows a link between the Ran gradient disruption and loss of heterochromatin in Progeria, where loss of heterochromatin may contribute to the disruption of Ran gradient and nuclear transport in HGPS cells. Together, this work suggests that the Ran gradient-dependent nuclear transport might be an important mediator of Progerin-induced cellular phenotypes.

ACKNOWLEDGEMENTS

First, I would like to thank my advisor Dr. Bryce M. Paschal for his exceptional mentoring. He has guided me throughout my graduate career and helped me become an independent thinker to approach a scientific question. I deeply appreciate his patience and effort in bringing out the best in me.

I would also like to thank my committee members, Drs. James Casanova, David Wotton and Patrick Grant, for their insightful comments, which helped in shaping the projects I worked on.

I was lucky to have great lab mates, who have always been very helpful and supportive. Chelsi Snow and Sutirtha Datta, have been great comrades both inside and outside of the lab, who have made the grad school experience a memorable one. Li Ni, Chun-Song Yang and Joshua Kelley have been incredible mentors, and their constructive criticisms during the lab meeting have been really helpful. Adam Spencer deserves a special mention here. He has always been the patient problem-solver in the lab. I would like to thank him specially for doing the last radioactive assay for me, which I could not do because of my pregnancy. Thanks to the new members of the lab, Kasey Jividen and Natalia Dworak, for their support and concern during my paper submission and thesis writing. I would specially like to thank the administrators at the Center for Cell Signaling, and Mary Hall at the Department of Cell Biology for making the grad school years smooth-sailing.

Friends outside the lab have made our six-odd years in Charlottesville a wonderful one. It was like a home away from home because of them. I would like to thank all of them for making our life in Charlottesville truly memorable.

Finally, last but by no means the least, I would like to thank my family – my husband, Budhaditya, who always stood by me through thick and thin. His immense faith in my capabilities, even beyond my own, has allowed me to gather determination in life. It would not have been possible for me to reach where I am today without his love and encouragement. My parents, Prottyush and Chitra Chatterjee, have always been a great support in my life. They let me follow my dreams of pursuing my higher studies in a land far away from home. I know it was not easy for them! No ‘Thank you’ is enough for what they have done for me. My elder brother, Rajarshi Chatterjee, is the one, who always is very proud of me no matter what I do. I would like to thank him for having such a high confidence in me. I would also like to thank my parents-in-law and my extended family members, who I am very close to, for their love and support.

TABLE OF CONTENTS

ABSTRACT.....	ii
ACKNOWLEDGEMENTS.....	iii
TABLE OF CONTENTS.....	v
LIST OF FIGURES & TABLES.....	ix
LIST OF ABBREVIATIONS.....	xi
CHAPTER 1: GENERAL INTRODUCTION	
<i>Nucleocytoplasmic transport</i>	2
<i>Classical protein import</i>	3
<i>Ran system/ gradient and its role in nuclear transport</i>	8
<i>Nuclear lamina and its function</i>	9
<i>Role of nuclear lamina in transcription and its association with chromatin</i>	13
<i>Nuclear lamina and diseases</i>	16
<i>Hutchinson-Gilford Progeria Syndrome (HGPS)</i>	18
<i>Therapeutic intervention</i>	23
<i>Oxidative stress</i>	26
<i>Oxidative stress and HGPS</i>	31
<i>Oxidative stress and nuclear transport</i>	31
<i>Regulator of Chromosome Condensation 1 (RCC1)</i>	32
<i>Ran-RCC1 interaction</i>	37
<i>RCC1-chromatin interaction</i>	41

<i>Objective of this thesis</i>	45
CHAPTER 2: DISRUPTION OF THE RAN SYSTEM BY CYSTEINE	
OXIDATION OF RCC1	
<i>Abstract</i>	48
<i>Introduction</i>	49
<i>Results</i>	53
<i>Diamide-induced oxidative stress reversibly inhibits RCC1</i> <i>exchange activity</i>	53
<i>Spatial arrangement and oxidative modification of cysteines</i> <i>in RCC1</i>	57
<i>Cys93 of RCC1 is important for its exchange activity</i>	64
<i>Cys93 of RCC1 is required for Ran-RCC1 binding</i>	68
<i>Oxidative stress alters RCC1-chromatin interaction</i>	71
<i>Diamide-induced oxidative stress inhibits Ran-dependent</i> <i>nuclear transport</i>	71
<i>Stress signaling disrupts Ran gradient via RCC1-dependent</i> <i>and -independent mechanisms</i>	77
<i>Discussion</i>	82
<i>Materials and methods</i>	90
<i>Cell culture and transfection</i>	90
<i>Plasmids</i>	90
<i>Immunofluorescence microscopy (IF) and fluorescence</i> <i>recovery after photobleaching (FRAP)</i>	91

<i>Recombinant proteins and Ran-binding assays</i>	94
<i>Nucleotide binding assay</i>	95
<i>Immunoblotting</i>	96
<i>Mass spectrometry</i>	96
<i>Protein modeling</i>	98
<i>Permeabilized cell assay</i>	98
<i>Acknowledgements</i>	100

CHAPTER 3: INTERPLAY BETWEEN HETEROCHROMATIN AND THE RAN
GTPase SYSTEM IN HUTCHINSON-GILFORD PROGERIA SYNDROME
(HGPS)

<i>Abstract</i>	102
<i>Introduction</i>	104
<i>Results</i>	107
<i>Loss of H3K9-methylation disrupts the Ran distribution</i>	107
<i>Nuclear levels of Histone methyltransferases (HMTases) are reduced in Progeria</i>	111
<i>Constitutive membrane attachment of lamin A is sufficient for downregulation of the HMTases</i>	114
<i>Loss of heterochromatin partially contributes to the Ran gradient disruption</i>	120
<i>Progerin expression causes import defect of histones H3 and H4</i>	123
<i>Imp4, the import receptor of H3-H4 dimer is mislocalized</i>	

<i>in presence of Progerin</i>	126
<i>Discussion</i>	130
<i>Materials and methods</i>	136
<i>Cell culture and drug treatment</i>	136
<i>Plasmids and siRNAs</i>	136
<i>Transfection and knock-down</i>	137
<i>RT-PCR</i>	137
<i>IF and microscopy</i>	138
<i>Immunoblotting</i>	140
 CHAPTER 4: DISCUSSION AND FUTURE DIRECTIONS	
<i>Significance</i>	142
<i>Relevance in normal aging</i>	147
<i>Future directions</i>	148
<i>Role of nuclear transport in cardiac hypertrophy</i>	151
<i>Role of nuclear transport in epigenetic changes in stem cell aging</i>	153
<i>Conclusion</i>	154
REFERENCES	158

LIST OF FIGURES & TABLES

Fig. 1.1: Nuclear transport in cells is regulated by Ran GTPase.....	6
Fig. 1.2: Post-translational processing of lamin A.....	11
Fig. 1.3: Crystal structure of RCC1.....	35
Fig. 1.4: Crystal structure of Ran-RCC1 in complex.....	39
Fig. 2.1: Oxidative stress induced by diamide reversibly inhibits RCC1 exchange activity.....	55
Fig. 2.2: Spatial arrangement and modification of cysteines in RCC1.....	59
Fig. 2.3: Mass spectrometry analysis of RCC1 from cells treated with diamide..	61
TABLE 1. Modification and accessibility of cysteines in RCC1.....	63
Fig. 2.4: Cys93 in RCC1 is crucial for exchange activity.....	66
Fig. 2.5: RCC1 binding to Ran requires Cys93.....	69
Fig. 2.6: Diamide treatment reduces RCC1 release from chromatin.....	73
Fig. 2.7: Diamide treatment reduces Ran-dependent nuclear import.....	75
Fig. 2.8: Stress signaling disrupts the Ran system via RCC1-dependent and RCC1-independent mechanisms.....	78
Fig. 2.9: Assay for Caspase 3 cleavage in response to stress.....	80
Fig. 2.10: Working model that summarizes oxidative stress effects on the Ran system described in this study.....	88
Fig. 3.1: Loss of heterochromatin disrupts Ran distribution and causes TPR mislocalization in human primary fibroblasts.....	109
Fig. 3.2: Nuclear intensity of G9a and GLP1 are significantly reduced in HGPS patient cells.....	112

Fig. 3.3: Histone methyltransferases are downregulated in Lopinavir-treated human fibroblasts.....	116
Fig. 3.4: Downregulation of histone methyltransferases is rescued by FTI-277 treatment of HGPS patient cells.....	118
Fig. 3.5: Loss of heterochromatin-induced Ran gradient disruption is much less severe compared to that caused by constitutive attachment of Prelamin A.....	121
Fig. 3.6: Histones H3 and H4 import defect in presence of Progerin.....	124
Fig. 3.7: Importin 4, the import receptor of histones H3 and H4 is mislocalized in presence of Progerin.....	128
Fig. 3.8: Model 1. Effect of Progerin on Ran gradient is more severe than that observed by loss of heterochromatin alone. Model 2. Model showing how Progerin-induced loss of heterochromatin affects Ran gradient.....	134
Fig. 4.1: Model integrating different pathways engaged by Progerin in order to cause age-associated phenotypes.....	156

LIST OF ABBREVIATIONS

AU- Arbitrary Unit

CAS- Cellular Apoptosis Susceptibility

DCF- Dichloro Fluorescein Diacetate

DMSO- Dimethyl Sulfoxide

EDMD- Emery-Dreifuss Muscular Dystrophy

FLIP- Fluorescence Loss in Photobleaching

FRAP- Fluorescence Recovery After Photobleaching

FTI- Farnesyl Transferase Inhibitor

GAP- GTPase Activating Protein

GEF- Guanine-nucleotide Exchange Factor

GFP- Green Fluorescence Protein

GNBP- Guanine nucleotide binding protein

H₂O₂- Hydrogen peroxide

HGPS- Hutchinson-Gilford Progeria Syndrome

HP1- Heterochromatin Protein 1

IBB- Importin β -Binding Domain

LMNA- lamin A

LPV- Lopinavir

N:C- Nuclear: Cytoplasmic

NEM- N-Ethyl maleimide

NES- Nuclear Export Sequence

NLS- Nuclear Localization Sequence

NPC- Nuclear Pore Complex

NTF2- Nuclear Transport Factor 2

NTR- N-terminal region

NUP- Nucleoporin

RCC1- Regulator of Chromosome Condensation 1

ROS- Reactive Oxygen Species

TPR- Translocated Promoter Region

UV- Ultra-violet

CHAPTER 1

General Introduction

Nucleocytoplasmic transport

Formation of compartments in the cell is one of the characteristic features of eukaryotes that distinguishes them from the prokaryotes. With the increasing amount of cellular complexity, including complex genetic material and mRNA splicing, division of a cell into several compartments for designated functions is important. The spatial separation of transcription and translation necessitates a regulated mechanism of transport of macromolecules between the nucleus and the cytoplasm. The constitutive nuclear proteins, such as histones and the transcription factors, undergo transport into the nucleus after their synthesis in the cytoplasm, and the mRNAs and tRNAs after transcription and the assembled ribosomal subunits are exported to the cytoplasm from the nucleus. Moreover, there are several proteins that continuously shuttle between these two compartments. All these different kinds of macromolecule trafficking comprise the bi-directional, highly regulated phenomenon, called nucleocytoplasmic transport.

In interphase cells, where the nuclear envelope acts as a barrier for the free exchange of macromolecules between these two compartments, transport occurs through a specialized structure called the Nuclear Pore Complex (NPC) (Fahrenkrog and Aebi, 2003; Görlich and Kutay, 1999; Macara, 2001; Stewart, 2007). There are numerous NPCs present all over the nuclear envelope and they span the entire nuclear envelope. NPCs allow for free diffusion of molecules below ~40 kDa, and receptor-mediated active transport of molecules above the diffusion limit of the NPC.

The vertebrate NPCs are huge assemblies of ~30 different proteins, called nucleoporins (Nups), with a mass of ~125 MDa. Transport through NPCs can be rapid, an estimated rate being ~1000 translocations per second per pore. (Ribbeck and Gorlich, 2001). Both passive diffusion of small molecules and receptor-mediated active transport of large cargoes occur through the NPCs. These pores can facilitate both import and export. NPCs consist of a central cylindrical core, which the cargoes translocate through, the cytoplasmic filamentous structures and a basket-shaped extension on its nucleoplasmic side. Many of the Nups contain distinctive hydrophobic phenylalanine-glycine (Phe-Gly or FG) sequence motifs that are important for the translocation of the cargo-carrier complex through the NPC (Bayliss et al., 2000; Rout et al., 2000).

Classical protein import

Nuclear protein import is initiated when the cargo is bound by the carrier, import receptor, followed by the translocation of the cargo-carrier complex through the NPC into the nucleus, dissociation of the complex with the release of the cargo in the nucleus, and finally recycling of the carrier back to the cytoplasm. Import receptor, Importin α , first binds its cargo in the cytoplasm. The cargoes harbor one or two clusters of basic amino acids, termed as mono- or bi-partite nuclear localization sequence (NLS) respectively, which is recognized and bound by Importin- α (Conti et al., 1998; Dingwall and Laskey, 1991; Fontes et al., 2000). Importin α contains tandemly arranged Armadillo (ARM) repeats, which form the binding site for the basic residues of the NLSs (Stewart, 2007). The N-terminus

of Importin- α binds Importin- β through its Importin- β binding (IBB) domain. Importin- β is considered to be the component of this complex that facilitates translocation through the NPC, whereas Importin- α acts as the adaptor protein. Importin- β can also directly bind some cargo proteins. The IBB domain of Importin- α is a stretch of basic amino acids, similar to the NLSs, and therefore, is capable of binding the NLS-binding site of Importin- α , auto-inhibiting Importin- α -cargo binding (Harreman et al., 2003; Kobe, 1999). Hence, the affinity of Importin- α for its cargo increases when in complex with Importin- β .

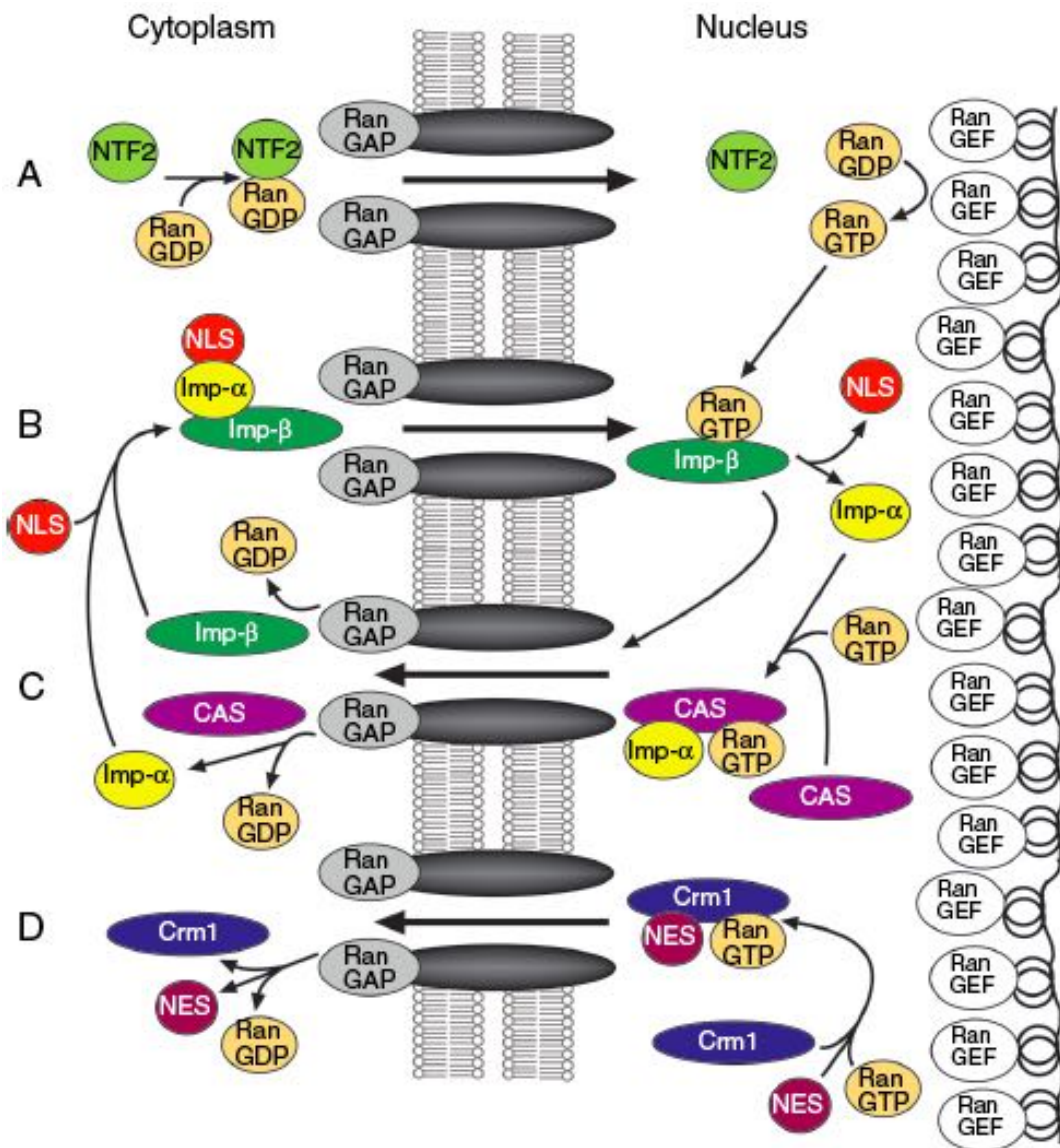
The cargo-carrier complex then traverses through the central pore of NPCs, where the side-chains of Phe of FG-repeats make weak and transient contacts with Importin- β to enable rapid transport (Stewart, 2007; Yang and Musser, 2006). However, the exact mechanism of translocation of the cargo-carrier complex through the NPC is still not clearly understood.

Once the import complex reaches the nucleus, RanGTP, which is abundant in this compartment binds Importin- β (Stewart, 2007). This brings about a conformational change in Importin- β that leads to the release of the IBB domain and dissociation of the import complex (Lee et al., 2005; Stewart, 2007). Now the free IBB domain competes with NLS-binding by Importin- α to dissociate the cargo by an auto-inhibitory mechanism. Importin- β , complexed with RanGTP, is recycled back to the cytoplasm, and Importin- α is actively exported out of the nucleus by the export receptor CAS in presence of RanGTP (Stewart, 2007). RanGAP in the cytoplasm hydrolyzes GTP to GDP on Ran, which releases the import receptors to carry out another import cycle.

Along with the recycling of the import receptors, two molecules of Ran get exported out of the nucleus with each transport cycle. Continuous import and export would deplete the nuclear pool of Ran, unless there is a mechanism to bring Ran back into the nucleus at a rate higher than that of the nuclear export. NTF2 binds Ran in the cytoplasm and imports it into the nucleus through the NPCs (Ribbeck et al., 1998; Smith et al., 1998). NTF2 has a high affinity for binding GDP-bound Ran, found in the cytoplasm (Paschal and Gerace, 1995; Paschal et al., 1996). But as soon as the NTF2-RanGDP complex enters the nucleus, the nucleotide exchange on Ran leads to dissociation of the complex.

Fig. 1.1: Nuclear transport in cells is regulated by Ran GTPase. A. NTF2 binds RanGDP in the cytoplasm and imports it into the nucleus. RCC1 converts RanGDP to RanGTP in the nucleus. B. Import complex assembly occurs in the cytoplasm where import receptor binds the nuclear localization sequence (NLS) of cargo, the complex is translocated to the nucleus, where dissociation of the import complex occurs in presence of high concentration of RanGTP. C. Importin α , while bound to RanGTP and CAS, and Importin β bound to RanGTP, are exported out to the cytoplasm, where RanGAP hydrolyzes RanGTP to RanGDP, and the export complex dissociates. D. Export complex assembly occurs in the nucleus in presence of high concentration of RanGTP, where export receptor Crm1 binds nuclear export sequence (NES) of a cargo and exports it to the cytoplasm. This figure is based on the following article: Pemberton & Paschal, *Traffic* 2005; 6: 187–198.

Fig. 1.1



Ran system/ gradient and its role in nuclear transport

Ran is a small *Ras*-like GTPase that exists in both GDP- and GTP-bound state (Ren et al., 1993). Ran continuously shuttles between the nucleus and the cytoplasm. However, it is predominantly a nuclear protein. At a steady state, the ratio of nuclear to cytoplasmic Ran is approximately 3:1 (Kelley and Paschal, 2007). It is accomplished by the nuclear import of Ran by its import factor NTF2. This is referred to as the Ran protein gradient.

The proteins that regulate the nucleotide-state of Ran are located in two distinct compartments. The Guanine-nucleotide Exchange Factor for Ran (RanGEF), also called Regulator of Chromosome Condensation 1 (RCC1), is localized in the nucleus, whereas the GTPase-Activating Protein for Ran (RanGAP) is present in the cytoplasm. RCC1 removes GDP from Ran and loads Ran with GTP in the nucleus (Bischoff and Ponstingl, 1991). Once RanGTP is exported to the cytoplasm, RanGAP hydrolyzes RanGTP to generate RanGDP. Therefore, there is another gradient present across the nuclear membrane, namely the RanGTP gradient, which is much steeper than the Ran protein gradient (nuclear : cytoplasmic is ~ 100:1) (Görlich et al., 2003).

Both Ran protein and RanGTP gradient are important for nucleocytoplasmic transport in cells. RanGTP gradient imparts directionality to the transport machinery (Izaurralde et al., 1997). Since the presence of RanGTP causes dissociation of the import complex and assembly of the export complex, high concentration of RanGTP in the nucleus and lack of it in the cytoplasm

ensures that cargo import and export occur in the correct direction (Izaurralde et al., 1997; Stewart, 2007). As described earlier, each nuclear transport cycle causes export of two RanGTP molecules from the nucleus. NTF2-mediated Ran-import replenishes this depletion (Ribbeck et al., 1998; Smith et al., 1998). Hence, disruption of Ran import into the nucleus might, potentially, cause collapse of the RanGTP gradient, affecting nucleocytoplasmic transport. Ran protein and RanGTP gradients are two integrated cycles that are crucial for the maintenance of the nucleocytoplasmic transport of macromolecules. RanGTPase is rightly thought as the master regulator of this process.

Nuclear lamina and its function

Nuclear lamina is the filamentous meshwork located between the inner nuclear membrane and the peripheral heterochromatin. It is composed of type V intermediate filament proteins, namely lamin A, B and C (Gerace and Blobel, 1980; Goldman et al., 1986). There are three lamin genes in most vertebrates – LMNA, LMNB1 and LMNB2, which generate several isoforms of lamin proteins by alternative splicing (Goldman et al., 2002). Lamins A and C are derived from LMNA gene, and LMNB1 and LMNB2 encode lamins B1 and B2, respectively (Lin and Worman, 1993; Peter et al., 1989; Vorburger et al., 1989). While lamin A expression is developmentally regulated, at least one type of lamin B is present in all cell types throughout development (Benavente et al., 1985; Lehner et al., 1987; Schatten et al., 1985). Like all intermediate filaments, lamins have a tripartite organization- an N-terminal head domain, a central α -helical rod domain

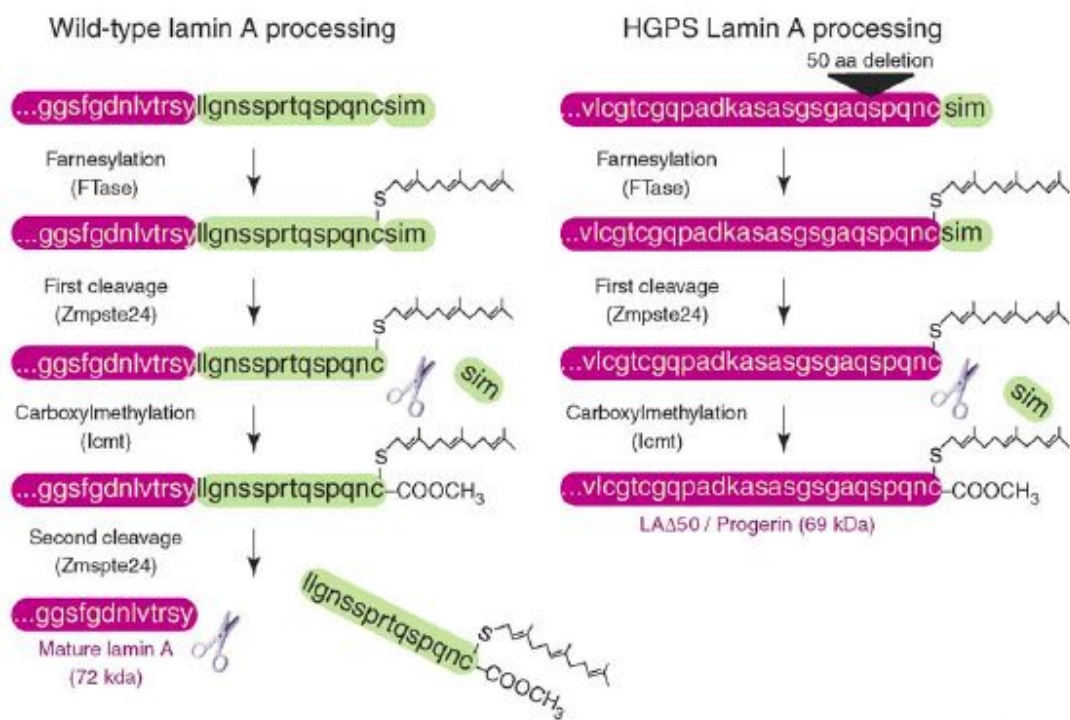
and a C-terminal tail domain (Stuurman et al., 1998). The nuclear localization signal (NLS) is situated in the tail domain close to the central rod domain (Loewinger and McKeon, 1988).

Lamins are synthesized as prelamins, which undergo several posttranslational modifications to finally form the mature form of lamins (Fig. 1.2). The prelamins contain a C-terminal –CAAX box (a Cys residue, followed by two aliphatic amino acids, and X stands for variable amino acid) (Dechat et al., 2008). The Cys residue of the –CAAX box is first farnesylated by a farnesyltransferase, followed by the removal of the –AAX residues by an endopeptidase (Rce1 and/or Zmpste24). The Cys residue is then carboxymethylated by isoprenylcysteine carboxyl methyltransferase (Icmt). Maturation of B-type lamin ends at this step, but prelamins A is further processed. Following carboxymethylation, Zmpste24 cleaves prelamins A one more time to remove 15 amino acids near the C-terminal end to generate mature lamin A.

Lamins play important roles in a number of cellular processes. They are crucial for the maintenance of the nuclear architecture. Lamin A-deficient nuclei have been shown to exhibit increased deformability under mechanical strain (Houben et al., 2007; Lammerding et al., 2004). Deletion or mutation of the LMNA gene leads to abnormal nuclear morphology and alters the organization of several proteins associated with the nuclear envelope (Goldman et al., 2004; Muchir et al., 2003). Lamins are thought to be involved in DNA replication, however the exact mechanism is not known yet. Lamin B3 has been shown to be important for DNA replication in *Xenopus* extract (Goldberg et al., 1995; Meier et al., 1991).

Fig. 1.2: Post-translational processing of lamin A. Post-translational modification of wild-type lamin A and Progerin, HGPS mutant of lamin A. This figure is adopted from the following publication: Mattout et al, *Current Opinion in Cell Biology* 2006, 18:335–341.

Fig. 1.2



Disruption of the lamin organization specifically affects the elongation phase of replication (Moir et al., 2000; Spann et al., 1997). Moreover, interaction of the Ig-fold of the C-terminal domain of lamins with the DNA replication elongation factor Proliferating Cell Nuclear Antigen (PCNA) suggests a direct role of nuclear lamins in DNA synthesis (Shumaker et al., 2008). In laminopathies, such as Hutchinson-Gilford Progeria Syndrome (HGPS), the progressive accumulation of γ H2AX foci, a marker for DNA double-strand breaks and impaired recruitment of the DNA repair proteins are indicative of defective DNA repair mechanism, and suggest some role of lamin A in DNA repair machinery (Liu et al., 2005; Scaffidi and Misteli, 2006). Downregulation of lamins can disrupt nuclear envelope assembly following mitosis, thereby arresting cell cycle progression (Lenz-Böhme et al., 1997). In HGPS, the mutant form of lamin A, Progerin, forms aggregates during mitosis unlike wildtype lamin A (Cao et al., 2007; Dechat et al., 2007; Goldman et al., 2004). This causes delay in mitosis in HGPS, suggesting that lamins are important for cell cycle progression.

Role of nuclear lamina in transcription and its association with chromatin

From the evidence that suggests the role of lamins in DNA synthesis, nuclear lamina appears to act as a scaffold for the proteins involved in DNA replication. Similarly, lamins can be thought of playing an analogous role in transcription and gene expression as well (Goldman et al., 2002). Interactions of lamins with chromatin at the nuclear periphery and evidence of transcriptional repression in that region support this idea. Spatial organization of every human

chromosome in lymphoblast cells and human fibroblasts revealed that the gene-poor chromosomes were peripherally located, whereas the gene-rich chromosomes were present in the center of the nucleus (Boyle et al., 2001). Moreover, the genes associated with *GAL-4* operator in the nuclear periphery were shown to be repressed in SIR (Silent Information Regulator) protein-dependent manner in *S. cerevisiae* (Andrulis et al., 1998). SIR proteins are involved in transcriptional silencing of genes in telomere and silent mating type loci in budding yeast (Palladino et al., 1993; Smith and Boeke, 1997). More direct evidence of the role of lamins in gene transcription came from the studies where the organization of the nuclear lamina was disrupted by introducing an N-terminal deletion mutant of lamin A (Δ NLA) and RNA polymerase II activity was inhibited in presence of Δ NLA in both mammalian cells and nuclei of *X. laevis*, without affecting RNA polymerases I and III-mediated transcription (Spann et al., 2002). Silencing lamin B1 not only altered the lamina meshwork and promoted nuclear blebbing in cells, it also affected the chromatin organization (Shimi et al., 2008). The nuclear lamina in the blebbed region of the lamin B1-silenced cells predominantly comprised of A-type lamin. The chromatin in the blebs showed enrichment of acetylated histone H3, indicative of euchromatin and a decrease in heterochromatin mark H3K9me². It was also shown that RNA polymerase II-mediated transcription elongation was inhibited in this region.

Although these observations suggest that the components of nuclear lamina are important for transcription, it is not clear what role they play in the process. There are several lines of evidence that show the localization of

transcription factors at the nuclear periphery interacting with the lamina leading to transcriptional repression (Gruenbaum et al., 2003). A collagenase repressor, Oct-1, colocalizes with lamin B in immortalized cells (Imai et al., 1997). During cellular aging, Oct-1 dissociates from the nuclear lamina leading to collagenase expression. Hypophosphorylated pRb, in a complex with the E2F transcription factor, binds lamin A/C and also LAP2 α , a lamin-binding protein (Gruenbaum et al., 2003; Mancini et al., 1994). Phosphorylation releases pRb from the lamina, and dissociates the pRb-E2F complex, with subsequent induction of E2F-mediated transcription. SREBP-1, a transcription factor involved in cholesterol biosynthesis and adipogenesis also interacts with lamin A (Lloyd et al., 2002). This interaction was found to be impaired in diseases like familial partial lipodystrophy (FPLD) that involves loss of subcutaneous adipose tissue. Lamin-binding protein Lamin B receptor (LBR) has been shown to bind Heterochromatin protein 1 (HP1) (Dechat et al., 2008; Gruenbaum et al., 2003). Therefore, nuclear lamina might regulate gene expression through interactions with the transcription factors or with the proteins responsible for modifying the chromatin state. Besides interacting with the transcription factors to modulate gene expression, lamins have been shown to directly bind chromatin. There are likely to be two chromatin binding sites in lamin A/C- one in the central rod domain, which requires lamin polymerization for binding histones, and the other in the C-terminal region (Dechat et al., 2009). Besides interacting with the histones, lamins have also been shown to bind DNA, mainly through the Ig-fold of the C-

terminal region (Stierlé et al., 2003). Hence, all these data strongly suggest the involvement of the nuclear lamina in gene regulation.

Furthermore, global loss of heterochromatin due to mutation in lamin A gene in HGPS suggests the role of nuclear lamina in the regulation of chromatin organization and indicates a possible mechanism of controlling gene activity by nuclear lamina (Scaffidi and Misteli, 2006; Shumaker et al., 2006). The changes in chromatin state due to alterations in the lamin organization were reflected in histone modifications, including reduction in H3K9me³ and H3K27me³, and increase in H4K20me³. Changes in H3K9me³ have also been observed in cells from old healthy individuals expressing Progerin (Scaffidi and Misteli, 2006). HP1 α , which interacts with H3K9me³ mark, was also found to be down-regulated in HGPS (Scaffidi and Misteli, 2006). Together, these observations suggest that alteration in the structure of nuclear lamina can impair the chromatin organization, which might lead to changes gene expression.

Nuclear lamina and diseases

Given the role of nuclear lamina in so many different cellular processes, it is very likely that mutation in the components of the lamina structure would result in multiple human diseases. Currently there are no known diseases associated with LMNB1 or LMNB2. It is speculated that mutations in these genes are lethal. However, >150 mutations in LMNA gene have been discovered that are linked to several human diseases. These diseases are collectively called “laminopathies”. The first human disease found to be associated with a gene encoding an inner

nuclear membrane protein was X-linked Emery-Dreifuss muscular dystrophy (X-EDMD) (Bione et al., 1994). This disease is caused by a mutation in a lamin-binding protein Emerin (Bione et al., 1994; Clements et al., 2000). A condition similar to this, autosomal dominant- EDMD (AD-EDMD) was discovered later, which was caused by a mutation in LMNA gene (Bonne et al., 1999). Familial partial lipodystrophy (FPLD) is also a result of a mutation in the LMNA gene (Cao and Hegele, 2000; Shackleton et al., 2000). It is caused by a heterozygous mutation of R482Q in the LMNA gene, resulting in a complete or partial loss of adipose tissue. Laminopathies are not just restricted to muscular dystrophy, skeletal defects and lipodystrophy. Lamin mutations can also result in dermopathy affecting the skin fibroblasts and peripheral neuropathy causing Charcot-Marie-Tooth disorder type 2 (De Sandre-Giovannoli et al., 2002; Navarro et al., 2005). A homozygous R298C amino acid substitution has been identified as the causal mutation of Charcot-Marie-Tooth disorder type 2. Perhaps the most dramatic phenotype caused by lamin A mutation is observed in early aging disease, Hutchinson-Gilford Progeria Syndrome (HGPS), affecting multiple organs in an individual.

Such a broad spectrum of phenotypes observed in laminopathies suggests that the function of lamin A is cell type-specific. Although the mutation linked to HGPS affects multiple cell types, in case of EDMD, the mutation in LMNA gene acts only on muscle cells. The structural weakness of the nuclear envelope and alterations in the gene expression due to lamin mutations are thought to be responsible for laminopathies (Hutchison and Worman, 2004).

Hutchinson-Gilford Progeria Syndrome (HGPS)

Hutchinson-Gilford Progeria Syndrome (HGPS), commonly called Progeria, is an early-aging disease that was first described in late 19th century by Jonathan Hutchinson and Hastings Gilford (Gilford, 1897; Hutchinson, 1886). Almost a century later, works by multiple groups unraveled the cause of this disease- a mutation in the LMNA gene (Cao and Hegele, 2003; De Sandre-Giovannoli et al., 2003; Eriksson et al., 2003).

This is a rare disease affecting the children, where they appear normal at birth, but within a year start showing the symptoms of aging that include loss of hair, loss of subcutaneous fat, musculoskeletal defects and cardiomyopathy. Their average lifespan is approximately 13 years, and the cause of their death is usually myocardial infarction. The molecular basis of this disease was found to be a heterozygous C → T transition at nucleotide 1824 in exon 11 of the LMNA gene (De Sandre-Giovannoli et al., 2003; Eriksson et al., 2003). This is a silent mutation G608G at the protein level. However, this activates a cryptic splice site in exon 11 of the LMNA gene, which leads to the deletion of 50 amino acids near the C-terminal end of lamin A. This mutant form of lamin A is termed Progerin. This deletion also abolishes the Zmpste24 cleavage site in prelamin A during lamin processing, due to which Progerin remains constitutively farnesylated and aberrantly attached to the nuclear membrane causing distortion of the nuclei and other downstream effects.

The cellular phenotypes associated with HGPS are many and the severity of the phenotypes progressively increases with accumulation of Progerin

(McClintock et al., 2007; Rodriguez et al., 2009). The most common characteristic feature of Progerin-expressing cells is nuclear blebbing (Eriksson et al., 2003; Goldman et al., 2004). As the passage number increases, the HGPS patient cells exhibit irregular-shaped nuclei with a lobulated appearance (Goldman et al., 2004). Even expression of Progerin in normal cells drives similar phenotype in a dominant-negative manner (Goldman et al., 2004). Both HGPS patient cells and *Zmpste24*-deficient cells, which arrest lamin A processing at the same stage as HGPS, show increased DNA damage, delay in the recruitment of the DNA damage repair machinery and hypersensitivity to DNA-damaging agent (Liu et al., 2005), indicating the role of lamin A in the maintenance of genomic integrity. Liu et al observed that the recruitment of the proteins involved in DNA damage repair, such as 53BP1 and Rad51, was delayed at the site of γ -H2AX, and also the repair foci persisted longer in HGPS and *Zmpste24*-deficient cells. This might suggest that in HGPS, the altered lamina architecture failed to provide the scaffold for the accumulation of the DNA repair machinery, and the lamina network stalled the replication fork, which caused the persistence of the repair foci (Misteli and Scaffidi, 2005). HGPS cells also exhibit downregulation of proteins involved in the heterochromatin formation, including heterochromatin protein HP1 and histone methyltransferase EZH2 (Scaffidi and Misteli, 2006; Shumaker et al., 2006). Furthermore, these cells have altered histone modification patterns involving heterochromatin, for example reduced histone H3 Lys9 trimethylation ($H3K9me^3$) and histone H3 Lys27 trimethylation ($H3K27me^3$) (Scaffidi and Misteli, 2006; Shumaker et al., 2006). Changes in the structural and

mechanical properties of the nuclear membrane are observed in HGPS cells, reflected by its resistance to external mechanical forces (Dahl et al., 2006). However, they do not show mechanical fragility, like those from Emery-Dreifuss muscular dystrophy. But the structural rigidity of the nuclear membrane might explain the defects in the endothelial and smooth muscle cells contributing to the changes in vasculature in HGPS.

In case of cells with open mitosis, the nuclear envelope breaks down before cell division starts and new nuclear envelope forms around the daughter nuclei after cytokinesis. In HGPS cells, the accumulation of Progerin along with some nuclear lamina components forming insoluble cytoplasmic aggregates during G1 phase and mitosis suggested cell cycle defects (Cao et al., 2007; Dechat et al., 2007). The time taken from metaphase/anaphase transition to the initiation of the cleavage furrow was longer in HGPS than in control cells (Dechat et al., 2007). So was the time taken from metaphase/anaphase transition to the formation of two daughter nuclei in HGPS cells. Supporting this observation, Cao et al. also observed that the time spent in the late mitotic stages is longer in Progerin-expressing cells than in the WT lamin A-expressing cells (Cao et al., 2007). Progerin expression also resulted in a significant increase in lagging chromosomes during anaphase and binucleated cells, suggesting chromosome segregation defects in Progeria. They also exhibited a delay in the recruitment of Progerin to the nuclear envelope at the end of mitosis. These observations suggest defects in cell cycle progression in HGPS cells.

Like normal aging, many pathological phenotypes in HGPS are thought to be inflicted, at least in part, by the increasing amount of oxidants produced endogenously. Fibroblasts from HGPS patients show significantly increased amount of reactive oxygen species (ROS), as depicted by the increase in the fluorescence intensity of dichlorofluorescein (DCF) in the patient cells, in addition to an increase in the expression of antioxidant enzyme, manganese-containing superoxide dismutase (MnSOD) (Viteri et al., 2010). The carbonylated protein levels, indicative of oxidation-mediated protein damage, were also increased in these cells compared to the age-matched control cells. Decreased ATP levels and proteasomal activity in HGPS cells also indicated the accumulation of damaged protein in cells, leading to cellular dysfunction.

Another recent addition to the plethora of cellular defects in HGPS was the disruption of Ran gradient, accompanied by mislocalization of a Ran-dependent cargo, TPR, and reduction of nuclear SUMOylation by SUMO2/3 in HGPS patient fibroblasts, and also in cells ectopically expressing Progerin (Kelley et al., 2011). The loss of nuclear SUMOylation was attributed to the defective import of the SUMO-conjugating enzyme Ubc9. This has been shown to result in the disruption of the Ran protein gradient, leading to TPR import defect. Knocking-down Ran import receptor, NTF2, resulted in the mislocalization of Ubc9 (Datta et al., 2014). The fact that Ubc9 distribution depends on the intact Ran gradient suggests that a feed-forward loop is likely to exist between Ran gradient disruption and Ubc9 mislocalization in HGPS. Later it was shown that Progerin does not affect nuclear import globally, but it tends to inhibit the transport of large

cargoes into the nucleus (Snow et al., 2013). Although the size of Ubc9 is below the diffusion limit of NPCs, in presence of oxidative stress Ubc9 dimerizes with E1 enzyme Uba2/Aos1, via a disulfide bond (Datta et al., 2014) that makes the import of the complex sensitive to Ran gradient disruption.

Exhaustion of stem cell population in HGPS patients has been implicated in some of the premature aging phenotypes of the disease (Halaschek-Wiener and Brooks-Wilson, 2007). Mesoderm-derived vascular epithelium, bone and adipocytes are a few of the major tissues affected in Progeria. Progerin expression in human mesenchymal stem cells (hMSCs) resulted in the expression of both general and lineage-specific differentiation markers, such as endothelial markers collagen IV and MCAM (Scaffidi and Misteli, 2008a). Upon induction of osteogenesis hMSCs showed enhanced differentiation in presence of Progerin as well. However, adipogenic differentiation was markedly inhibited by Progerin expression. These observations indicated toward the depletion of stem cell population in HGPS, which might be responsible for the defects in osteogenesis and adipogenesis in these patients. Progerin-induced activation of Notch signaling has been shown to be responsible for this alteration in the differentiation program of MSCs (Scaffidi and Misteli, 2008a). Moreover, *Zmpste24*^{-/-} mice, which phenotypically mimic HGPS mutation, were shown to have defects in both self-renewal and differentiation potential of hair follicle stem cells, and Wnt signaling was ascribed to this (Espada et al., 2008; Hernandez et al., 2010). Reduction in the stem cell population also in keratinocytes from Progeria mouse-model was reflected by a decrease in $\alpha 6$ -integrin^{high}CD34^{high}

cells compared to the wild type keratinocytes (Rosengardten et al., 2011). Epidermal wound healing was also impaired in Progeria mice. Reprogramming of the dermal fibroblasts from HGPS patients to derive induced pluripotent stem cells (iPSCs) was a leap forward towards understanding the disease mechanism in HGPS (Liu et al., 2011; Zhang et al., 2011). This approach helped to study the role of Progerin in the development of tissue-specific phenotypes, which can potentially aid to overcome the lack of autopsy-based analyses due to the rarity and young mortality in the disease. The iPSCs were differentiated into both mesenchymal and non-mesenchymal lineages. It was found that the expression of Progerin in mesenchymal stem cells (MSCs), vascular smooth muscle cells (VSMCs) and fibroblasts was the highest among the cell-types tested, whereas the lowest expression was found in the neural progenitors (Zhang et al., 2011). HGPS-derived MSCs and VSMCs were sensitive to hypoxia, and failed to restore the blood flow in the ischemic limb of a mouse. Although MSCs survive in low-oxygen niches in vivo, based on these observations it was proposed that Progerin expression resulted in the depletion of MSC pool, which, in turn, led to at least some of the phenotypes in HGPS patients.

Therapeutic intervention

The disease phenotypes in HGPS are driven by the membrane accumulation of Progerin through its constitutive farnesylation (De Sandre-Giovannoli et al., 2003; Eriksson et al., 2003). Therefore, the therapeutic approaches have mainly been directed towards reducing the production of

Progerin in cells, and prevention of farnesylation of prelamin A. A morpholino complementary to the region in exon 11 of lamin A gene that contains the HGPS mutation, sterically blocked the cryptic splice site to prevent the access of the splicing machinery (Scaffidi and Misteli, 2008b). This strategy reduced the production of Progerin significantly, with concomitant improvement in the nuclear morphology, and the restoration of the normal levels of LAP2, HP1 α and nuclear H3K9-trimethylation. Splicing correction of lamin A pre-mRNA also restored the expression of some of the genes, misregulated in Progeria. A similar approach that involved two morpholinos, one that bound the lamin A splice-donor site in exon 10 and the other targeted to the C1824T mutation in exon 11, successfully reduced the expression of Progerin, improved subcutaneous fat layers and decrease in senescence (Osorio et al., 2011). shRNA against Progerin has also been used to reduce Progerin levels in HGPS cells, which improved nuclear morphology, cell viability and the number of senescent cells (Huang et al., 2005). However, this procedure seems inapplicable to whole organisms.

Another successful endeavor was the application of farnesyltransferase inhibitors (FTIs), which prevent farnesylation of Progerin, and therefore, its aberrant association with the nuclear membrane. It has been shown that treating Progeria fibroblasts with a farnesyltransferase inhibitor (FTI), Lonafarnib, could, at least partially, reverse the cellular phenotypes, including nuclear morphology, and also improved bone density, adipose tissue mass, body weight and lifespan of progeroid mice (Capell et al., 2005; Fong et al., 2006; Glynn and Glover, 2005; Toth et al., 2005; Yang et al., 2006). FTI treatment solubilized significant amount

of Progerin in Progerin-expressing cells (Cao et al., 2007). Progeria fibroblasts, treated with FTI showed a rescue of Ran gradient, TPR mislocalization, nuclear SUMOylation and H3K9-trimethylation (Kelley et al., 2011). Based on the success of FTIs in the mouse model of Progeria, the drug Lonafarnib was incorporated in the clinical trial of HGPS in 2007, and the results were encouraging with some patients exhibiting increase in body weight, and improved cardiovascular stiffness, bone structure and audiological status (Gordon et al., 2012). Currently, a clinical trial with a combination of three drugs- Lonafarnib, Pravastatin for lowering cholesterol thus ameliorating cardiovascular defects, and Zoledronic acid for the treatment of osteoporosis- is underway (Trial # NCT00916747, clinicaltrials.gov).

A few other recent studies have shown some promise in treating HGPS phenotypes. Rapamycin, a drug that is known to inhibit mTOR signaling, and frequently used in transplant patients as an antirejection drug, has been shown to rescue nuclear blebbing and delay cellular senescence in HGPS fibroblasts (Cao et al., 2011b). It decreased Progerin levels in those cells, and also facilitated the clearance of Progerin aggregates in autophagic manner. The Progeria mice models show an increase in the tissue-nonspecific alkaline phosphatase activity and diminished ATP levels due to mitochondrial dysfunction (Villa-Bellosta et al., 2013). This leads to a decrease in the extracellular pyrophosphate levels that causes vascular calcification. Therefore, administering pyrophosphate to the progeroid mice inhibited aortic calcification. In another study, in a *Zmpste24*^{-/-} Progeria mouse model a hypomorphic allele of Isoprenylcysteine carboxyl

methyltransferase (ICMT) was made. Reduced ICMT activity generated prelamin A that was unable to target to the nuclear membrane, and delayed senescence in those mice, improved weight gain and reduced bone fractures (Ibrahim et al., 2013). These studies suggested additional mechanisms for the treatment of HGPS, in addition to the existing treatment regimen.

HGPS fibroblasts have high reactive oxygen species (ROS), which is thought to play some part in causing some of the cellular defects, such as DNA damage (Richards et al., 2011; Viteri et al., 2010). Treatment with ROS scavenger, N-acetyl cysteine (NAC) eliminated ROS-induced DNA damage significantly and improved population-doubling time. This result suggests a significant contribution of oxidative stress in HGPS phenotype.

Oxidative stress

Under normal physiological conditions, aerobic respiration unavoidably generates reactive oxygen species (ROS), which include superoxide anions, hydroxyl radicals and hydrogen peroxide (Finkel and Holbrook, 2000). Superoxide and hydroxyl radicals are extremely unstable, whereas hydrogen peroxide is relatively stable and freely diffusible through the cell membrane. According to the 'free-radical-theory', these endogenously produced oxygen radicals cause cumulative damage to the cell, which ultimately shortens the lifespan of the organism (Finkel and Holbrook, 2000). A balance exists between the pro-oxidants and the anti-oxidants in the cell in order to maintain homeostasis. But as an organism ages, the oxidant production surpasses the ability of the cells

to combat it leading to the accumulation of oxidative damage, which is postulated to be a major causal factor for senescence.

ROS is produced both exogenously and from endogenous sources. NADPH oxidases in both immune and non-immune cells potently generate ROS (Finkel and Holbrook, 2000). However, the majority of intracellular ROS production occurs at complex I (NADPH dehydrogenase) and complex III (ubiquinone-cytochrome c reductase) of the electron transport chain (ETC) in mitochondria (Finkel and Holbrook, 2000). In complex III, reduced coenzyme Q generates an intermediate, free radical semiquinone anion species ($\bullet Q^-$), while transferring an electron to cytochrome c. This intermediate then transfers an electron to molecular oxygen to produce superoxide radical. Therefore, ROS production is directly related to the metabolic rate in an organism. P450 complex and peroxisomes also generate ROS in cells.

An abundance of non-enzymatic and enzymatic cellular antioxidants limits the effects of ROS in a well-orchestrated manner. Among the non-enzymatic antioxidants, such as vitamins C and E, and carotenoids etc., glutathione (GSH) probably plays the most important role in counteracting ROS, primarily because of its abundance (millimolar concentration) in the cells (Finkel and Holbrook, 2000). It directly reduces the disulfide bonds, formed in cellular proteins as a consequence of oxidative damage, by serving as an electron donor. In the process, GSH itself gets oxidized to glutathione disulfide (GSSG), which is then recycled back to its reduced form (GSH) by glutathione reductase. Often, the ratio of GSH to GSSH in the cell is considered as a measure of cellular oxidative

stress. The antioxidant enzymes include superoxide dismutase (SOD), catalase, glutathione peroxidase and thioredoxin peroxidase (peroxiredoxin) (Finkel and Holbrook, 2000; Veal et al., 2007). SOD converts superoxide to hydrogen peroxide, whereas catalase, glutathione peroxidase and thioredoxin peroxidase catalyze the decomposition of hydrogen peroxide to water (Finkel and Holbrook, 2000; Veal et al., 2007).

Although cells grown in presence of low level of oxidative stress generate an adaptive response, high oxidative stress results in telomere shortening leading to a reduced lifespan (Finkel and Holbrook, 2000; Zglinicki et al., 1995). The role of oxidative stress in aging is further underscored by several genetic studies in *C. elegans*. Mutating *ctl-1* gene that encodes a cytosolic catalase resulted in reduced lifespan in *C. elegans* (Taub et al., 1999). As a consequence of oxidative stress, cellular proteins, lipids and DNA are modified, which lead to alterations in their activities or their degradation due to misfolding. Increased level of oxidation-induced DNA damage has been reported in aging cells (Finkel and Holbrook, 2000). Interestingly, mitochondrial DNA is found to be more susceptible to such damages than the nuclear DNA, which can be attributed to its proximity to the site of ROS generation, and the lack of antioxidant machinery in mitochondria. This causes mitochondrial dysfunction that acts as a vicious cycle to produce more ROS in the cell (Finkel and Holbrook, 2000). Lipid peroxidation in mitochondrial membrane has been proven to be deleterious as well (Alleman et al., 2014). Cardiolipin is a major component of the inner mitochondrial membrane, and constitutes a considerable amount of the membrane lipids.

Cardiolipins are highly susceptible to peroxidation, which causes a decline in the activity of electron transport chain that eventually leads to apoptosis. Lipid peroxidation has also been implicated in schizophrenia (Okusaga, 2014).

Oxidation-mediated modifications of proteins have been fairly widely studied recently. Amino acids undergo both reversible and irreversible modifications by oxidation. Only three of the amino acids are modified reversibly- Cysteine (Cys), Methionine (Met) and Selenocysteine (Sec) (Go and Jones, 2013). The thiol of Cys is the most well-characterized component of the redox proteome. 214,000 Cys residues are encoded in the human genome (Go and Jones, 2013). Approximately, 5-12% of the total protein Cys is oxidized in cells and tissues, which can be significantly increased by the addition of oxidants. Oxidation of Cysteine residues plays a critical role in modifying the structure and function of many proteins. However, elucidating the function of these oxidative post-translational modification (oxPTMs) in normal physiology or disease has been difficult, largely because of the labile nature of these modifications and also due to lack of specificity in detecting these modifications in a complex biological system.

Oxidation of a single thiol can lead to the formation of a sulfenic acid group (-SOH), while oxidation of two thiol groups in the vicinity of each other produces disulfide bond (-S-S-), either in the same protein molecule (intra-chain) or between two proteins (inter-chain) (Go and Jones, 2013; Hancock, 2009). These two post-translational modifications of Cys residues represent the reversible redox proteome. Disulfide formation includes S-glutathionylation (-S-

SG), S-cysteinylation (-S-S-Cys), and protein-protein disulfide (Protein-S-S-Protein) formation. These modifications are known to protect the Cys residues from getting irreversibly modified under oxidative stress. However, sulfenic acid group can get further oxidized to sulfinic (-SO₂H) or sulfonic (-SO₃H) group, which are irreversible modifications. Cys residues in proteins also react with other molecules, such as nitric oxide (NO) or hydrogen sulfide (H₂S) to result in S-nitrosylation (-S-NO) or S-sulfhydration (-S-S-) respectively (Go and Jones, 2013). While irreversible oxidation of Cys residues leads to protein degradation, reversible modifications alter the activity of the protein by various mechanisms. Oxidation of a Cys at the active site of the phosphatase PTP1B renders it inactive (van Montfort et al., 2003), whereas oxidation of NF-κB inhibits its DNA-binding capability (Toledano and Leonard, 1991). Moreover, a disulfide bond between two thioredoxin (Trx) molecules results in a decreased interaction with thioredoxin reductase (Watson et al., 2003).

Accumulation of oxidized proteins is common in aging cells, which results from an imbalance between the rate of their generation and that of their removal from the cells (Holbrook et al., 1996). Mitochondrial dysfunction, inefficiency of the antioxidant mechanism, and/or increased availability of transition metal-ions due to the lack of metal binding by proteins in these cells often increase the production of ROS that leads to high degree of protein oxidation. Age-dependent decrease in the proteolytic activity might also contribute to an accumulation of oxidized proteins in aging cells.

Oxidative stress and HGPS

The first evidence of high oxidative stress in HGPS fibroblasts came from the observation that these cells produced significantly higher fluorescence intensity of dichlorofluorescein-diacetate (DCF-DA) compared to their age-matched control cells (Viteri et al., 2010). DCF-DA is a compound that fluoresces upon oxidation, and, therefore, provides a measure of ROS in cells (Royall and Ischiropoulos, 1993). These cells also exhibited high level of protein oxidation (Viteri et al., 2010). Mitochondrial superoxide dismutase (SOD) was also upregulated in these cells in response to high oxidative stress with some decrease in the ATP content. A decrease in proteasomal activity was also observed. Accumulation of double strand breaks (DSBs) and poor growth of the HGPS cells were shown to be caused due to an increase in ROS in them, as treating those cells with ROS scavenger, N-acetyl cysteine (NAC), improved both cell growth and the number of DSB foci (Richards et al., 2011). These findings also suggest an additional therapeutic strategy for treating HGPS. Recently, It has been shown that the cells pre-adapted to oxidative stress are resistant to the effects of Progerin on Ran and Ubc9 distribution, which suggests that Progerin exerts its effects on the Ran system via oxidative stress (Datta et al., 2014). However, this study also reported that disruption of the Ran gradient was sufficient to induce oxidative stress, which suggested the presence of a feedback loop between the Ran system and the ROS production in HGPS cells.

Oxidative stress and nuclear transport

The Ran system has been shown to be affected by different stress signaling in multiple studies. Oxidative, osmotic and UV stress have all been shown to mislocalize Ran, import receptors, and also nucleoporins in cells, which, in turn, causes defects in nuclear transport (Crampton et al., 2009; Czubryt et al., 2000; Kelley and Paschal, 2007; Kodiha et al., 2004; 2008; Miyamoto et al., 2004; Stochaj et al., 2000; Yasuda et al., 2006). MAPK signaling pathway has been implicated in the stress-mediated inhibition of the Ran system and nuclear transport (Czubryt et al., 2000; Kodiha et al., 2009b; Kosako et al., 2009). Addition of MEK-inhibitor has been shown to correct the mislocalization of Ran in presence of oxidative stress (Czubryt et al., 2000). Kosako et al. identified that ERK phosphorylates nucleoporin Nup50 to inhibit nuclear accumulation of importin- β (Kosako et al., 2009). Activated ERK failed to abrogate nuclear buildup of importin- β in presence of phosphorylation-deficient mutant of Nup50. However, this did not explain how activation of ERK signaling pathway disrupts Ran distribution during stress. RanGTPase itself has been shown to be oxidized at Cys112 residue by pervanadate, and is also S-nitrosylated (Ckless et al., 2004; Tao et al., 2005). But whether or not these oxidative modifications have any ramification on the Ran system or nuclear transport is unknown.

Regulator of Chromosome Condensation 1 (RCC1)

RCC1 (Regulator of chromosome condensation) was first discovered while identifying the factors required for chromosome condensation during G2 to M transition in cell cycle (Nishimoto et al., 1992). In tsBN2 cells, there is a

temperature-sensitive mutation in the RCC1 gene. At non-permissive temperature (39.5°C) RCC1 is degraded leading to premature chromatin condensation and entry into mitosis by activating p34^{cdc2}/Histone H1 kinase for the cells that are in S or G2 phase (Nishitani et al., 1991). Cells that are in G1 do not enter mitosis and remain arrested in G1. These data demonstrated a role for RCC1 in the cell cycle.

The RCC1 gene encodes a 2.5 kb poly(A)⁺ RNA that is well-conserved from yeast to human (Nishitani et al., 2008; Ohtsubo et al., 1987). The gene is located on human chromosome 1, encoding a 421 amino acid long protein with a molecular weight of 45kDa. RCC1 is the only known Guanine-nucleotide exchange factor (GEF) for Ras-related small nuclear GTPase Ran (Bischoff and Ponstingl, 1991). Ran or any other GTPase is known to exist in the cell in inactive GDP-bound and active GTP-bound states. RCC1 brings about the conversion of Ran-GDP to Ran-GTP in the nucleus. Ran has a similar binding affinity for both GDP and GTP in nanomolar to picomolar range (Klebe et al., 1995). Such high affinity causes slow dissociation rate of nucleotide from Ran, which is accelerated by RCC1 (Bos et al., 2007; Klebe et al., 1995). Nucleotide exchange of Ran by RCC1 is a multi-step process involving the formation of a binary complex consisting of RCC1 and nucleotide-free Ran and a ternary complex of Ran-GDP/GTP-RCC1 (Klebe et al., 1995).

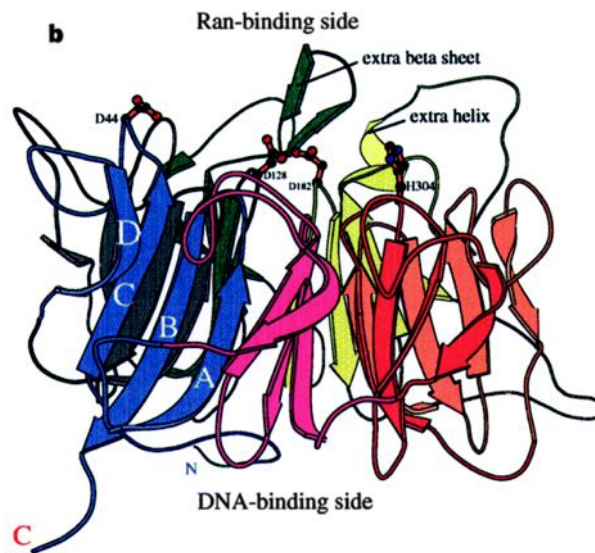
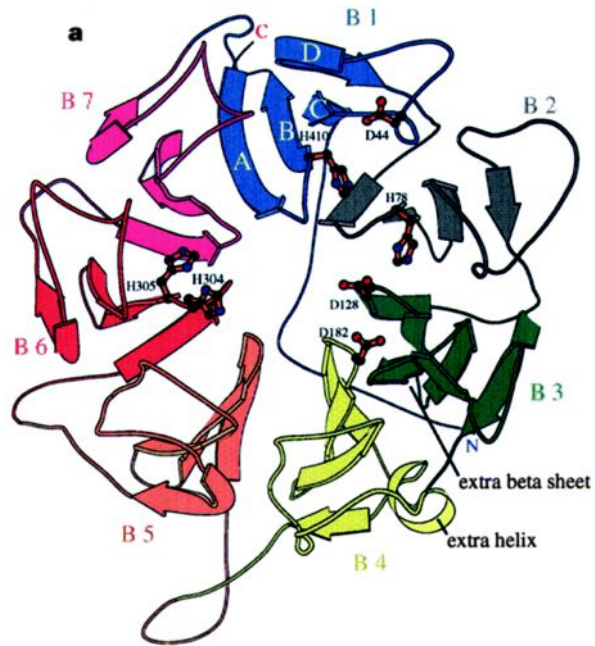
RCC1 has a seven-bladed β -propeller, with its N- and C-terminal tails sticking out of the same surface, the Ran-binding surface being the opposite one (Renault et al., 1998; Vetter and Wittinghofer, 2001) (Fig. 1.3). The N-terminal tail

makes contact with the chromatin. Each of the seven blades of RCC1 has four anti-parallel β -strands, the innermost strand being aligned to the water-filled central shaft of propeller (Hadjebi et al., 2008; Renault et al., 1998). There are seven repetitive sequences of 51-68 amino acids, which together form the RCC1-like domain (RLD), a characteristic of all RCC1 superfamily members. But these seven repeats do not align with the seven blades of the β -propeller, each repeat spanning the third and fourth β -strands of one blade and first and second of the next one. All the seven blades share structural similarity in the first three β -strands, suggesting that these three strands are important for the structural integrity of the molecule, whereas the outermost strands show variability implicating their role in interaction with different effector molecules. An extra β -sheet, called the β -wedge, protrudes from blade-3 towards the Ran-binding surface. This structure plays an important role in RCC1-Ran interaction by promoting the dissociation of GDP from Ran, and subsequent uptake of GTP. The propeller structure is stabilized by several turns composed of Glycine residues between the strands and hydrophobic interactions. Analysis of alanine scanning of RCC1 mutants revealed three invariant amino acid residues, D128, D182 and H304, mutation of which caused severe reduction in k_{cat} of nucleotide exchange reaction of RCC1, suggesting their role in GEF activity (Azuma et al., 1999; Renault et al., 1998). These residues have been found to be located in the center of the Ran-RCC1 interface (Azuma et al., 1999). D44 mutation has been shown to affect the K_M of the reaction, but does not have any effect on the k_{cat} .

Fig. 1.3: Crystal structure of RCC1. It is a seven-bladed β -propeller structure.

This figure is based on the following article: Renault et al, Nature, vol 392, 5, March 1998.

Fig. 1.3



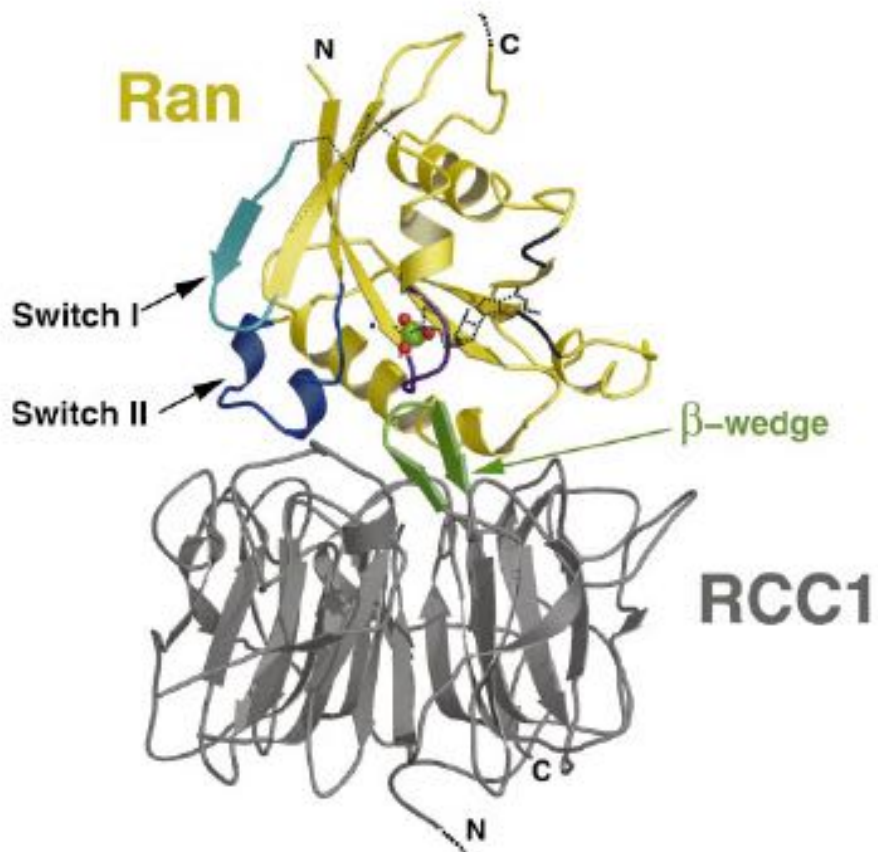
Ran-RCC1 interaction

All the guanine-nucleotide binding proteins (GNBPs) have a universal G-domain that is crucial for its function and carries out nucleotide exchange by a conserved mechanism (Vetter and Wittinghofer, 2001) (Fig. 1.4). There is a 6-stranded β -sheet and 5 α -helices in the G-domain of GNBPs. Switch region of the G-domain consisting of Switch I and II and the phosphate-binding loop, termed P-loop, is crucial for the nucleotide-binding and undergoes conformational switch upon binding nucleotides and GEF (Vetter and Wittinghofer, 2001). RCC1 interacts with Switch I and II of Ran-GDP and inserts residues close to the P-loop, thereby blocking the binding of phosphate group and Mg^{2+} ion, both of which are important for nucleotide binding by Ran (Bos et al., 2007; Vetter and Wittinghofer, 2001). This interaction of RCC1 with Ran results in a conformational change in the switch region, α -helices 3 & 4 and in the P-loop (conserved base binding motif NKxD) causing lower affinity between Ran and the nucleotide GDP (Renault et al., 2001; Vetter and Wittinghofer, 2001). All blades of the RCC1 β -propeller participate in the Ran interaction (Renault et al., 2001). The β -wedge of RCC1 interacts with the P-loop, Switch II and helix α 3 of Ran. Presence of a sulphate anion keeps the P-loop intact, except it shifts towards its base binding site NKxD. Switch II region in Ran-GDP causes severe clash with RCC1, thereby inhibiting stable Ran-GDP-RCC1 complex formation. RCC1 binding to Ran results in major rearrangement in this area. RCC1 interacts with helices α 3/4 and the adjoining area, which is close to the base-binding motif NKxD of P loop. Therefore, subsequent changes in this area cause dissociation

of nucleotide GDP from Ran. Since the P loop remains intact upon RCC1 binding, phosphate binding and Mg^{2+} binding can occur easily prior to the incorporation of GTP into Ran. Moreover, switch I and base binding motif also remains unaffected, which ensures smooth entry of GTP into the complex lowering the binding affinity between RCC1 and Ran (Bos et al., 2007; Renault et al., 2001).

Fig. 1.4: Crystal structure of Ran-RCC1 in complex. The β -wedge of RCC1 physically interacts with Ran and replaces RanGDP with RanGTP. This figure is based on the following publication: Renault et al, Cell, Vol. 105, 245–255, April 20, 2001.

Fig. 1.4



RCC1-chromatin interaction

RCC1 is localized in the nucleus during interphase and on the chromosome during mitosis (Hutchins et al., 2004; Li et al., 2003). RCC1 is known to interact with the chromatin through its N-terminal tail, removal of which results in weaker binding to the chromatin (Moore et al., 2002). It has been shown that binding of RCC1 with H2A/H2B significantly increases its GEF activity (Nemergut et al., 2001). An in-vitro nucleotide exchange assay revealed a significant increase in exchange activity of RCC1 and twofold increase in dissociation rate constant for nucleotide in presence of H2A/H2B. A similar experiment in presence of the Ran-binding protein RanBP3 and histones showed that GEF activity of RCC1 was stimulated by histones and RanBP3 in an additive manner (Nemergut et al., 2002). The same group also showed that RanBP3 interacted with RCC1 in a Ran-dependent way, since it failed to bind free RCC1. This interaction is different from the RCC1-chromatin interaction, because it is Ran-independent.

There are several factors that can influence RCC1 interaction with the chromatin during mitosis, for example, nucleotide-exchange on Ran (Ran-GTP), Ran-GTPase itself, the amino terminal region (NTR) of RCC1, and post-translational modification of amino acid residues (phosphorylation, methylation) present in the NTR of RCC1.

RCC1 interaction with chromatin is highly dynamic during both interphase and mitosis, as shown by Fluorescence Recovery After Photobleaching (FRAP) experiment. When 3T3 cell nucleus expressing RCC1-GFP was photobleached, most of the fluorescence recovery occurred very rapidly during both interphase

and mitosis (Hutchins et al., 2004; Li et al., 2003). Consistent with this, Fluorescence Loss in Photobleaching (FLIP) experiments showed that interaction of RCC1 with the chromatin is more dynamic during mitosis compared to that in interphase cells (Li et al., 2003). Interaction of RCC1 with isolated chromatin or H2A/H2B stimulates its GEF-activity on Ran (Nemergut et al., 2001). RCC1 couples its interaction with chromatin to nucleotide exchange on Ran, thereby generating a steep Ran-GTP gradient on and around the chromosome (Li et al., 2003). Li et al. also showed that the binary complex of Ran-RCC1 exhibited stable association with chromatin, but following nucleotide exchange on Ran both RCC1 and Ran-GTP dissociated from the chromatin. Therefore, Ran-GTP causes lowering of binding affinity of RCC1 to chromatin. This release of RCC1 from chromatin ensures its binding to Ran-GDP or nucleotide-free Ran to form stable binary complex, which then associates with chromatin to generate more of Ran-GTP on the chromatin for proper spindle formation or nuclear envelope assembly. However, when GFP-RCC1^{D182A} (RCC1 mutant with lower affinity for Ran) is expressed in mitotic cells, some cells do exhibit RCC1 localization to the chromosome like the wild-type RCC1, but the percentage of cells with diffused localization is significantly higher in the mutant expressing cells compared to the wild-type (Moore et al., 2002). This observation implies that RCC1 interaction with chromatin during mitosis is facilitated by Ran. Hao et al. proposed an Allosteric Switching model to explain the role of Ran on RCC1 interaction with chromatin (Hao and Macara, 2008). This model suggests that upon Ran binding, N-terminal tail of RCC1 undergoes a conformational change that causes effective

binding of the tail to DNA and also exposes the histone binding site of RCC1 leading to stronger binding to the chromatin (Hao and Macara, 2008).

The N-terminal tail of RCC1 harbors several amino acid residues that get modified during mitosis, along with a Lysine-rich bipartite nuclear localization signal sequence (NLS) (Hao and Macara, 2008). It has been shown experimentally that removal of this N-terminal region (NTR) results in several defects in spindle phenotype, similar to those found in mitotic cells expressing Ran^{T24N} (Ran mutant lacking nucleotide binding capacity) and Ran^{Q69L} (Ran mutant deficient in GTPase activity) (Moore et al., 2002). Moreover, it has been shown that GFP-Δ27-RCC1, lacking the N-terminal 27 amino acid residues, failed to localize exclusively on the chromosome of mitotic cells and exhibited a rather diffused localization instead. A caveat to this is GFP-GST-(1-27) RCC1, carrying only the N-terminal 27 amino acid residues, also failed to localize to the chromosome and showed a diffused distribution. However, from the FRAP data of Hutchins et al. it is evident that the mobility of GFP-Δ27-RCC1 is comparable to that of GFP-GST, which is not expected to bind chromatin (Hutchins et al., 2004). Together these data imply that the NTR is necessary, but not sufficient, for RCC1 localization to the chromatin during mitosis.

The NTR of RCC1 is subjected to several modifications during mitosis. Li et al. and Hutchins et al. have shown that recombinant human RCC1 gets phosphorylated by Cdk1/CyclinB in mitotic *Xenopus* egg extract and mitotic human cell extract (Hutchins et al., 2004; Li and Zheng, 2004). Among the four putative phosphorylation sites in the NTR of RCC1, they found that mutating only

two residues (Ser2 and Ser11) caused reduction in phosphorylation (Hutchins et al., 2004; Li and Zheng, 2004). Fluorescence Loss in Photobleaching (FLIP) experiment data showed that when these two residues were mutated to Alanine, the cells expressing the GFP-fused double mutant (RCC1S2,11A-GFP) exhibited higher rate of fluorescence loss compared to the wild-type, indicating the requirement of phosphorylation of these two residues for efficient binding between RCC1 and chromatin (Li and Zheng, 2004). When all four residues were mutated to Alanine, the cells expressing GFP-RCC1^{AAAA} showed significantly reduced FRAP rate, compared to the wild-type, whereas, the cells expressing the phosphomimetic mutant GFP-RCC1^{EEEE} showed a FRAP rate similar to that of the wild-type, indicating that lack of phosphorylation reduces the dynamicity of RCC1 interaction with the chromatin (Hutchins et al., 2004). In support of this, the γ -isoform of RCC1 that has a 17 amino acid insert in its NTR, is most highly phosphorylated at Ser11 residue among all the three RCC1 isoforms during mitosis, which is probably responsible for its stronger interaction with chromatin than that of RCC1- α (Hood and Clarke, 2007).

The N-terminal tail of RCC1 has also been shown to be methylated at Ser2 residue during mitosis (Chen et al., 2007). The initial methionine residue gets cleaved and the exposed α -amino group of Ser2 is methylated by a α -N-terminal methyltransferase. Mono-, di- and tri-methylated RCC1 have been found in cell lysates of both interphase and mitotic cells. Two amino acids Proline and Lysine downstream of the Ser2 residue are thought to be important for the recognition by the methyltransferase enzyme. Therefore RCC1 carrying K4Q

mutation is a methylation defective protein. Fixed mitotic cells expressing GFP-RCC1K4Q mutant showed a more diffused distribution than GFP-RCC1 during mitosis instead of being localized to the chromosome, which implies that methylation of NTR of RCC1 is crucial for its interaction with the chromatin.

Objective of this thesis

RCC1 is one of the central components that is necessary for the maintenance of the Ran gradient in cells. Inhibition of RCC1 nucleotide-exchange activity disrupts the Ran gradient and leads to the inhibition of nuclear transport. The goal of this thesis is to study the regulation of RCC1 activity in the context of Progeria. Progerin expression induces oxidative stress in cells (Viteri et al., 2010), and causes disruption of the Ran gradient (Kelley et al., 2011). Although there is evidence that oxidative stress alters the Ran distribution and causes mislocalization of several components of the nuclear import machinery (Czubryt et al., 2000; Miyamoto et al., 2004; Yasuda et al., 2006; 2012), it was not clear how oxidative stress exerts these effects. In Chapter 2, I have addressed how oxidative stress inhibits RCC1 activity to transduce its effects on the Ran gradient.

Reduction in heterochromatin marks is considered as one of the characteristic features of HGPS cells. Both H3K9me³ and H3K27me³ marks are significantly reduced in Progeria patient cells (Scaffidi and Misteli, 2006; Shumaker et al., 2006). RCC1 has been shown to have a preference for binding heterochromatin in budding yeast (Casolari et al., 2004). The fact that the

changes in histone modification alters RCC1 mobility on chromatin (Wong et al., 2008), and RCC1 couples its nucleotide exchange activity with chromatin binding to generate RanGTP gradient (Li et al., 2003), suggests that affecting the heterochromatin state in cells might alter RCC1 mobility on chromatin and affect the Ran gradient. This might potentially link the reduction in heterochromatin marks and the disruption of Ran gradient in HGPS cells, which addressed in Chapter 3.

Chapter 2

Disruption of the Ran System by Cysteine Oxidation of RCC1

*This chapter is based on the following manuscript accepted for publication in
Molecular and Cellular Biology.*
Mandovi Chatterjee^{1,2} and Bryce M. Paschal^{1,3}, “Disruption of the Ran System by
Cysteine Oxidation of the Nucleotide Exchange Factor RCC1”

ABSTRACT

Transport regulation by the Ran GTPase requires its nuclear localization and GTP loading by the chromatin-associated exchange factor, RCC1. These reactions generate Ran protein and Ran nucleotide gradients between the nucleus and cytoplasm. Cellular stress disrupts the Ran gradients, but the specific mechanisms underlying the disruption have not been elucidated. We used biochemical approaches to determine how oxidative stress disrupts the Ran system. RCC1 exchange activity was reduced by diamide-induced oxidative stress and restored with dithiothreitol. Using mass spectrometry we found that multiple solvent-exposed cysteines in RCC1 are oxidized in cells treated with diamide. Cysteines oxidized in RCC1 included Cys93, which is solvent-exposed and unique because it becomes buried upon contact with Ran. A Cys93Ser substitution dramatically reduced exchange activity through an effect on RCC1 binding to RanGDP. Diamide treatment reduced the size of the mobile fraction of RCC1-GFP in cells, and inhibited nuclear import in digitonin-permeabilized cell assays. The Ran protein gradient was also disrupted by UV-induced stress, but without affecting RCC1 exchange activity. Our data suggest that stress can disrupt the Ran gradients through RCC1-dependent and RCC1-independent mechanisms, possibly dependent on the particular stress condition.

INTRODUCTION

Regulation of nuclear transport by the Ran GTPase involves two integrated cycles, a nucleotide cycle and a nucleocytoplasmic shuttling cycle. The nucleotide cycle, which is a general feature of GTPases, depends on GTP loading onto Ran and a subsequent step of GTP hydrolysis (Pemberton and Paschal, 2005; Stewart, 2007). GTP loading onto Ran occurs in the nucleus through the action of the nucleotide exchange factor RCC1, which upon binding Ran promotes GDP release and GTP binding (Bischoff and Ponstingl, 1991; Ohtsubo et al., 1989). GTP binding to Ran is favored over GDP-rebinding because of the GTP:GDP ratio (~10:1) in cells (Bischoff and Ponstingl, 1991; Bourne et al., 1991). The nuclear export phase of the nucleocytoplasmic shuttling cycle occurs as a result of high affinity binding of RanGTP to nuclear transport receptors that translocate from the nucleus to the cytoplasm. In the cytoplasm, GTP hydrolysis by Ran, which promotes release from the transport receptors, occurs through association with the Ran GTPase Activating Protein (GAP) (Bischoff et al., 1994). RanGDP can then engage with a dedicated import receptor, NTF2, and undergo re-import (Paschal and Gerace, 1995; Paschal et al., 1996; Ribbeck et al., 1998; Smith et al., 1998). Thus, Ran undergoes import, nucleotide exchange, export, and nucleotide hydrolysis. These reactions generate two nuclear:cytoplasmic (N:C) Ran gradients, a Ran protein gradient (~3:1) and a RanGTP gradient (~100:1) (Izaurralde et al., 1997; Kelley and Paschal, 2007). Disrupting the Ran protein gradient by depleting NTF2 reduces Ran GTP-dependent import (Clarkson et al., 1997; Kelley et al., 2011), and

inhibiting GTP loading with a temperature-sensitive allele of RCC1 disrupts the Ran protein gradient (Tachibana et al., 1994). Because disruption of the Ran protein gradient perturbs the nucleotide cycle, and vice versa, the two cycles appear to be linked in the cell.

RCC1 is the only known nucleotide exchange factor for Ran, and the exclusive nuclear localization of RCC1 restricts the generation of RanGTP to the nuclear compartment (Ohtsubo et al., 1989). Together with the cytoplasmic distribution of RanGAP, subcellular localization of RCC1 and RanGAP generate “compartment identity” through Ran, in the sense that disassembly of import complexes and assembly of export complexes occur only in the nucleus (Izaurralde et al., 1997). The overall structure of RCC1 is that of a seven-bladed propeller (Renault et al., 1998). The Ran binding surface of RCC1 contains a small β -sheet termed the β -wedge that extends from Blade 3 (Renault et al., 1998). The β -wedge inserts into Ran and promotes GDP dissociation. RCC1 also binds directly to chromatin, and chromatin stimulates activation of RCC1 nucleotide exchange activity towards Ran (Li et al., 2003; Nemergut et al., 2001; Seino et al., 1992). RCC1 interactions with chromatin are mediated through multiple contacts that are distinct from the region that binds Ran. The major chromatin-binding site for RCC1 is the switchback loop, which contacts histones H2A and H2B in the nucleosome co-crystal (England et al., 2010; Makde et al., 2010). RCC1 also binds chromatin through its N-terminal tail and a DNA-binding loop (Chen et al., 2007; England et al., 2010; Hao and Macara, 2008; Makde et al., 2010; Seino et al., 1992). The N-terminal tail of RCC1 is methylated and

phosphorylated, and during mitosis these modifications help regulate chromatin binding and therefore RanGTP generation at the chromosomal surface (Chen et al., 2007; Li and Zheng, 2004).

Oxidative stress including the production of reactive oxygen species (ROS) has myriad effects on the cell, and depending on the context can be harmful or beneficial (Cai, 2005; Geiszt and Leto, 2004; Li et al., 2006; Sauer et al., 2000; Veal et al., 2007). ROS is generated through partial reduction of molecular oxygen during aerobic respiration (Finkel and Holbrook, 2000; Veal et al., 2007). The deleterious effects of oxidative stress, which range from DNA damage and lipid oxidation to protein modification, are combated in multiple ways including the expression of genes encoding anti-oxidant enzymes (Chen et al., 2003; Gasch et al., 2000).

Nuclear transport is one of the important pathways impacted by oxidative stress (Crampton et al., 2009; Kodiha et al., 2004; 2008; Miyamoto et al., 2004; Stochaj et al., 2000), but the specific mechanisms by which stress signals are sensed by the nuclear transport machinery are not well defined. Oxidative stress induced by hydrogen peroxide (H_2O_2) results in a reduced concentration of Ran in the nucleus (Stochaj et al., 2000; Yasuda et al., 2006). Cells treated with diethyl maleate undergo oxidative stress and display mislocalization of Importin- α and a reduced level of Crm1-mediated nuclear export (Crampton et al., 2009; Kodiha et al., 2008; Pemberton and Paschal, 2005; Stewart, 2007). Cells from patients with the premature aging syndrome Hutchinson-Gilford Progeria Syndrome (HGPS) have elevated ROS and a disrupted Ran protein gradient,

though the relationship between these phenomena is complex (Bischoff and Ponstingl, 1991; Datta et al., 2014; Ohtsubo et al., 1989; Viteri et al., 2010). These examples emphasize the inhibitory effects of oxidative stress on nuclear transport, but it should be mentioned that certain kinases and transcription factors undergo nuclear import in response to stress (Bischoff and Ponstingl, 1991; Bourne et al., 1991; Eisinger-Mathason et al., 2008; Toone et al., 1998). The biological effect of stress on nuclear transport likely depends on the type, magnitude, and duration of stress, and possibly the specific cargo undergoing transport.

In this study we set out to understand the relationship between oxidative stress and nucleocytoplasmic transport. Using the thiol oxidant diamide to trigger oxidative stress in cells, and employing multiple biochemical approaches, we determined that cysteine residues in RCC1 undergo modification in a manner that significantly reduces nucleotide exchange activity towards Ran. One of the cysteines in RCC1 that is modified by oxidative stress is Cys93, a residue that is situated within the Ran binding site. We show that RCC1 Cys93 is critical for binding and nucleotide exchange on Ran. Cysteines in RCC1 that are outside of the Ran binding region are also modified by diamide, and based on Fluorescence Recovery After Photobleaching (FRAP) analysis, may be involved in the association with chromatin. Our data suggest that RCC1 can sense oxidative stress and transduce the effects to Ran-dependent transport in the cell.

RESULTS

Diamide-induced oxidative stress reversibly inhibits RCC1 exchange activity

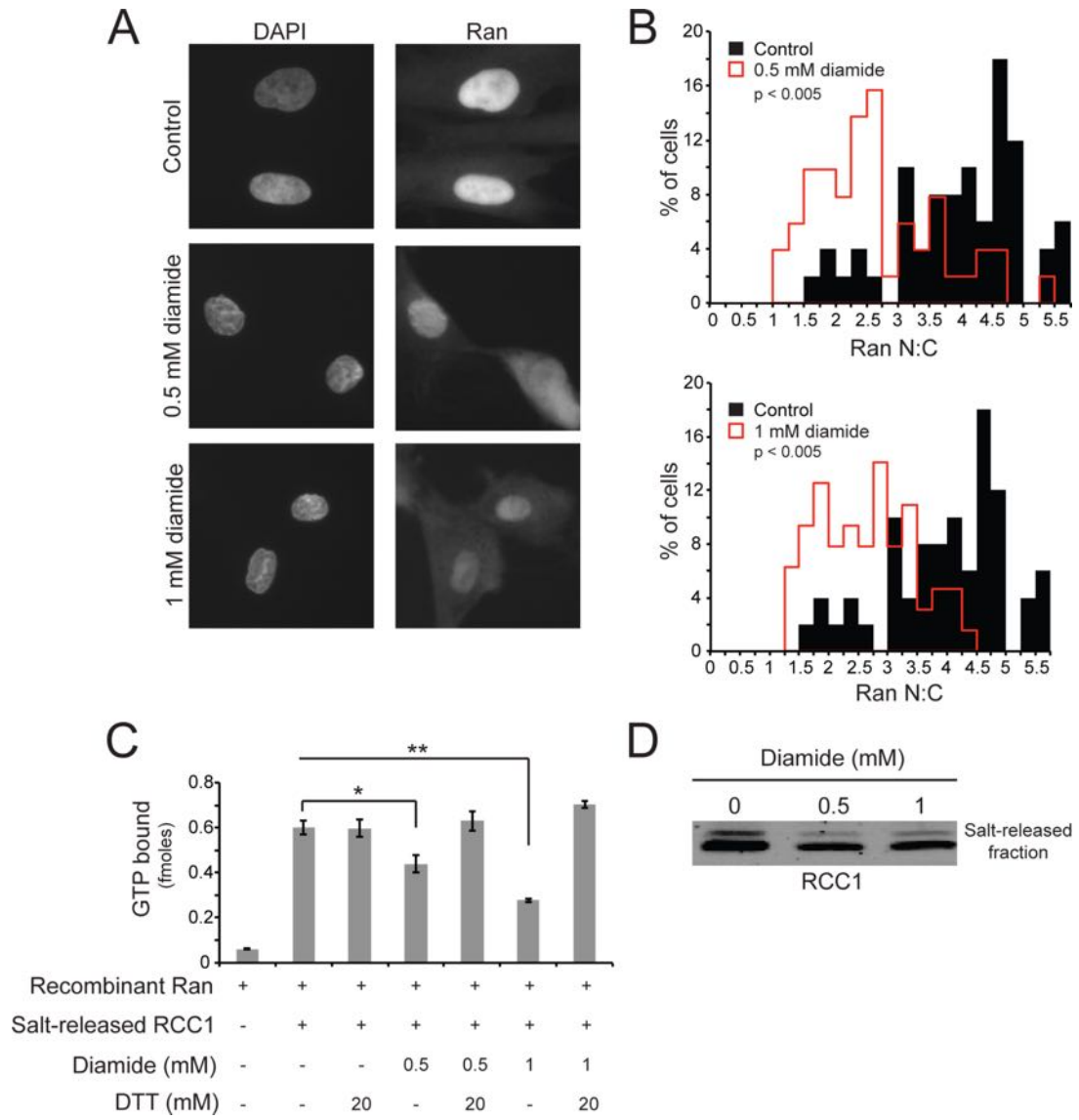
Oxidative stress causes a reduction in the N:C ratio of Ran and inhibits nuclear protein import in various cell types (Bischoff et al., 1994; Crampton et al., 2009; Kodiha et al., 2004; 2008; Miyamoto et al., 2004; Stochaj et al., 2000). To gain insight into how oxidative stress might induce changes in nuclear transport, we treated primary human fibroblasts with the thiol oxidant diamide and examined the effects on the Ran GTPase system. Diamide was chosen because of its selectivity for cysteines and its reversibility in vitro (Kosower and Kosower, 1995; Paschal and Gerace, 1995; Paschal et al., 1996; Ribbeck et al., 1998; Smith et al., 1998). Treating normal human fibroblasts with 0.5 and 1.0 mM diamide for 1 hr altered the Ran distribution, which by immunofluorescence (IF) microscopy appeared as an increase in the cytoplasmic level of Ran (Fig. 2.1 A). By quantitative analysis, diamide caused a significant reduction in the N:C ratio of Ran (Fig. 2.1 B; $p < 0.005$).

Ran undergoes rapid shuttling between the nucleus and the cytoplasm, and formation of the Ran protein gradient requires its nuclear-localized nucleotide exchange factor RCC1 (Bischoff and Ponstingl, 1991; Izaurralde et al., 1997; Kelley and Paschal, 2007; Ohtsubo et al., 1987). tsBN2 cells developed by the Nishimoto laboratory harbor a temperature sensitive allele of RCC1 and display a significant reduction in the Ran N:C distribution when cells are shifted at the non-permissive temperature (Clarkson et al., 1997; Kelley et al., 2011; Seki et al., 1996; Tachibana et al., 1994; Uchida et al., 1990). We reasoned that

the diamide effects on Ran distribution might be mediated by inhibition of RCC1, which is known to be inhibited by the sulfhydryl-directed compound N-ethylmaleimide (NEM) in vitro (Schwoebel, 1998; Tachibana et al., 1994). We used a biochemical approach to test whether diamide treatment of cells affects RCC1 nucleotide exchange activity towards Ran. We prepared chromatin from control and diamide-treated fibroblasts, used high salt to release RCC1 from chromatin (Fig. 2.1 D), and tested RCC1-mediated GDP-GTP exchange on recombinant Ran using a nucleotide binding assay (Ohtsubo et al., 1989; Steggerda and Paschal, 2000). We found that diamide treatment reduced the nucleotide exchange activity of RCC1, and that the inhibition was effectively reversed by treating the RCC1 protein with DTT (Fig. 2.1 C). Because the Ran gradient in cells depends on RCC1 activity (Izaurralde et al., 1997; Ren et al., 1993), RCC1 is the only exchange factor for Ran, and the effect of diamide on RCC1 is reversible by DTT treatment (Fig. 2.1 C), our data suggest that diamide disrupts the Ran protein gradient by oxidizing one or more cysteine residues in RCC1 that are critical for its activity.

Fig. 2.1: Oxidative stress induced by diamide reversibly inhibits RCC1 exchange activity. A. Ran protein distribution in control and diamide-treated human fibroblasts. B. Histogram showing Ran N:C in control and diamide-treated cells. C. In-vitro nucleotide exchange activity of endogenous RCC1 from control and diamide-treated fibroblasts. Statistical significance as measured by Student's t-test: * $p = 0.04$; ** $p = 0.006$. D. Western-blot showing the expression of RCC1 in cells.

Fig. 2.1



Spatial arrangement and oxidative modification of cysteines in RCC1

The crystal structures of RCC1 alone and in various co-complexes provide a context for considering how oxidation by diamide could affect RCC1 function. RCC1 forms a seven bladed β -propeller (Azuma et al., 1999; Renault et al., 2001; 1998) and contains 8 cysteines, four of which are solvent exposed (Cys93, Cys198, Cys228, Cys280) (Fig. 2.2 A; models based on pdb 1A12). None of the cysteines in RCC1 appear to form intra-chain disulfides, but several cysteines are located in positions that might influence protein-protein interactions related to its exchange activity. RCC1 Cys93 and Cys198 are situated on the “side” of RCC1 that binds Ran (Fig. 2.2 A, purple) (Renault et al., 2001; 1998), and Cys228 and Cys280 are near the region of RCC1 that contacts histones in chromatin (England et al., 2010; Li et al., 2003; Makde et al., 2010; Nemergut et al., 2001; Seino et al., 1992), which could be significant, given that RCC1 exchange activity is stimulated by chromatin (England et al., 2010; Makde et al., 2010; Nemergut et al., 2001).

Because cysteine oxidation by diamide is reversed by DTT, and samples for mass spectrometry (MS) are prepared under reducing conditions, we developed a procedure that incorporates modification of RCC1 with NEM, which is irreversible and detectable by MS as a mass shift of +125 daltons. The rationale for the procedure is that cysteines modified in response to diamide in cells should be protected from subsequent modification by NEM. We determined that NEM modification of RCC1 released from chromatin results in virtually complete inhibition of exchange activity, and as expected, RCC1 activity is not

restored by DTT treatment (Fig. 2.2 B, C). If the cells are pre-treated with diamide prior to incubation with NEM, DTT treatment results in an increase in exchange activity (Fig. 2.2 B). For preparation of samples for MS, the diamide-modified cysteines were reversed by DTT, and then oxidized by iodoacetamide (IA) (Fig. 2.2 D). Thus, the Cys-containing peptides derived from RCC1 are a mixture of masses reflecting modification by NEM and IA. The relative abundance of NEM- and IA-modified peptides for a given sequence provides a readout of the susceptibility of specific RCC1 cysteines to modification by diamide. Plots generated from the MS analysis are shown (Fig. 2.3 A, B), along with a summary of the results (Table I). Four cysteines in RCC1 (Cys93, Cys198, Cys228, and Cys280) showed a high degree of labeling by NEM (>30%) that was reduced in cells treated with diamide. These data are consistent with the accessible surface areas (solvent exposure) of these residues in the RCC1 crystal structure, that range from 5-36 Å² depending on the particular cysteine (Table I). Cys93 has the largest accessible surface area of any cysteine in RCC1 (36.05 Å²) and, notably, it is the only cysteine whose surface area becomes buried by contact with Ran (Table I, www.ebi.ac.uk/pdbe/pisa/).

Fig. 2.2: Spatial arrangement and modification of cysteines in RCC1. A. Crystal structure of RCC1 (upper panel) showing the location of the Cys residues (in yellow), including those that are solvent-exposed (lower panel). Regions in RCC1 that become buried by contact with Ran are indicated (purple). B. In-vitro exchange activity of transfected RCC1 from diamide-treated (1 mM for 1hr) tsBN2 cells, and in presence of N-ethylmaleimide (NEM) (1 mM) and the recovery of activity by DTT (20 mM) treatment. Statistical significance as measured by Student's t-test: * $p < 0.005$. C. Western blot showing the expression of transfected RCC1 that are released from chromatin by high salt. D. Scheme of sequential labeling of Cys residues to reveal the diamide-oxidized sites.

Fig. 2.2

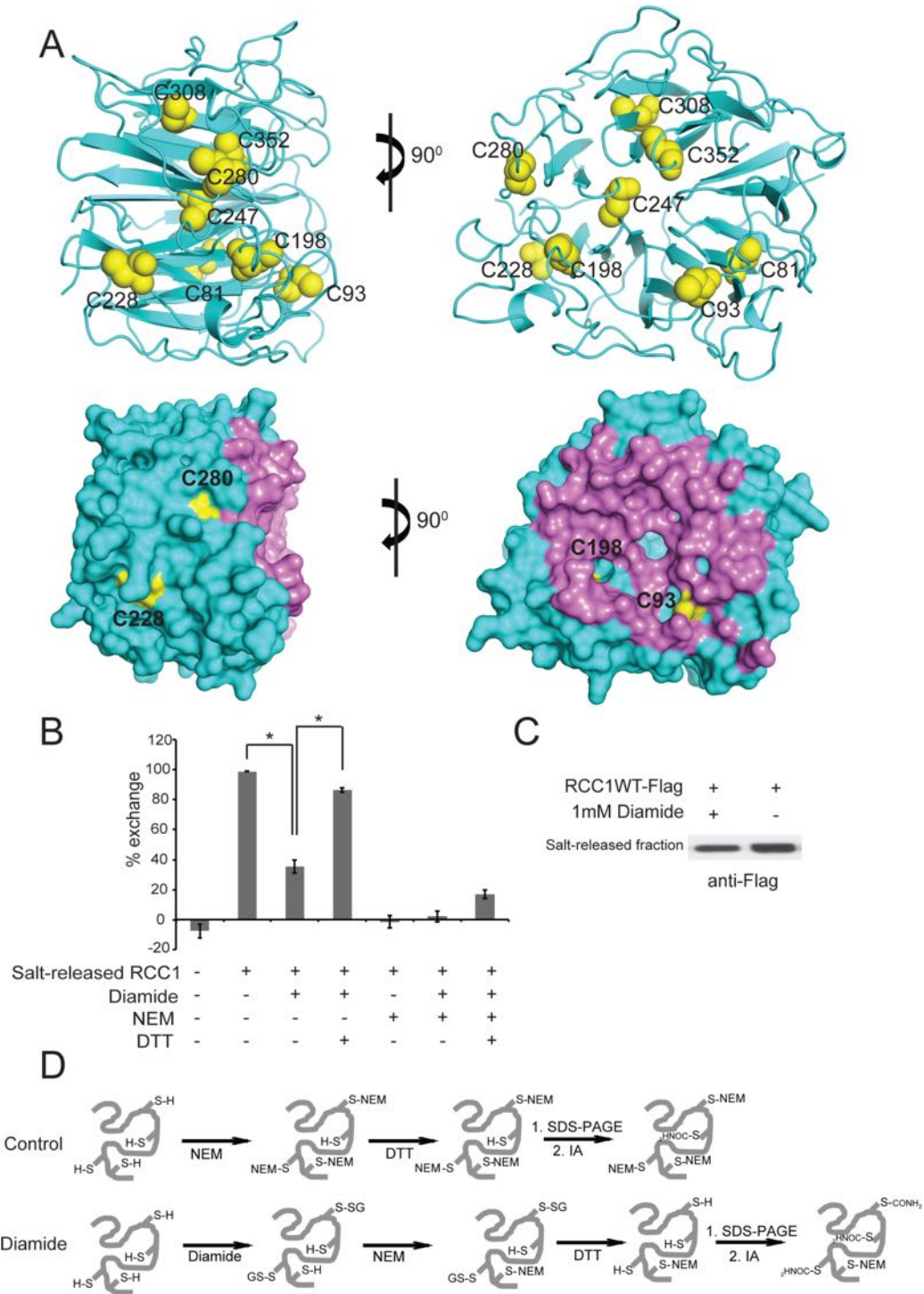


Fig. 2.3: Mass spectrometry analysis of RCC1 from cells treated with diamide. A & B. Mass spectra of control and diamide-treated RCC1.

Fig. 2.3

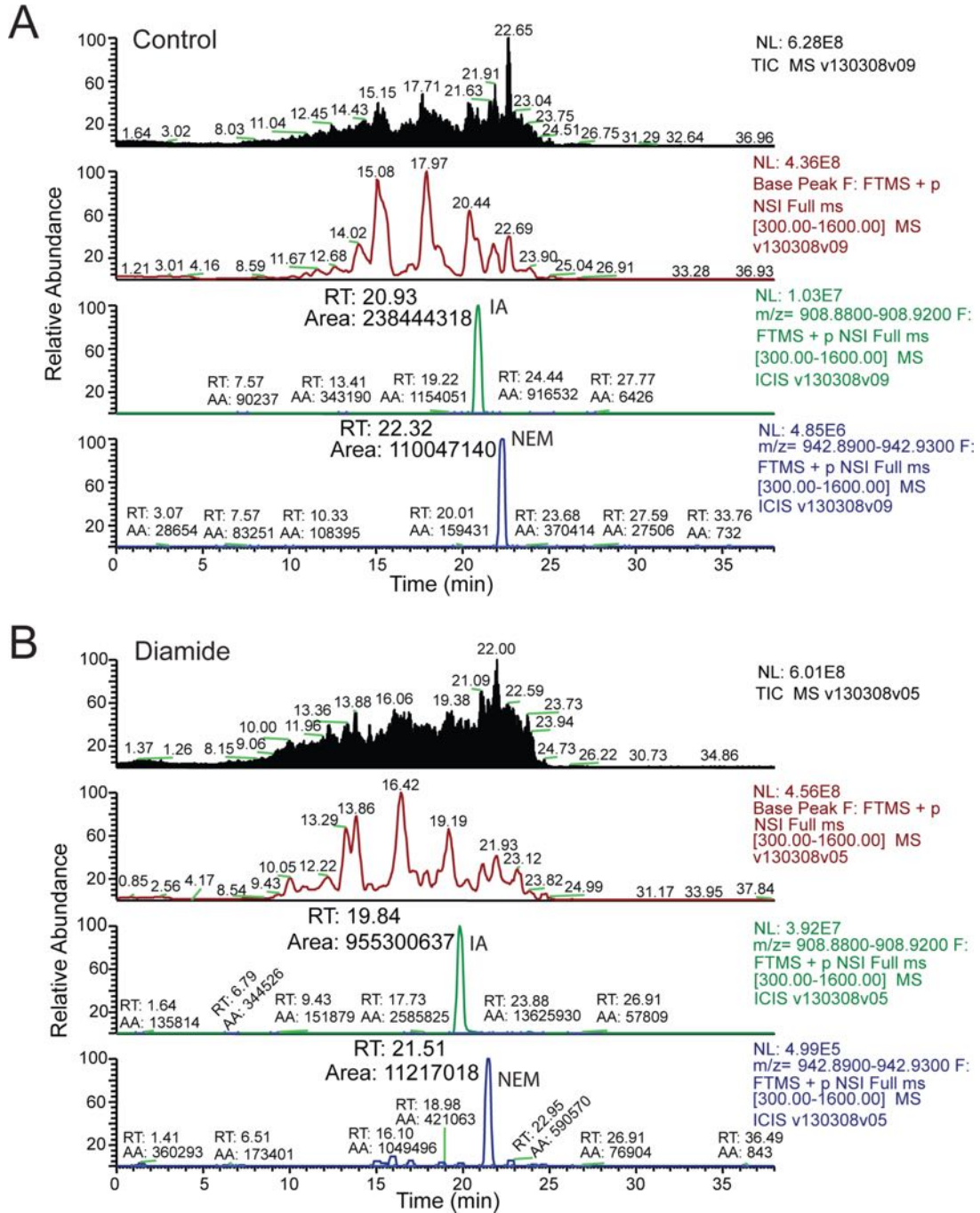


TABLE 1. Modification and accessibility of cysteines in RCC1.

% NEM modification was calculated by the following equation, $\% \text{ NEM modification} = \frac{\text{NEM}^{\text{Area}}}{(\text{IA}^{\text{Area}} + \text{NEM}^{\text{Area}})} \times 100$, where NEM^{Area} and IA^{Area} represent the areas under the curve corresponding to N-ethylmaleimide (NEM)-modified and iodoacetamide (IA)-modified Cys residue. Surface area and water accessibility are based on pdb structures 1A12 and 1I2M.

Residue	% NEM modification		Accessible surface area in free RCC1 (Å ²)	Surface area buried by Ran (Å ²)	Water accessible
	- Diamide	+Diamide			
C81	9.2%	2.1%	0.00	0.00	NO
C93	31.6%	1.1%	36.05	27.18	YES
C198	30.7%	4.2%	6.25	0.00	YES
C228	39.1%	2.0%	24.88	0.00	YES
C247	17.9%	2.0%	20.62	0.00	YES
C280	30.1%	2.1%	5.14	0.00	YES
C308	19.9%	3.5%	0.00	0.00	NO
C352	8.3%	0.7%	15.01	0.00	YES

Cys93 in RCC1 is important for its exchange activity

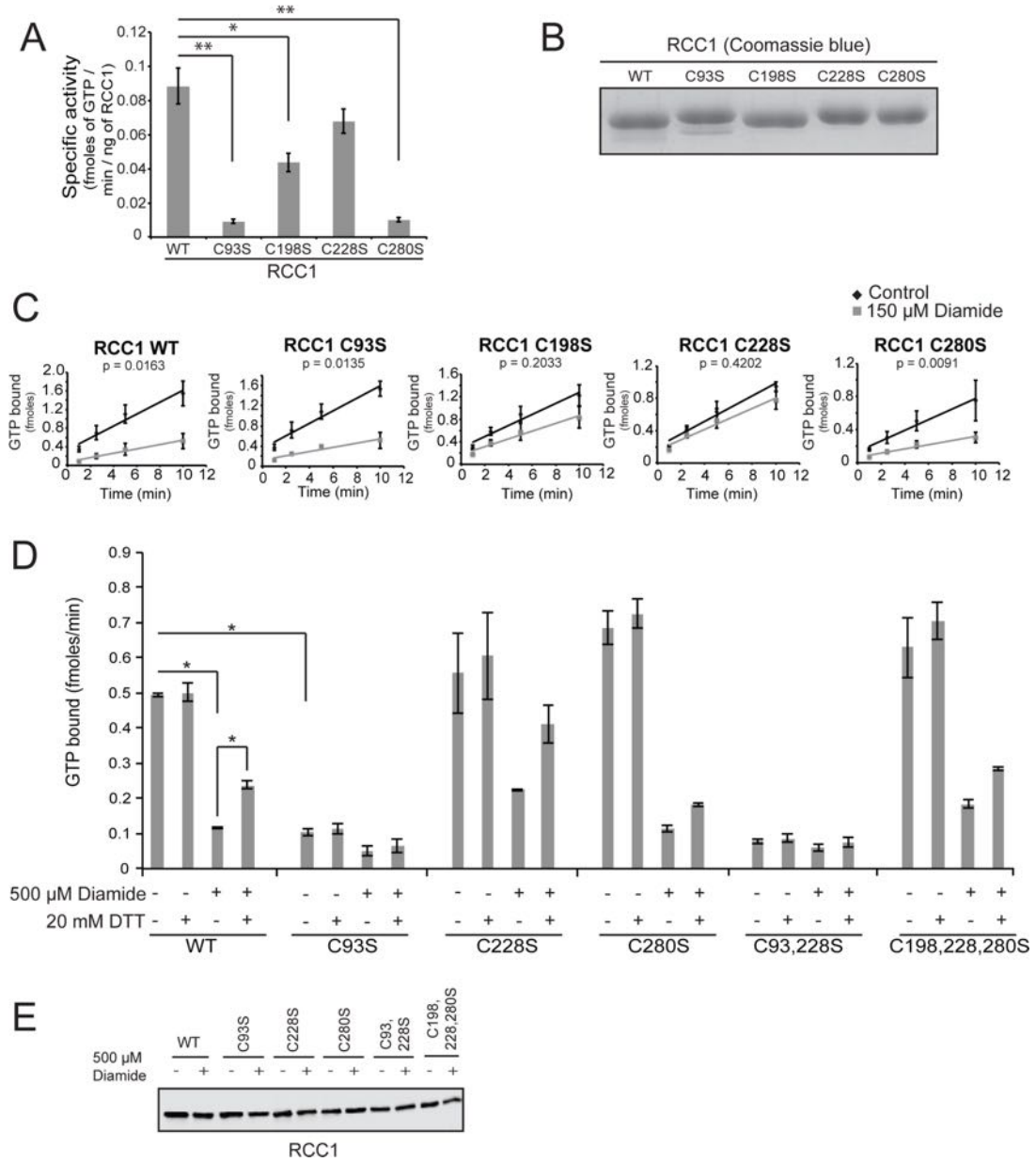
To determine whether individual cysteines contribute to RCC1 exchange activity, we engineered Cys to Ser substitutions in the four cysteines that showed the highest levels of modification by diamide. RCC1 mutant proteins (Cys93Ser, Cys198Ser, Cys228Ser, Cys280Ser) were expressed in bacteria, purified, and tested in GDP-GTP exchange assays using recombinant Ran. Serine substitutions at any one of these four cysteines reduced the exchange activity of recombinant RCC1 (Fig. 2.4 A, B). WT RCC1 had a specific activity of 0.088 fmoles GTP loaded onto recombinant Ran per minute per ng RCC1. The largest reduction in activity was noted with the Cys93Ser (0.009 fmoles/min/ng) and Cys280Ser (0.010 fmoles/min/ng) RCC1 proteins (Fig. 2.4 A). To determine whether one of these cysteines is responsible for the diamide sensitivity of RCC1, we tested if any of the serine substitutions imparted resistance to diamide treatment in vitro, using nucleotide exchange to measure RCC1 activity. For this experiment we used a concentration of diamide (150 μ M) that gave ~80% inhibition of recombinant WT RCC1 (Fig. 2.4 C). RCC1 mutant proteins Cys198Ser and Cys228Ser were resistant to diamide under the conditions tested (Fig. 2.4 C). Thus, using purified recombinant RCC1, Cys198 and Cys228 appear to be the major sites of modification that can reduce RCC1 exchange activity.

Protein oxidation in the cell reflects the complex interplay between protein structure, protein interactions, and redox buffering. To gain insight into which RCC1 cysteines are targets of diamide and are important for exchange activity in

cells, we analyzed a series of RCC1 mutants expressed in mammalian cells. Plasmids encoding WT and mutant forms of RCC1 were transfected into tsBN2 cells, which harbor a temperature-sensitive allele of RCC1 that undergoes degradation at the non-permissive temperature (39.5°C). After transfection and expression of ectopic RCC1, cell growth at 39.5°C results in loss of endogenous RCC1. The transfected RCC1 was released from chromatin and assayed for nucleotide exchange activity, both from control and diamide-treated cells (Fig. 2.4 D). All of the mutants were expressed at similar levels (Fig. 2.4 E), suggesting the substitutions did not have deleterious effects on protein stability. RCC1 from control and diamide-treated cells was also incubated with DTT to test whether diamide effects on RCC1 activity are mediated via cysteine oxidation. We found that the Cys93Ser substitution had a profound inhibitory effect on exchange activity, consistent with the results obtained with RCC1 protein expressed in bacteria. Serine substitutions for Cys198, Cys228, and Cys280, including a triple mutant, had no significant effect on RCC1 exchange activity. Cys228Ser appeared to be slightly resistant to diamide, though the fact that the exchange activity of this mutant was enhanced by DTT treatment indicates other cysteines were modified in this mutant. From these results we conclude that Cys93 is critical for the nucleotide exchange activity of RCC1, but that several cysteines are involved in the diamide sensitivity.

Fig. 2.4: Cys93 in RCC1 is crucial for exchange activity. A. Specific activity of recombinant wild-type (WT) and mutant RCC1. Statistical significance as measured by Student's t-test: * $p < 0.05$; ** $p < 0.001$. B. Coomassie-stained SDS-PAGE of recombinant WT and mutant RCC1 (1 μg each). C. Sensitivity of recombinant WT and Cys mutants of RCC1 to diamide-treatment (150 μM). The amount of RCC1 mutants used in each assay was adjusted to give comparable levels of GDP-GTP exchange (WT: 2.85 ng, C93S: 28 ng, C198S: 4.77 ng, C228S: 2.24 ng, C280S: 11.25 ng). D. In-vitro nucleotide-binding assay with WT or Cys mutants of RCC1, transfected into tsBN2 cells, in presence of diamide (500 μM) and/or DTT (20 mM). Statistical significance as measured by Student's t-test: * $p < 0.005$. E. The expression of WT and Cys mutants (C93S, C228S, C280S, C93,228S, C198,228,280S) of RCC1 in tsBN2 cells.

Fig. 2.4

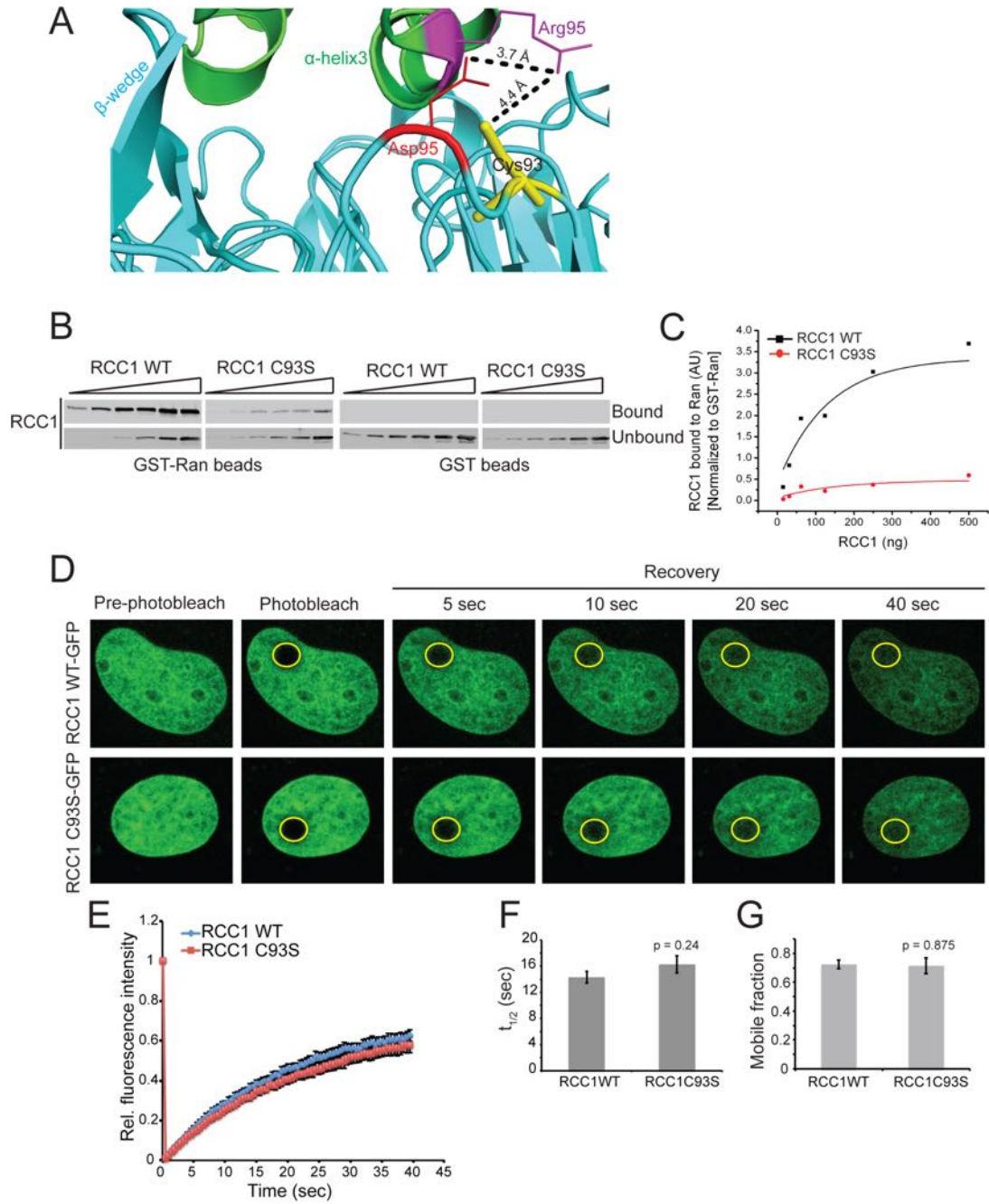


Cys93 of RCC1 is required for Ran-RCC1 binding

In the RCC1-Ran co-crystal, RCC1 Asp95 contacts Ran Arg95 (Chen et al., 2007; England et al., 2010; Hao and Macara, 2008; Makde et al., 2010; Renault et al., 2001; Seino et al., 1992), and the PDBePISA software predicted a hydrogen bond or salt-bridge between these two residues. RCC1 Cys93 is situated in Blade 2 approximately 4.4 Å from Ran Arg95 (Fig. 2.5 A) (Chen et al., 2007; Li and Zheng, 2004; Renault et al., 2001). Thus, the location of RCC1 Cys93 suggests it could also contribute to the bond formation involving RCC1 Asp95 and Ran Arg95. Given these considerations, we examined whether the reduced exchange activity of RCC1 Cys93Ser might be explained by reduced binding to Ran. We tested this hypothesis using binding assays that compared WT and mutant forms of recombinant RCC1. We found that the Cys93Ser substitution caused a substantial reduction (88% decrease) in RCC1 binding to Ran (Fig. 2.5 B, C). To determine whether Cys93 influences RCC1 binding to chromatin we used fluorescence recovery after photobleaching (FRAP; Fig. 2.5 D, E) since the intra-nuclear mobility of GFP-RCC1 in living cells reflects binding to and dissociation from chromatin (Cai, 2005; Cushman et al., 2003; Geiszt and Leto, 2004; Li et al., 2006; Sauer et al., 2000; Veal et al., 2007). We found that the Cys93Ser substitution in RCC1 had no significant effect on the $t_{1/2}$ for recovery or the size of the mobile fraction (Fig. 2.5 F, G). From these data we conclude that the primary effect of the Cys93 substitution, and thereby its function in RCC1, is related to Ran binding.

Fig. 2.5: RCC1 binding to Ran requires Cys93. A. Crystal structure of RCC1 (cyan), complexed with Ran (green), showing the Ran-binding surface of RCC1 near Cys93. B. GST-Ran binding assay showing the binding of wildtype and Cys93Ser mutant of RCC1 (RCC1 WT and RCC1 C93S) with Ran. C. Plotting of the relative binding of RCC1 WT and RCC1 C93S to GST-Ran. D. FRAP assay by live-cell imaging of tsBN2 cells, transfected with RCC1 WT-GFP and RCC1 C93S-GFP. E. Nuclear mobility of RCC1 WT-GFP and RCC1 C93S-GFP, measured by FRAP in tsBN2 cells. Error bars represent standard error of the mean (SEM). F, G. Plotting of $t_{1/2}$ (time taken to reach half-maximal value of fluorescence recovery) (F) and the mobile fraction (G) of the WT and C93S-mutant form of RCC1 in cells.

Fig. 2.5



Oxidative stress alters RCC1-chromatin interaction

To determine whether diamide affects RCC1 interactions with chromatin, perhaps in a manner that is independent of RCC1 Cys93, we treated cells with diamide and examined the levels of chromatin-associated and salt-released RCC1 (Fig. 2.6 A). The fraction of RCC1 released by these conditions was reduced by diamide treatment (Fig. 2.6 A; compare lanes 4-6 to lanes 8-10). By FRAP analysis, diamide treatment reduced the size of the mobile fraction of GFP-RCC1 (Fig. 2.6 B-E), consistent with an effect on dissociation from chromatin. Taken together, our data indicate that diamide can affect RCC1 interactions with both Ran and chromatin.

Diamide-induced oxidative stress inhibits Ran-dependent nuclear transport

To assess whether diamide reduces RCC1 activity to a level that limits nuclear import, we devised an assay that combines treating cells in culture with diamide and reconstituting nuclear import in the same cells after digitonin permeabilization. The assays were carried out in tsBN2 cells, which permit temperature-dependent manipulation of RCC1 levels prior to the nuclear import assay. In tsBN2 cells grown at the permissive temperature, diamide treatment inhibits nuclear import to about the same extent as the temperature shift that causes RCC1 degradation in the tsBN2 cells (Fig. 2.7 A, 33.5°C +Diamide vs. 39.5°C -Diamide). Transfection of WT RCC1 rescues the import defect of cells grown at the non-permissive temperature, though as expected, the cells remain sensitive to diamide treatment (Fig. 2.7 A, +RCC1, 39.5°C, \pm Diamide). These

data corroborate our biochemical data that RCC1 is a diamide-sensitive component of the nuclear transport machinery, and show that diamide inhibition of RCC1 reduces nuclear import.

Fig. 2.6: Diamide treatment reduces RCC1 release from chromatin. A. High salt-mediated release of RCC1 from the triton-resistant fraction in control and diamide-treated (1 mM) tsBN2 cells. B. FRAP assay by live-cell imaging of control and diamide-treated tsBN2 cells, transfected with RCC1 WT-GFP. C. Nuclear mobility of RCC1 WT-GFP, measured by FRAP of control and diamide-treated (500 μ M) cells. Error bars represent standard error of the mean (SEM). D, E. Plotting of $t_{1/2}$ (time taken to reach half-maximal value of fluorescence recovery) (D) and the mobile fraction (E) of RCC1 WT-GFP in control and diamide-treated cells.

Fig. 2.6

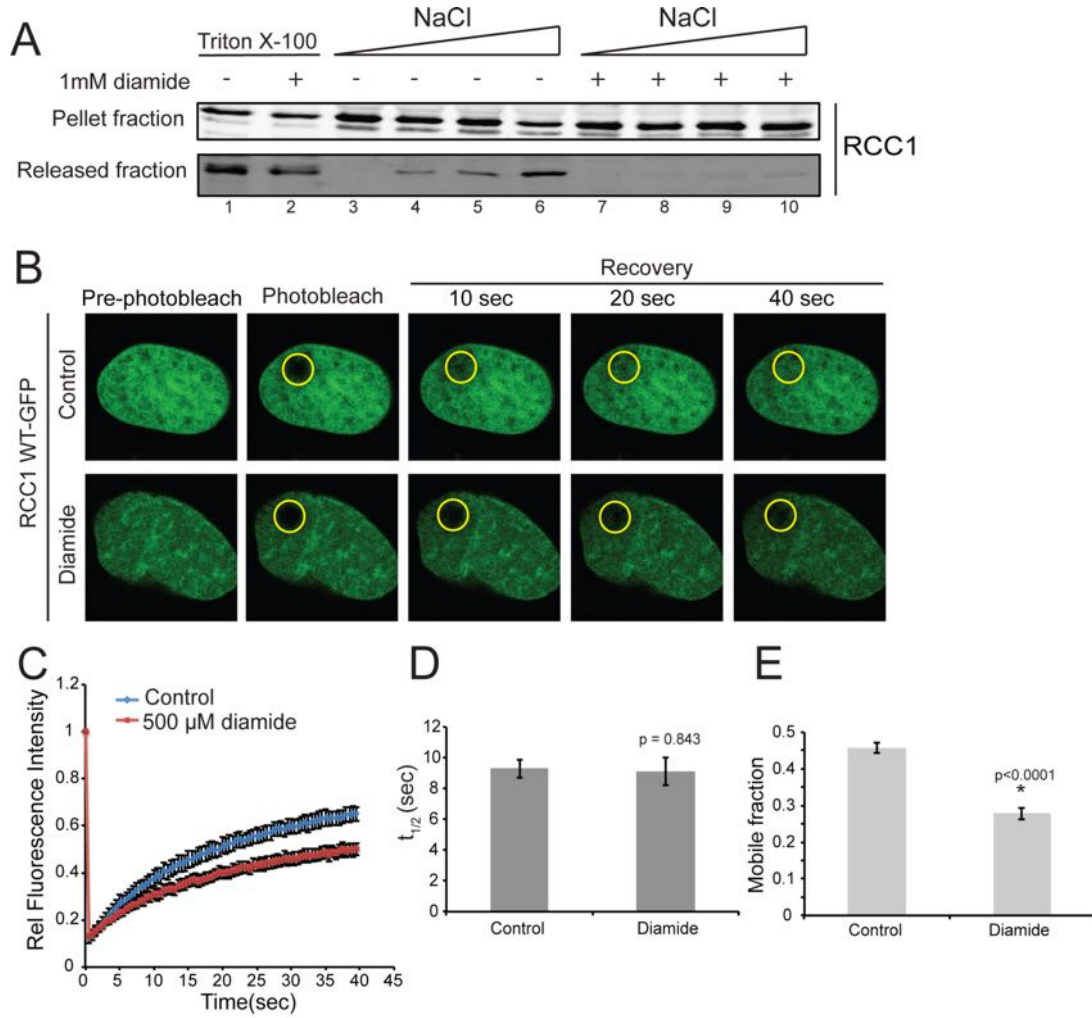
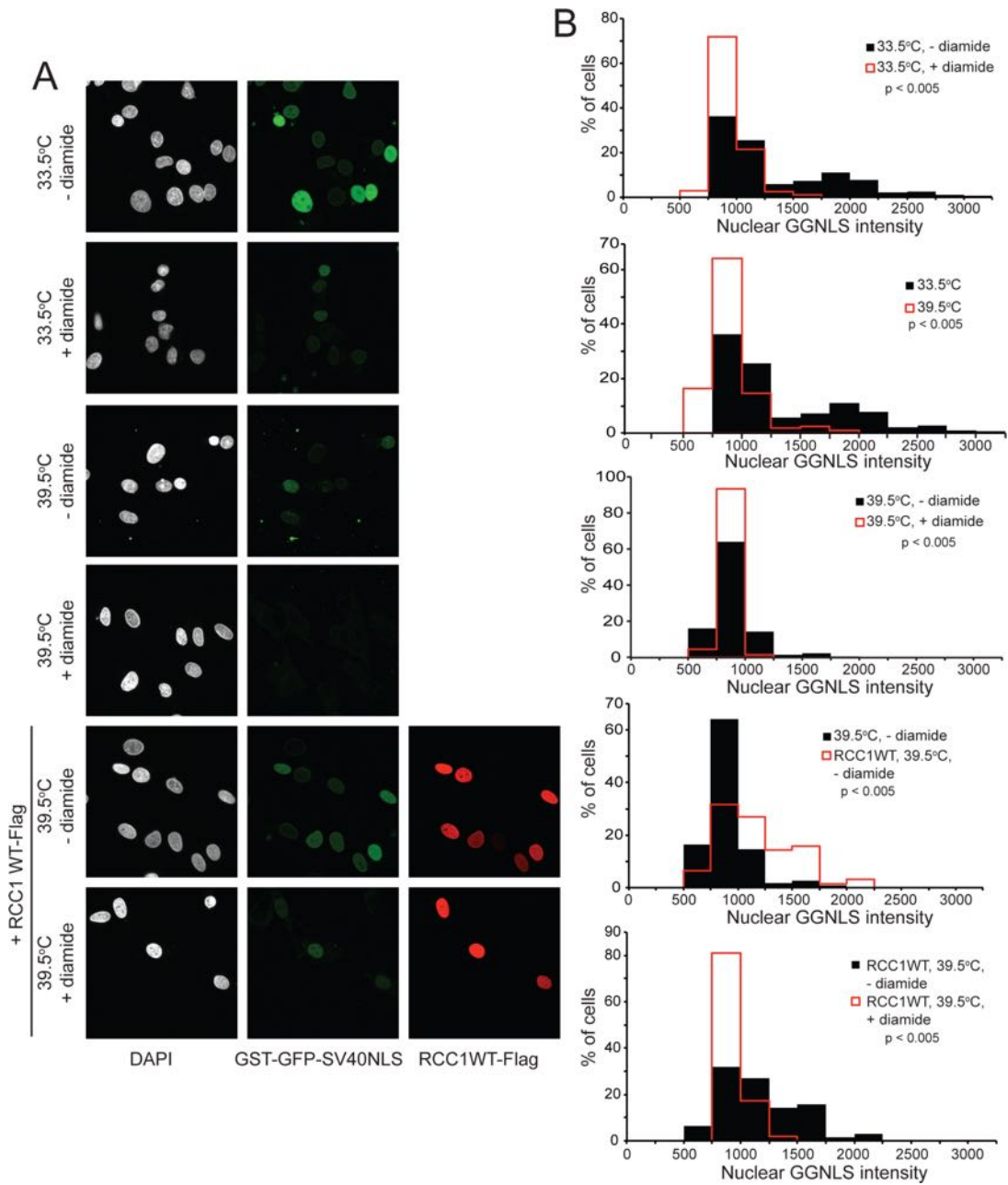


Fig. 2.7: Diamide treatment reduces Ran-dependent nuclear import. A. In-vitro transport of a fluorescently-labeled Ran-dependent cargo, GST-GFP-SV40NLS (GGNLS), in tsBN2 cells. B. Histograms showing the fluorescence intensity of GGNLS, transported into the nucleus of the permeabilized tsBN2 cells at different conditions.

Fig. 2.7



Stress signaling disrupts Ran gradient via RCC1-dependent and -independent mechanisms

Treatments including oxidative stress, osmotic shock, and UV have all been shown to disrupt the Ran protein distribution in cells (Finkel and Holbrook, 2000; Kelley and Paschal, 2007; Kodiha et al., 2004; Miyamoto et al., 2004; Stochaj et al., 2000; Veal et al., 2007). To determine whether reduced RCC1 activity is a common mechanism for transducing stress signaling to the nuclear transport machinery, we subjected tsBN2 cells (permissive temperature) to several conditions and analyzed the effect on Ran and RCC1. Diamide, H₂O₂, menadione, and UV each caused a significant reduction in the Ran protein gradient (Fig. 2.8 A, B). Under these conditions, RCC1 nucleotide exchange activity was reduced by diamide and menadione, and recovered by DTT treatment, but exchange activity was not reduced by the other stresses (Fig. 2.8 C). All of the conditions increased phospho-p38 to a similar level, indicating that tsBN2 cells mounted a stress response under the conditions tested (Fig. 2.8 D). Increasing the concentration of H₂O₂ to a level that gave a more severe disruption of the Ran gradient resulted in a reduced level of RCC1 exchange activity (Fig. 2.8 E-G). We conclude that stress signaling can disrupt the Ran system by RCC1-dependent and RCC1-independent mechanisms. Whether or not RCC1 activity is reduced by oxidation is likely to be dependent on the type and level of stress. As these stress conditions do not induce Caspase 3 cleavage, the effects on the Ran system appear to be independent of events associated with apoptosis (Fig. 2.9)

Fig. 2.8: Stress signaling disrupts the Ran system via RCC1-dependent and RCC1-independent mechanisms. A. Ran distribution in tsBN2 cells treated with different stress-inducers. B. Histograms showing Ran N:C in control and stress-treated cells. C. In-vitro exchange activity of endogenous RCC1 in tsBN2 cells in presence of diamide, H₂O₂, menadione, UV radiation, and/or DTT. Statistical significance as measured by Student's t-test: * p < 0.05. D. Western blot of samples from control and stress-treated cells. Effect of H₂O₂ (2.5 mM) on the Ran system. (E) Ran distribution by IF, (F) histograms showing Ran N:C and (G) in-vitro exchange activity of endogenous RCC1 in control and 2.5 mM H₂O₂-treated tsBN2 cells.

Fig. 2.8

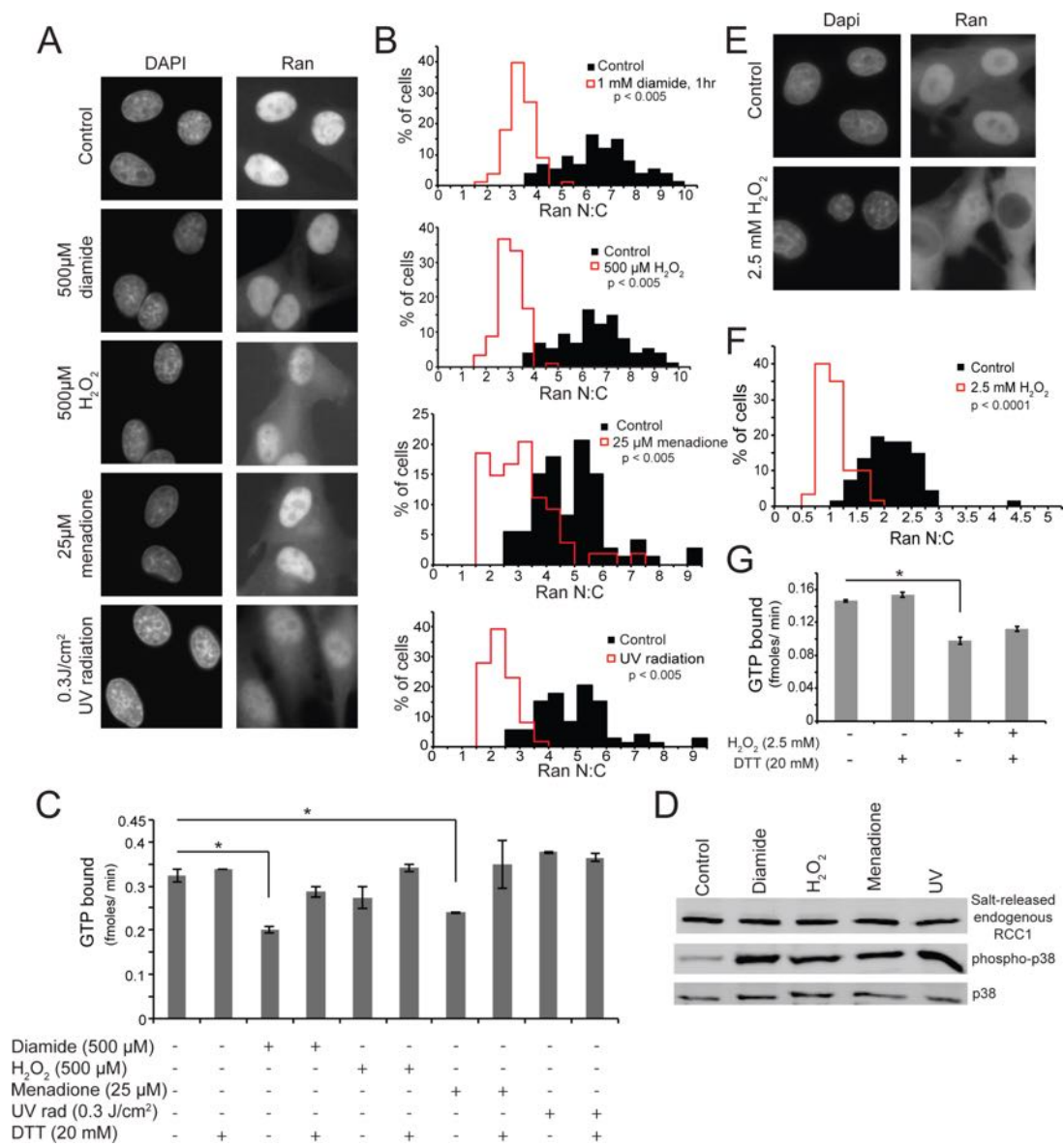
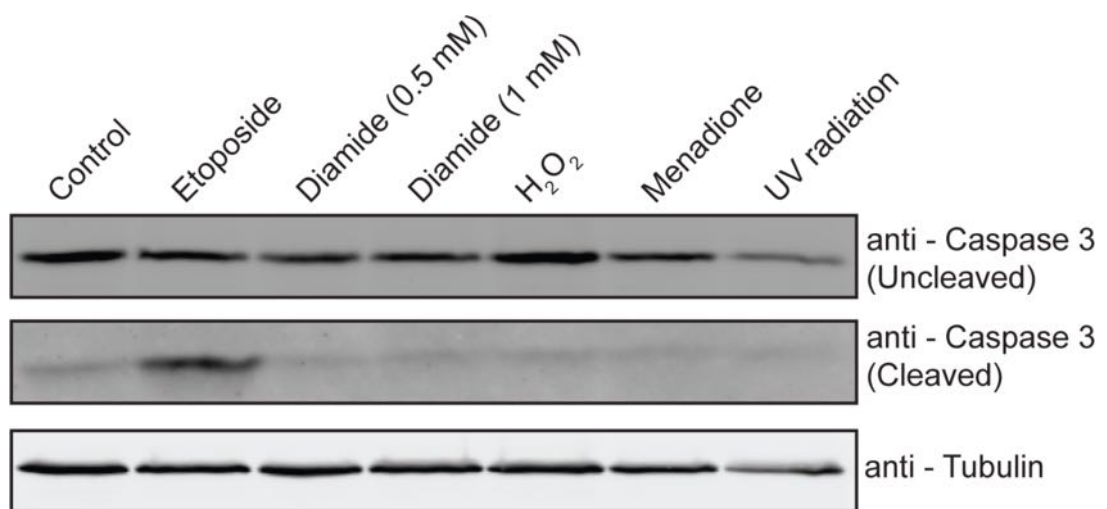


Fig. 2.9: Assay for Caspase 3 cleavage in response to stress. tsBN2 cells (permissive temperature) were treated with etoposide (20 $\mu\text{g}/\text{ml}$, 24 hrs), diamide (0.5 & 1 mM, 1 hr), H_2O_2 (0.5 mM, 15 min), menadione (25 μM , 30 min) and UV radiation (0.3 J/ cm^2) and subjected to immunoblotting with the indicated antibodies. Etoposide treatment induces Caspase 3 cleavage (lane 2) and apoptosis (Wong et al, 2008). In contrast, stress conditions sufficient to disrupt the Ran system (this study) do not induce Caspase 3 cleavage.

Fig. 2.9



DISCUSSION

The Ran GTPase is an essential regulator of nucleocytoplasmic transport in the interphase nucleus. Like other GTPases, the regulatory functions of Ran are intrinsically linked to the conformational differences between its GDP- and GTP-bound states. Ran-GDP is recognized in the cytoplasm by a dedicated import receptor, NTF2, which facilitates Ran translocation through the NPC (Chen et al., 2003; Gasch et al., 2000; Paschal et al., 1996; Ribbeck et al., 1998; Smith et al., 1998). Within the nucleus, the nucleotide exchange factor RCC1 catalyzes GDP-GTP exchange on Ran (Bischoff and Ponstingl, 1991; Crampton et al., 2009; Kodiha et al., 2004; 2008; Miyamoto et al., 2004; Stochaj et al., 2000). This reaction generates the steady supply of RanGTP needed to trigger nuclear import complex disassembly, and promote nuclear export complex assembly (Görllich and Kutay, 1999; Stochaj et al., 2000; Yasuda et al., 2006). RanGTP exits the nucleus bound to import and export receptors, encounters RanGAP in the cytoplasm, and undergoes GTP hydrolysis. This last step produces RanGDP, which can engage with NTF2 and re-enter the transport and nucleotide cycles. Nucleocytoplasmic shuttling together with nucleotide exchange therefore generates two Ran gradients, a Ran protein gradient and a RanGTP gradient.

The inhibitory effects of stress signaling on Ran distribution have been reported in a number of studies. Chemical, osmotic, and UV stress have all been shown to cause mislocalization of Ran and import receptors, and in some systems, the nucleoporins (Czubryt et al., 2000; Kelley and Paschal, 2007;

Kodiha et al., 2004; 2008; Miyamoto et al., 2004; Stochaj et al., 2000). All these changes, along with oxidative stress-mediated posttranslational modification of nucleoporins and activation of the MAPK pathway, have been suggested to contribute to the disruption of the Ran gradient and inhibition of nuclear transport (Czubryt et al., 2000; Kodiha et al., 2009a; Kosako et al., 2009). Although an altered Ran distribution is commonly observed in response to stress, the specific mechanism by which Ran levels in the nucleus are reduced have remained obscure. The RanGTPase itself has been shown to be oxidized at Cys112 residue in presence of pervanadate (Tao et al., 2005) and is also S-nitrosylated (Ckless et al., 2004). But whether these oxidation-mediated posttranslational modifications of Ran have functional consequences for nuclear transport events is not known. MAP and PI-3 kinases can modulate stress effects on nuclear transport, but the specific targets of signaling by these pathways, and how said targets might affect Ran distribution are also unknown. Given the nucleotide requirements for nuclear transport and the fact that stress generally reduces ATP levels in the cell, the conventional wisdom was that reduced levels of GTP should account for nuclear transport changes in response to stress (Yasuda et al., 2006). We tested this assumption in a previous study using the drug ribavirin, and showed that a dramatic reduction in GTP levels in the cell is not sufficient to reduce nuclear import to the extent observed in cells responding to hyperosmotic stress (Kelley and Paschal, 2007). Thus, while energy depletion might have a role in regulating Ran and nuclear transport in certain settings, this explanation does not seem to account for stress effects on the Ran system more generally.

Using temperature-sensitive alleles it has been shown that loss of RCC1 leads to disruption of the Ran protein gradient in both mammalian cells and in yeast. These genetic experiments provide definitive evidence that maintenance of the Ran protein gradient in interphase cells requires the nucleotide exchange activity of RCC1 (Tachibana et al., 1994). These data also provided a clue as to the possible basis of stress-induced disruption of the Ran protein gradient. We set out to test the hypothesis that oxidative stress-induced disruption of the Ran protein occurs through reduced function of RCC1. Our key observation was that treating cells with the thiol-modifying reagent diamide caused disruption of the Ran protein gradient, and reduced the nucleotide exchange activity of RCC1 in a biochemical assay. RCC1 exchange activity was restored by in vitro treatment with DTT, which is known to reverse oxidation caused by diamide treatment (Kosower and Kosower, 1995). These observations provide clear evidence that RCC1 is a key protein affected by oxidative stress in the cell, and that its oxidation state impacts its nucleotide exchange activity towards Ran. In response to diamide, the functionally-relevant cysteines in RCC1 are likely oxidized to the sulfenic state, and/or form a mixed disulfide with glutathione, since the higher oxidation states (sulfinic and sulfonic forms) are not reversible with DTT (Poole and Nelson, 2008; Reddie and Carroll, 2008).

To determine which cysteines in RCC1 are oxidized, we utilized a MS approach wherein cysteine residues that underwent diamide-mediated modification in cells were protected from NEM modification in vitro. Using this strategy, we determined that all eight cysteines in RCC1 showed some level of

modification in cells treated with diamide. We selected four cysteines for more detailed analysis (Cys93, Cys198, Cys228, Cys280) based on fold-changes in labeling with NEM (control vs. diamide) and solvent accessibility in the RCC1 crystal structures. Using recombinant RCC1 made in *E. coli* and chromatin-associated RCC1 prepared after transfection in mammalian cells, we determined that Cys93 is critically important for the nucleotide exchange activity of RCC1, and Cys93 modification mediates, at least in part, the inhibitory effects of diamide. By mass spectrometry, Cys93 labeling by NEM is reduced 28-fold in diamide-treated cells. Both *E. coli*-expressed and mammalian cell-derived RCC1 Cys93Ser showed markedly lower levels of exchange activity towards Ran. The basis of the reduced exchange activity by Cys93Ser can be explained by the location of this residue and its effect on Ran binding. Cys93 has the largest accessible surface area of any cysteine in RCC1 (36 Å²), and it is the only cysteine that is buried (27 Å²) when RCC1 contacts Ran (Table 1). With recombinant proteins, Cys93Ser RCC1 binding to Ran is reduced by ~88% relative to WT RCC1. Based on these data we propose that oxidation of RCC1 Cys93 contributes to the reduction in Ran binding and nucleotide exchange caused by diamide-induced oxidative stress. From the atomic structures published by other groups, it is possible that Cys93 contributes to the Ran interaction through hydrogen bonding to Ran Arg95 in helix 3 (Renault et al., 2001). While Cys93 plays an important role in RCC1 activity, the other three solvent-exposed Cys residues of RCC1 likely make contributions as well. The C93S mutant displayed some sensitivity to diamide treatment (Fig. 2.4 C),

indicating other cysteine residues of RCC1 are modified and contribute to the nucleotide exchange activity.

In addition to Ran-binding, diamide reduced the salt-dependent release of RCC1 from chromatin, and it reduced the size of the mobile fraction of RCC1 measured by FRAP (Figs. 2.6 A - E). Because chromatin stimulates the exchange activity of RCC1 (Nemergut et al., 2001), it seems likely that diamide reduces RCC1 activity through a mechanism that is distinct from its effect on Ran-binding. Consistent with this idea, FRAP analysis showed that intranuclear mobility of RCC1 Cys93 was indistinguishable from RCC1 WT. Thus, the diamide effect on RCC1 mobility probably involves cysteines outside of the Ran-binding side.

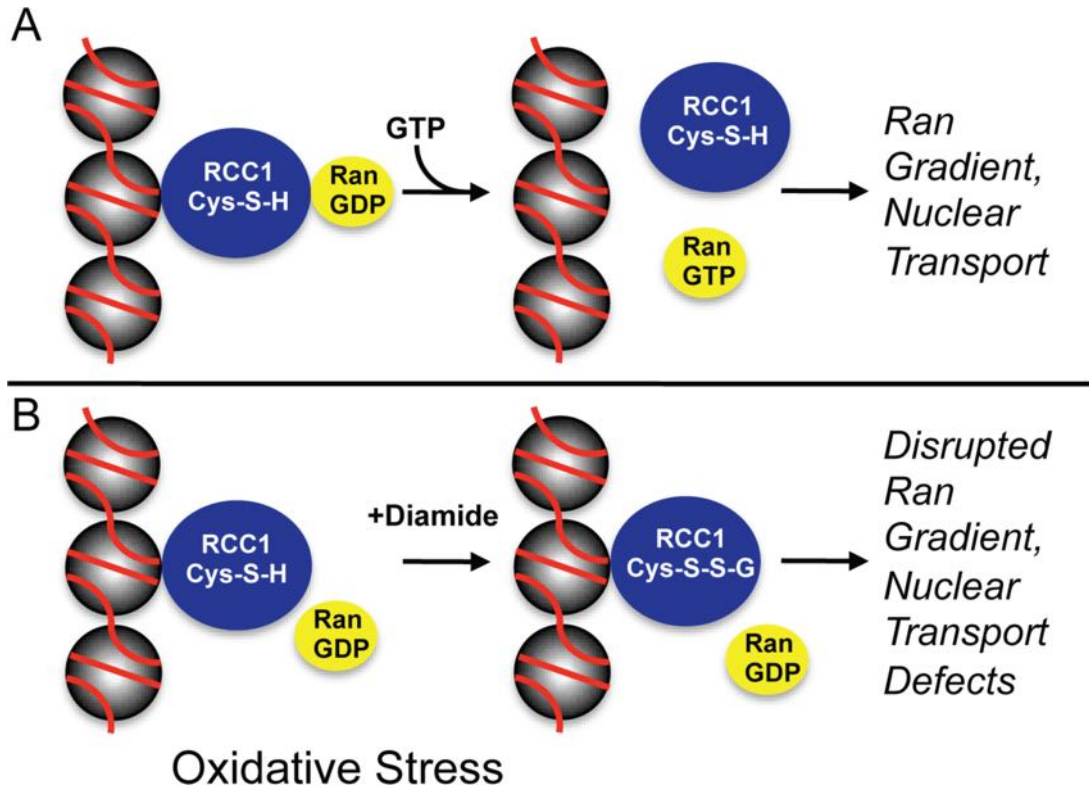
Several post-translational modifications influence RCC1 interactions with chromatin, at least during mitosis. RCC1 is phosphorylated at the N-terminal tail by Cdk1/CyclinB in mitotic extracts (Hutchins et al., 2004; Li and Zheng, 2004), which regulates chromatin binding. The γ -isoform of RCC1 that has a 17 amino acid insert in its N-terminal tail is highly phosphorylated at Ser11. This modification is proposed to account for the enhanced interaction with chromatin during mitosis (Hood and Clarke, 2007). The N-terminal tail of RCC1 is also methylated at Ser2 residue in mitotic cells (Chen et al., 2007). Inhibiting this methylation causes RCC1 to have a diffused distribution during mitosis instead of being localized to the chromosome. Whether or not these modifications affect RCC1 exchange activity or RCC1-chromatin interactions during interphase has not been reported.

The effects of oxidative stress on the cell are complex and involve multiple compartments and pathways. The inhibitory effects of stress on the Ran system imply there could be global effects on nuclear transport. This is an oversimplification, however, given the clear examples of kinases and transcription factors that undergo nuclear import as part of a stress response. It is probable that the net effect of stress on the nuclear transport apparatus depends on the particular cell and tissue, and the type and duration of the stress. For example, a concentration of H₂O₂ typically applied to cells in culture induces activation of multiple kinases and nuclear translocation of Erk2 (Kodiha et al., 2009a; 2007). In contrast, under severe oxidative stress conditions the integrity of the NPC can be compromised and apoptotic mechanisms may be activated (D'Angelo et al., 2009). In our experiments, treating cells with diamide was sufficient to disrupt the Ran gradient and inhibit nuclear import without obvious effect on nuclear integrity.

In summary, we identified RCC1 as a target of oxidative stress and showed that several cysteines, including Cys93, are oxidized when cells are treated with the thiol oxidant diamide. Given that RCC1 Cys93 is critical for Ran binding and nucleotide exchange, our data suggest that oxidation of this site is part of the mechanism for transducing stress signaling to the nuclear transport machinery (Fig. 2.10). We propose that RCC1 oxidation inhibits nucleotide exchange, which, in turn, disrupts the Ran protein and nucleotide gradients. These events are predicted to generate nuclear transport defects, particularly for cargoes that are highly sensitive to nuclear levels of RanGTP (Snow et al., 2013).

Fig. 2.10: Working model that summarizes oxidative stress effects on the Ran system described in this study. A. RCC1 in its reduced state binds RanGDP and mediates GDP-GTP exchange, presumably on the surface of chromatin (Li & Zheng, 2003; Nemergut et al, 2001; Makde et al, 2010). RCC1 activity generates Ran protein and RanGTP gradients that facilitate nuclear transport. B. Diamide-mediated oxidation of RCC1 is predicted to glutathionylate RCC1 adding RCC1-Cys-S-SG adduct, which reduces RanGDP binding, GDP-GTP exchange, and possibly its dissociation from chromatin. Diminished RCC1 activity is predicted to reduce RanGTP production, disrupt the formation of interphase Ran protein and RanGTP gradients, and thereby negatively impact nuclear transport pathways.

Fig. 2.10



MATERIALS AND METHODS

Cell Culture and Transfection

tsBN2 cells carrying a temperature-sensitive mutation in RCC1 gene were grown at 33.5°C (permissive temperature) in 5% CO₂ in Dulbecco's modified Eagle's medium (DMEM) (Gibco/Invitrogen, Carlsbad, CA) containing 10% fetal bovine serum (Atlanta Biologicals, Lawrenceville, GA). Six hrs after transfection, the cells were shifted to the non-permissive temperature (39.5°C) for 6 hrs (FRAP) or 12 hrs (for all other experiments). For stress experiments, tsBN2 cells were treated with H₂O₂, diamide, and menadione (all from Sigma-Aldrich) under the conditions stated in the legends. Cells were also treated with UV radiation (0.3 J/cm²), allowed to recover for 1 hr at 33.5°C, and processed for IF microscopy. For UV radiation, a Hoefer UVC500 UV crosslinker, equipped with a UV lamp, 8W, 254 nm (Amersham Biosciences, Cat. 80-6223-64) was used. During the UV treatment, cells were maintained in standard growth medium (DMEM supplemented with 10% fetal bovine serum). Samples were also harvested for immunoblotting and nucleotide binding assays. One day after plating, tsBN2 cells were transfected with pK-RCC1-Flag or pEGFP-RCC1-GFP plasmids (WT and mutants) using Lipofectamine-2000 (Invitrogen by Life Technologies) following manufacturer's guidelines. After transfection (6-9 hrs), tsBN2 cells were transferred to non-permissive temperature (39.5 °C) for 6 or 12 hours, and then subjected to analysis.

Plasmids

Mammalian and bacterial expression plasmids encoding RCC1 (pK-RCC1-Flag, pEGFP-RCC1-GFP and pET22b-HIS-RCC1) were kindly provided by Ian Macara. Mutations were engineered into RCC1 using the Quik-Change II site-directed mutagenesis kit (Stratagene/Agilent-Technologies, Santa Clara, CA) to generate a collection of cysteine point mutants (C93S, C198S, C228S, C280S, C93,228S and C198,228,280S). Ran was expressed from pET11d-HIS-Ran WT, and kindly provided by Dr. Ralph Kehlenbach. RCC1 and Ran were expressed in BL21 E. coli and purified by standard methods.

Immunofluorescence microscopy (IF) and Fluorescence Recovery After Photobleaching (FRAP)

IF microscopy was performed using standard methods as previously described (Kelley et al., 2011). Cells were grown on glass coverslips, washed with PBS, and fixed for 20 min with 3.75% formaldehyde, followed by permeabilization in 0.2% Triton X-100 for 5 min. Cells were blocked for 1 hr in blocking buffer (2% FBS and 2% BSA in PBS). Primary antibody was diluted in blocking buffer, and incubation was performed for 2 hrs at room temperature or overnight at 4°C. The primary antibodies used for IF were Ran mAb (catalog number 610341; BD) and Flag-rabbit polyclonal or D-8 (catalog number sc807; Santa Cruz Biotechnology). Secondary antibodies were diluted in blocking buffer, and incubation was performed at room temperature for 1 hr. Secondary antibodies used were FITC-labeled donkey anti-mouse and Cy3-labeled donkey anti-rabbit (Jackson ImmunoResearch Laboratories, Inc.). Slides were mounted

for imaging.

Images were acquired using wide-field and confocal microscopes. Most of the fixed-cell imaging was performed using an upright microscope (Eclipse E800; Nikon) using a 40x, 1.0 NA oil immersion objective and were captured with a charge-coupled device camera (C4742-95; Hamamatsu Photonics) with OpenLab software (PerkinElmer). The images of Fig. 7 were acquired on a microscope (LSM 700; Carl Zeiss) equipped with a 40x, 1.3 NA oil immersion objective and ZEN software (Carl Zeiss). All imaging was performed at room temperature (~24°C).

Quantitative analysis of IF images (ratios of the nuclear intensity to the cytoplasmic intensity, N:C ratios) was performed as described previously (Kelley and Paschal, 2007; Kelley et al., 2011) using ImageJ (National Institutes of Health). Both nuclear and cytoplasmic regions of each cell were selected, and the mean IF was determined by ImageJ software. $n:c \text{ ratios} = (\text{mean fluorescence of nucleus})/(\text{mean fluorescence of cytoplasm})$. All histograms were made and statistical tests (Student's t test) were performed using Microsoft Excel. All IF images shown were processed in Photoshop (Adobe). Adjustments to brightness and contrast were performed using the levels function and images of all conditions in an experiment were treated equally.

For live cell imaging, tsBN2 cells were grown on Delta T dishes (Fisher Scientific, Pittsburgh, PA). One day after transfection with RCC1WT-GFP or RCC1C93S-GFP, tsBN2 cells were transferred to the non-permissive

temperature (39.5°C) for 6 hrs. The media was then changed to CO₂-independent phenol red-free media (Hank's balanced salt solution, supplemented with 10% FBS, 25mM HEPES, non-essential amino acid and 5mM CaCl₂), alone or containing 500µM diamide. FRAP was performed by using an LSM 700 confocal microscope (Carl Zeiss, Thornwood, NY) equipped with a 40x, 1.3 NA oil immersion objective, ZEN software (Carl Zeiss) and a Biotech stage warmer. A single Z-section was imaged before and at 500 millisecond intervals after the photobleaching for 40 seconds. The photobleaching was performed using both 488 and 405nm laser line at maximum power of 50 iterations in the boxed regions.

Images were then quantified using ImageJ software (National Institutes of Health) and statistical analysis (n = 10 cells per condition) was done using Microsoft Excel. The fluorescence intensity of the bleached region of interest (ROI), the background (Bg) and the total nucleus (Tot) was measured. To account for the loss of fluorescence intensity due to photodamage, the measured ROI intensity was calculated using the following equation, Normalized intensity of the bleached region = (ROI – Bg) / (Tot – Bg). And finally, it was normalized to the fluorescent intensity of the region of interest before bleaching. These values were plotted as the relative fluorescent intensity as a function of time.

The nonlinear curve fit function of OriginPro (OriginLab Corp.) was used to fit the equation $F = A_1 - A_2 e^{-kt}$, where F is the fluorescence intensity, t is the time after bleaching and A1 is the upper asymptote or the intensity at the end of recovery (F_{end}). The half-life ($t_{1/2}$) equals $\ln(2)/k$. The mobile fraction (M_f) is

calculated using the following equation, $M_f = (F_{\text{end}} - F_{\text{post}}) / (F_{\text{pre}} - F_{\text{post}})$, where F_{end} is the upper asymptote, F_{post} is the intensity at bleaching and F_{pre} is the intensity before bleaching. P values were calculated with Microsoft Excel.

Recombinant proteins and Ran-binding assay

Human Ran protein was expressed as both GST- and HIS-tag fusions. Human RCC1 protein (WT and mutants) was expressed as a HIS-tag fusion in *E. coli* (BL21) using 1 mM Isopropyl β -D-1-thiogalactopyranoside (IPTG) in the presence of 2% ethanol. GST-Ran protein was purified using Glutathione-agarose beads (Cat. G4510, Sigma) in PBS with 1% Triton X-100 and protease inhibitors and was eluted in a buffer containing 50 mM Tris pH 8, 10 mM glutathione and protease inhibitors. HIS-tagged proteins were purified using TALON metal affinity resin (Cat. 635502, Clontech) in TALON buffer (50mM sodium phosphate pH 7, 300 mM NaCl, 10 mM imidazole and protease inhibitors) and were eluted in TALON buffer with 150-200 mM imidazole.

For Ran-binding assay, recombinant GST protein and GST-tagged Ran (2 μ g per reaction) were bound to glutathione-agarose beads at 4°C overnight in PBS with 0.5 mg/ml BSA and protease inhibitors. The beads were then washed three times in a wash buffer (25 mM Tris pH 7.5, 0.5 mg/ml BSA, 50 mM NaCl, 5 mM MgCl₂, 0.1 mM EDTA, 0.1% NP-40 and protease inhibitors), and incubated with recombinant RCC1 (wildtype and C93S mutant) at 4°C for 3 hours. The beads were then washed again and both the bound and the unbound fractions were collected for Western blotting with RCC1 and GST antibodies. The Western

blot data were quantified using Odyssey v3.0 software and the nonlinear curve fit function of OriginPro (OriginLab Corp.) was used to fit the data.

Nucleotide binding assay

tsBN2 cells, transfected with wildtype or mutant RCC1, were subjected to triton x-100-mediated fractionation. Cells were washed three times with cold phosphate-buffered saline (PBS), followed by lysis in 0.05% triton x-100 in PBS and protease inhibitors on ice for 8 min. Lysed cells were centrifuged to obtain the pellet containing chromatin and chromatin-associated proteins. 300 mM NaCl in a buffer (20 mM Hepes pH 7.4, 100 mM KOAc, 2 mM MgOAc, 0.5 mM EGTA and protease inhibitors) was used to release chromatin-associated protein, including RCC1, from the pellet, followed by centrifugation at 13000 rpm for 15 min at 4°C. Bradford assay was performed with the supernatant to determine the protein concentration, and then it was used for in-vitro nucleotide binding assay.

Nucleotide binding assay was performed as previously described (Steggerda and Paschal, 2000). Gel-filtered Ran- $[\gamma\text{-}^{32}\text{P}]\text{-GTP}$ (final concentration ~ 400 nM) or recombinant HIS-Ran WT (final concentration 10 μM) with GTP (mix of hot and cold GTP) (final concentration 100 μM) was incubated with recombinant RCC1 (~2 ng of WT) or RCC1 released by high salt treatment from the triton-resistant fraction of cells in GEF buffer (20 mM Hepes pH 7.4, 100 mM KOAc, 2 mM MgOAc, 0.5 mM EGTA and 5 mM MgCl_2) for 10 min at 30 °C. The reaction was stopped by dilution into 5 ml of GEF buffer containing 5 mM MgCl_2 . The radiolabeled nucleotide that remained bound to Ran or that became

associated with Ran was measured by filter binding to nitrocellulose membranes (0.45 μm , Cat. HAWG02500, Millipore) in liquid scintillation counter (Beckman LS6500).

Immunoblotting

SDS-PAGE and immunoblotting were performed by standard methods. The primary antibodies used for immunoblotting were a mouse monoclonal RCC1 antibody (KAM-CC225; StressGen), a mouse monoclonal GST antibody (B-14) (sc-138, Santa Cruz Biotechnology), a mouse monoclonal pan-p38 MAPK antibody (9217S, Cell Signaling) and a rabbit polyclonal phospho-p38 MAPK (T180, Y182) antibody (9211S, Cell Signaling). The IR dye-conjugated secondary antibodies- Alexa Fluor 800-conjugated donkey anti-mouse IgG and Alexa Fluor 680-conjugated donkey anti-rabbit IgG, were used and the Odyssey system was used for detection and analysis.

Mass spectrometry

tsBN2 cells, transfected with RCC1 WT-Flag, were transferred to the non-permissive temperature (39.5°C) for approx. 12 hours, followed by diamide (1 mM) treatment for 1 hour. RCC1 was extracted from the triton-resistant fraction of both control and diamide-treated cells by 300 mM NaCl, followed by N-ethylmaleimide (NEM) treatment for 30 min at room temperature, and then 20 mM DTT treatment. The samples were then run in an SDS-PAGE and the

Coomassie-stained band specific for RCC1 was subjected to mass spectrometry (MS) analysis.

The gel piece was destained in 50% methanol overnight, dehydrated in acetonitrile and then rehydrated and reduced in 10 mM DTT in 0.1 M ammonium bicarbonate at room temperature for 30 min, followed by alkylation in 50 mM iodoacetamide (IA) in 0.1 M ammonium bicarbonate at room temperature for 30 min. After complete removal of the reagents the samples were digested with 20 ng/ μ l (Trypsin, Glu-C and Chymotrypsin) overnight at 37°C. The peptides were then evaporated for MS analysis. The LC-MS system consisted of a Thermo Electron Orbitrap Velos ETD mass spectrometer system with a Protana nanospray ion source interfaced to a self-packed 8 cm x 75 μ m id Phenomenex Jupiter 10 μ m C18 reversed-phase capillary column. The peptides were eluted from the column by an acetonitrile/ 0.1 M acetic acid gradient at a flow rate of 0.5 μ L/ min over 30 min. The nanospray ion source was operated at 2.5 kV. The digest was analyzed using the double play capability of the instrument acquiring full scan mass spectra to determine peptide molecular weights followed by product ion spectra to determine amino acid sequence in sequential scans. The data were analyzed by database searching using the Sequest search algorithm. The mass spectrometry was performed by W. M. Keck Biomedical Mass Spectrometry Lab at the Univ. of Virginia.

For each of the peptides, the mass spectra of NEM-modified Cys and IA-modified Cys were obtained. The areas under the curve of NEM-modified (NEM^{area}) and IA-modified (IA^{Area}) spectra were calculated. Then, the % NEM

modification for each of the Cys residues was determined using the following equation, % NEM modification = $[\text{NEM}^{\text{Area}} / (\text{NEM}^{\text{Area}} + \text{IA}^{\text{Area}})] \times 100$.

If the % NEM modification for a particular Cys is high in the control sample (-diamide) and low in +diamide sample, then it would indicate that the Cys residue is modified by diamide, and therefore, protected from NEM modification.

Protein modeling

The crystal structure of RCC1 (PDB ID 1A12) and co-crystal of Ran and RCC1 (PDB ID 1I2M) published in RCSB Protein Data Bank (PDB) were rendered using PyMOL software. The interface area, solvent exposed and buried surface area in Ran-RCC1 co-crystal were determined using PDBePISA [<http://www.ebi.ac.uk/pdbe/pisa/>]. PDBePISA software also predicted the hydrogen bonds and salt-bridges across the interface between Ran and RCC1.

Permeabilized cell assay

For import assays, tsBN2 cells were grown on coverslips and transfected with wildtype RCC1. 6 hrs after transfection they were transferred to the non-permissive temperature (39.5°C) for approx. 12 hrs. The cells were then treated with 500 µM diamide for 1 hr. After washing in ice-cold transport buffer (20 mM HEPES pH 7.4, 100 mM KOAc, 2 mM MgOAc, 0.5 mM EGTA, 2 mM DTT and protease inhibitors), the cells were permeabilized with digitonin (0.005%; Calbiochem) in transport buffer for five min on ice. Permeabilization was stopped by washing the samples in ice-cold transport buffer and adding 10 mg/ml BSA in

transport buffer for 2 min at 25°C. The import assay consisted of the import substrate, GST-GFP-SV40NLS (0.06 mg/ml) (GGNLS, Welch et al, 1999), a rabbit reticulocyte lysate (50% vol/vol), KPNA2 (0.02 mg/ml) and an energy-regenerating system (16 mg/ml phosphocreatine, 10 mM ATP, 10 mM GTP, 20 U/ml creatine phosphokinase) in 4 mg/ml BSA/transport buffer. Transport reaction was carried out at 30°C for 20 min for GGNLS, and terminated by washing (3x) in transport buffer. The cells were then fixed in 4% formaldehyde in 1x PBS for 20 min, permeabilized in 0.2% Triton X-100 for 5 min, blocked for 1 h in blocking buffer (2% FBS and 2% BSA in PBS), followed by primary antibody incubation with rabbit polyclonal Flag antibody (sc807; Santa Cruz Biotechnology) at room temperature overnight. Cells were then washed, incubated with Cy3-conjugated donkey anti-rabbit secondary antibody at room temperature for an hour, stained with DAPI and visualized by confocal microscopy.

ACKNOWLEDGEMENTS

We thank Dr. Zygmunt Derewenda for his help with interpreting crystal structures, Dr. Nicholas Sherman for performing the mass spectrometry (W. M. Keck Biomedical Mass Spectrometry Laboratory at the Univ. of Virginia), and Dr. Mark Conaway for guidance with statistical analyses. We also thank Dr. Dennis Templeton for suggesting the use of diamide as a thiol oxidant in these studies. We thank Adam Spencer for technical assistance, and Drs. Chelsi J. Snow and Chun-Song Yang for reading the manuscript.

This work was supported by National Institutes of Health award 1RO1AG040162 (to B.M. Paschal)

Chapter 3

Interplay between Heterochromatin and Ran GTPase System in Hutchinson-Gilford Progeria Syndrome (HGPS)

ABSTRACT

Hutchinson-Gilford Progeria Syndrome (HGPS) is a premature aging disease that is caused by the accumulation of a mutant form of lamin A, Progerin, in the nuclear lamina. This results in a number of phenotypic changes in the cells, including reduction in heterochromatin marks, which is predicted to alter gene expression at a large-scale. Progerin expression also disrupts the Ran gradient in cells, leading to nuclear transport defects. In this study, we find that loss of heterochromatin by treating the cells with BIX01294, a small-molecule inhibitor of histone methyltransferase G9a, alters the RanGTPase distribution in cells. Reduced nuclear levels and mRNA expression levels of histone methyltransferases (HMTases) in HGPS patient cells and Lopinavir-treated human fibroblasts, contribute, at least partially, to the Ran gradient disruption. Lopinavir causes constitutive attachment of prelamin A to the nuclear envelope. This suggests that constitutive attachment of Progerin is responsible for the downregulation of histone methyltransferases. The reduction in HMTase nuclear intensities in HGPS patient cells is rescued by treating with farnesyltransferase inhibitor, FTI-277. We also observed that the effects on the Ran gradient by Lopinavir treatment was more severe than that caused by knocking down histone methyltransferases. We further showed that Progerin expression resulted in nuclear import defect of histones H3 and H4, and also mislocalized their import receptor Importin 4. Therefore, we propose that loss of heterochromatin alone contributes partially to the disruption of Ran gradient in HGPS cells, and Progerin-induced nuclear import defect of histones H3 and H4 might further

amplify the effect on heterochromatin and chromatin organization in cells by a feedback loop leading to severe Ran gradient defect.

INTRODUCTION

Hutchinson-Gilford Progeria Syndrome (HGPS) is a premature aging disease, caused by a mutation in the lamin A gene (De Sandre-Giovannoli et al., 2003; Eriksson et al., 2003). HGPS is characterized by several symptoms similar to aging, including hair loss, delayed dentition, loss of subcutaneous fat, osteoporosis, muscular atrophy and arteriosclerosis (Gilford, 1897; Hutchinson, 1886). A Cytosine to Thymine (C > T) mutation in base 1824 of the lamin A gene (LMNA) introduces a cryptic splice site that results in the deletion of 50 amino acids near the C-terminus of lamin A. This deletion mutant is termed Progerin. Unlike lamin A, Progerin lacks a protease cleavage site and therefore, remains constitutively tethered to the inner nuclear membrane (Dechat et al., 2008; Eriksson et al., 2003).

HGPS patient fibroblasts exhibit several cellular phenotypes associated with the dominant-negative effect of Progerin attachment to the nuclear membrane, which include a misshapen nucleus and a reduction of heterochromatin marks in patient cells (Eriksson et al., 2003; Goldman et al., 2004; Scaffidi and Misteli, 2006; Shumaker et al., 2006). Loss of heterochromatin in HGPS cells has been demonstrated by the reduction in epigenetic marks, namely histone H3 Lys9 trimethylation (H3K9me³) and histone H3 Lys27 trimethylation (H3K27me³), and also reduced level of heterochromatin protein 1 (HP1) (Scaffidi and Misteli, 2006; Shumaker et al., 2006). The histone methyltransferase, EZH2, responsible for the methylation of H3 Lys27 is also downregulated in HGPS (Shumaker et al., 2006). The association of the

components of nuclear lamina with the peripheral heterochromatin and the role of lamins in transcription have led to the question whether or not the loss of heterochromatin is causal to the alterations of gene expression and other phenotypes in HGPS (Hutchison, 2002; Spann et al., 2002).

Our recent studies have identified several other phenotypes associated with HGPS, including alterations in RanGTPase distribution and Ran gradient-dependent nuclear import (Datta et al., 2014; Kelley et al., 2011; Snow et al., 2013). Ran is a small GTPase that shuttles rapidly between the nucleus and the cytoplasm (Görllich and Kutay, 1999; Ren et al., 1993). However, at a steady-state there is more nuclear Ran than its cytoplasmic counterpart (~3:1) (Kelley et al., 2011). We observed that Ran was mislocalized to the cytoplasm in HGPS patient fibroblasts (Kelley et al., 2011). These cells also exhibited altered localization of Ran gradient-dependent cargoes, such as TPR and Ubc9 (Datta et al., 2014; Kelley et al., 2011).

RCC1 is a chromatin-associated RanGEF and histones H2A and H2B stimulate the nucleotide-exchange activity of RCC1 (Ohtsubo et al., 1989) (Bischoff and Ponstingl, 1991; Nemergut et al., 2001). In yeast, the RCC1 homolog Prp20 shows binding preference for transcriptionally inactive genes, in other words, heterochromatin (Casolari et al., 2004). Epigenetic modification of histone H2B (H2BSer14 phosphorylation) has been shown to affect the interaction between RCC1 and chromatin in apoptotic cells causing reduction in the nuclear RanGTP level (Wong et al., 2008). We showed earlier that Progerin slowed down RCC1 mobility on chromatin (Kelley et al., 2011). RCC1 is required

for the Ran protein gradient (Ren et al., 1993). Based on these observations, we reasoned that the altered chromatin organization in HGPS cells might transduce its effects on Ran distribution via RCC1.

In the present study, we sought to determine a link between the loss of heterochromatin and Ran gradient disruption in HGPS cells. Using a histone methyltransferase inhibitor, BIX01294, which specifically targets G9a, we showed that loss of heterochromatin disrupted Ran distribution in cells. The nuclear intensities of histone methyltransferases- G9a, GLP1 and EZH2, were significantly reduced in HGPS patient cells. Treatment of patient cells with farnesyltransferase inhibitor, FTI-277, reversed these phenotypes. Along with EZH2, the mRNA level of Suv39HI was also reduced in response to Lopinavir treatment. However, G9a and GLP1 mRNA levels did not change. Knocking down four of the histone methyltransferases – G9a, GLP1, Suv39HI and EZH2, slightly disrupted the Ran gradient in HeLa cells. However, the degree of disruption was much less severe compared to that in Progerin-expressing cells or Lopinavir-treated cells observed earlier. Our data suggest that although loss of heterochromatin is sufficient to alter Ran distribution in cells, its effects alone are not robust enough to cause age-related Ran gradient disruption and nuclear transport defects observed in Progeria. Therefore, lamin A mutation in Progeria is likely to employ multiple mechanisms, including loss of heterochromatin, to transduce its effects on the Ran system in cells.

RESULTS

Loss of H3K9-methylation disrupts the Ran distribution

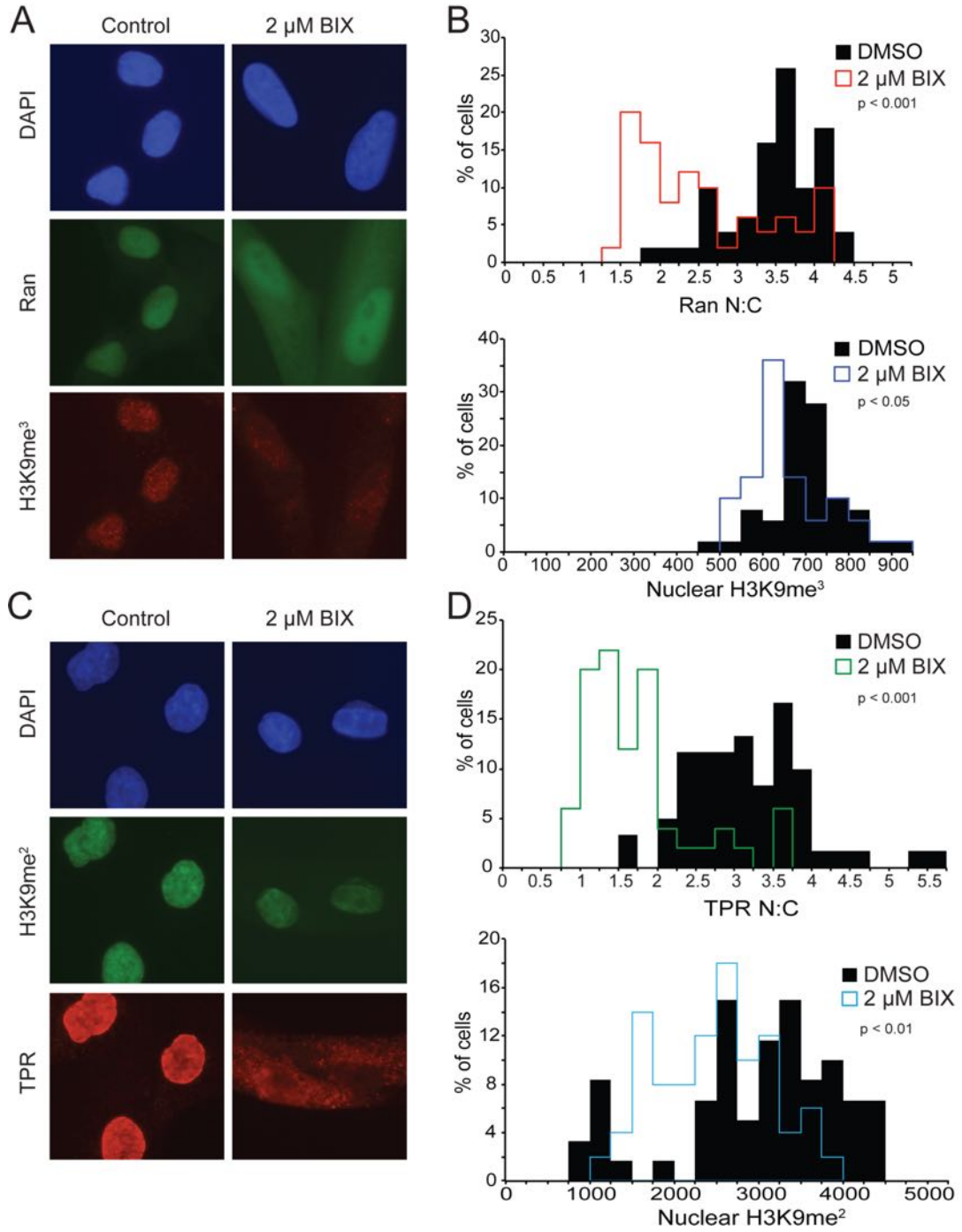
Loss of heterochromatin and disruption of Ran gradient are characteristic features of HGPS patient cells (Kelley et al., 2011; Scaffidi and Misteli, 2006; Shumaker et al., 2006). The defects in the chromatin organization are thought to be one of the early events in Progeria, due to its proximity and physical association with the nuclear lamina (Dechat et al., 2009; Stierlé et al., 2003). In order to determine how loss of heterochromatin might affect Ran distribution in cells, we treated human fibroblasts with BIX01294, an inhibitor of a histone methyltransferase, G9a (Kubicek et al., 2007), and examined the effects of loss of heterochromatin on Ran distribution by indirect immunofluorescence. G9a di- and tri-methylates the Lys9 residue of histone H3 (Tachibana et al., 2002; 2005). Successful inhibition of G9a was reflected by the reduction in histone H3 di- and tri-methylation (H3K9me² and H3K9me³) (Fig. 3.1 A-D). Reduction in heterochromatin modification due to G9a inhibition also altered the Ran distribution moderately, but significantly in cells, where increased Ran intensity was observed in the cytoplasm compared to the control, significantly decreasing Ran nuclear:cytoplasmic (Ran N:C) ratio ($p < 0.001$) (Fig. 3.1 A & B). Distribution of TPR, a Ran-dependent cargo, also changed due to the loss of heterochromatin in cells (Fig. 3.1 C & D). TPR normally exhibits a characteristic nuclear rim staining in addition to a nucleoplasmic staining. In response to the loss of heterochromatin, TPR was found to form aggregates in the cytoplasm along with its disappearance from the nuclear rim and reduction in nucleoplasmic

staining. Our data suggest that loss of heterochromatin, which is thought to be an early event in Progeria, might be responsible, at least partly, for the disruption of Ran gradient and Ran-dependent nuclear transport.

Fig. 3.1: Reduction in heterochromatin modification disrupts Ran distribution and causes TPR mislocalization in human primary fibroblasts.

A. Ran protein distribution and histone H3 Lys9 tri-methylation (H3K9me³) in control and BIX01294-treated cells. B. Histograms showing Ran N:C (top panel) and nuclear H3K9me³ fluorescence intensity (bottom panel) in control and BIX-treated cells. C. TPR localization and histone H3 Lys9 di-methylation (H3K9me²) in control and BIX01294-treated cells. D. Histograms showing TPR N:C (top panel) and nuclear H3K9me² fluorescence intensity (bottom panel) in control and BIX-treated cells.

Fig. 3.1

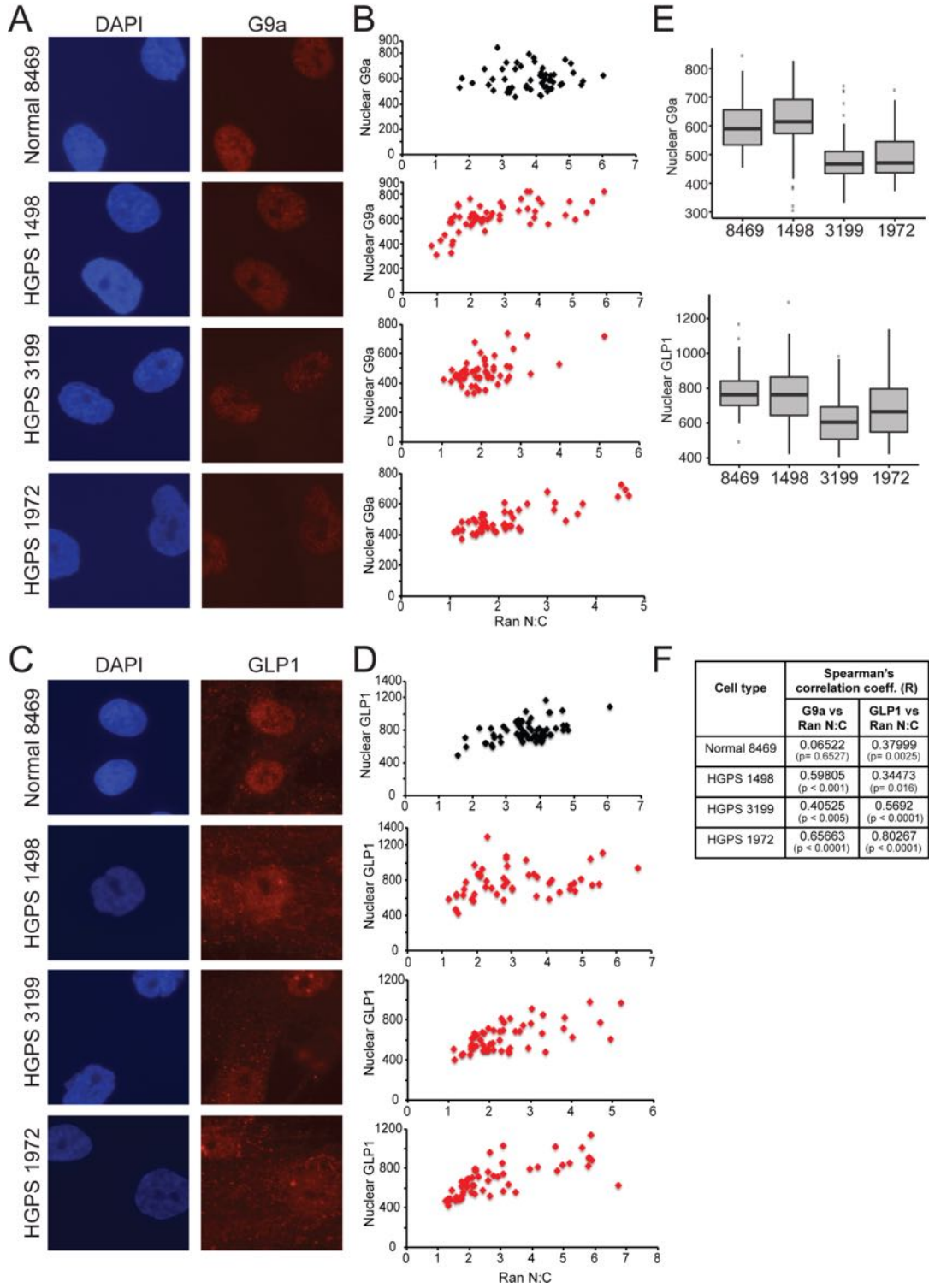


Nuclear levels of histone methyltransferases (HMTases) are reduced in Progeria

We also examined the expression level of several HMTases in HGPS patient cells. It has been previously reported that the expression level of histone methyltransferase EZH2, responsible for trimethylation of histone H3 Lys27 (H3K27me³), is significantly reduced in HGPS (Shumaker et al., 2006). We found that at least in two different HGPS patient cell lines, in addition to EZH2 the nuclear intensities of two other HMTases, namely G9a and GLP1, are significantly reduced ($p < 0.001$) (Fig. 3.2 A & C; Fig. 3.2 E). Less abundance of these methyltransferases in the primary cells makes it difficult for detection by Western blot. Both G9a and GLP1 are known to methylate histone H3 Lys9 residue (Shinkai and Tachibana, 2011; Tachibana et al., 2002; 2005). We have previously shown that Ran N:C ratios in normal and HGPS cells correlated with histone mark H3K9me³ and HP1 γ levels (Kelley et al., 2011). Here we show that Ran N:C ratio correlated with the nuclear levels of both G9a and GLP1 (Fig. 3.2 B & D). The Spearman's rank correlation coefficients are shown in Fig. 3.2 F. This data further confirmed that the epigenetic state of chromatin is linked to the Ran system in HGPS cells, where the downregulation of the HMTases might affect the Ran distribution or the disruption of Ran gradient dependent transport of HMTases might alter the epigenetic state or a combination thereof.

Fig. 3.2: Nuclear intensity of G9a and GLP1 are significantly reduced in HGPS patient cells. A. G9a localization in normal (8469) and three of the patient (1498, 3199 & 1972) fibroblasts. B. Ran N:C is plotted as a function of nuclear G9a levels. The Spearman's correlation coefficients (R) are recorded in Fig. F. C. GLP1 localization in normal (8469) and three of the patient (1498, 3199 & 1972) fibroblasts. D. Ran N:C is plotted as a function of nuclear GLP1 levels. The Spearman's correlation coefficients (R) are recorded in Fig. F. E. Box plot showing the nuclear levels of G9a and GLP1 in normal and HGPS patient cells. F. Table showing Spearman's correlation coefficients (R) and p-values.

Fig. 3.2



Constitutive membrane attachment of lamin A is sufficient for downregulation of the HMTases

Lamin A is synthesized as Prelamin A that undergoes several post-translational modifications, for example, farnesylation and carboxymethylation, near its C-terminal end (Dechat et al., 2008). The farnesylated form remains attached to the inner nuclear membrane. Finally, it is cleaved by a protease, Zmpste24, followed by the release of the mature lamin A. The mutant form of lamin A, Progerin, lacks the protease-cleavage site due to the 50 amino acid deletion near its C-terminal end (Eriksson et al., 2003). Hence, it remains constitutively attached to the nuclear membrane.

Here, we treated normal human fibroblasts with a protease inhibitor, Lopinavir (LPV), and examined the nuclear levels of the HMTases – G9a, GLP1 and EZH2. LPV inhibits Zmpste24, leading to the constitutive attachment of Prelamin A to the nuclear membrane (Coffinier et al., 2007), giving rise to the similar conditions as HGPS. We showed that LPV treatment resulted in a significant reduction in the nuclear level of the HMTases tested (Fig. 3.3 A & B). The mRNA levels of EZH2 and Suv39HI also reduced in response to LPV treatment ($p\text{-value} \leq 0.05$) (Fig. 3.3 C), without much effect on the mRNA levels of G9a and GLP1.

Farnesyltransferase inhibitor, FTI-277 or Lonafarnib, which prevents farnesylation of Progerin, has been successfully used in the clinical trial of HGPS (Gordon et al., 2012). This drug has also been shown to reverse several cellular phenotypes associated with Progeria, including Ran gradient, TPR

mislocalization and H3K9 tri-methylation (Kelley et al., 2011). In this study, treating the HGPS patient cells with FTI-277 rescued the reduced nuclear level of histone methyltransferases, G9a and GLP1 (Fig. 3.4 A & B). This further confirms that constitutive membrane attachment of Progerin drives the changes in the expression level and localization of the histone methyltransferases. However, we cannot distinguish between localization and expression of the proteins by immunofluorescence, and the protein levels in these cells were not readily detected by Western blot.

Fig. 3.3: Histone methyltransferases are downregulated in Lopinavir-treated human fibroblasts. A. G9a, GLP1 and EZH2 localization in control and Lopinavir (40 μ M, 2 days)-treated cells. B. Histograms showing nuclear levels of G9a, GLP1 and EZH2 in control and Lopinavir-treated cells. C. mRNA expression levels of G9a, GLP1, Suv39H1 and EZH2 in control and Lopinavir-treated cells.

Fig. 3.3

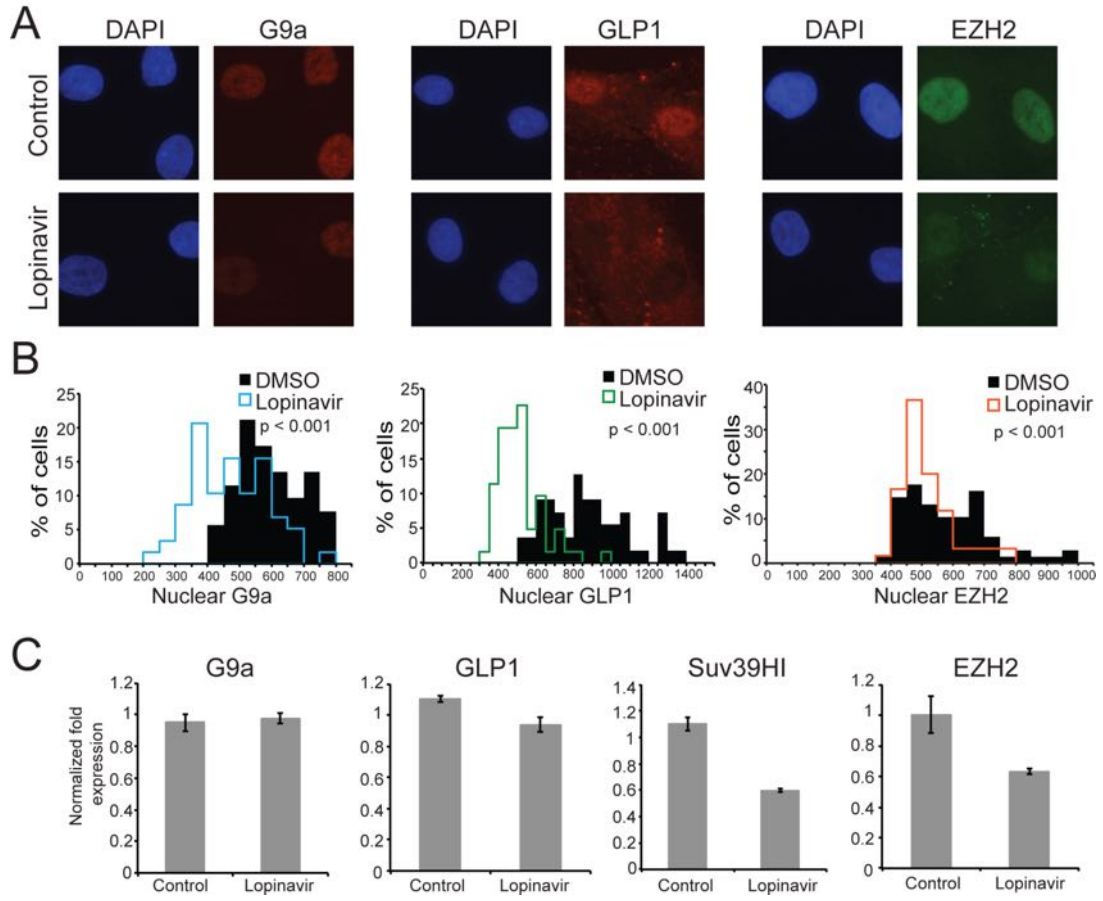
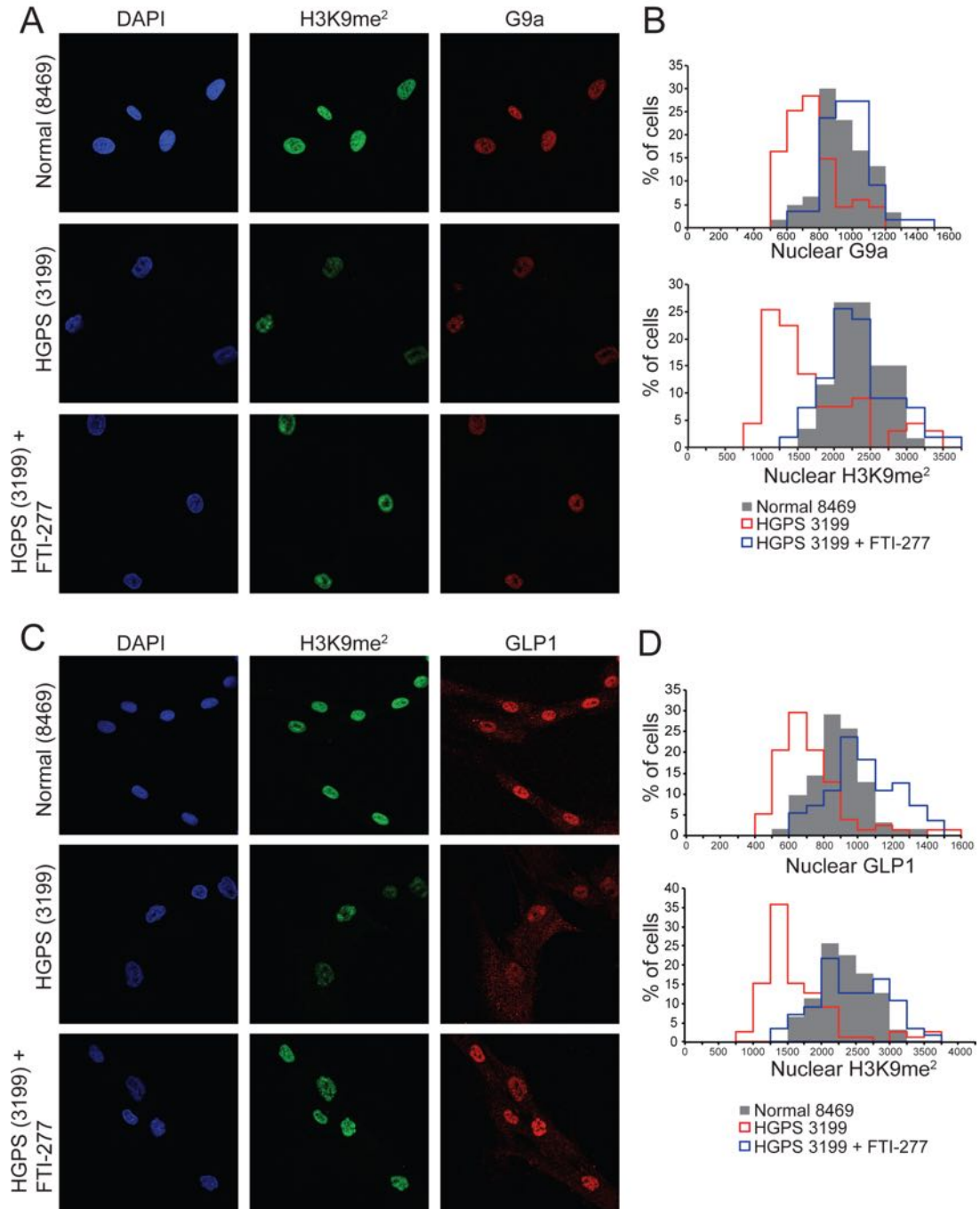


Fig. 3.4: Downregulation of histone methyltransferases is rescued by FTI-277 treatment of HGPS patient cells. A. Localization of H3K9me² (green) and G9a (red) in normal (8469), HGPS patient (3199) fibroblasts, and 3199 treated with FTI-277 (3 μM for 4 days). B. Histograms showing nuclear G9a and H3K9me² intensities in normal (8469) (grey bars), HGPS patient (3199) fibroblasts (red lines), and 3199 treated with FTI-277 (blue lines). C. Localization of H3K9me² (green) and GLP1 (red) in normal (8469), HGPS patient (3199) fibroblasts, and 3199 treated with FTI-277. D. Histograms showing nuclear GLP1 and H3K9me² intensities in normal (8469) (grey bars), HGPS patient (3199) fibroblasts (red lines), and 3199 treated with FTI-277 (blue lines).

Fig. 3.4

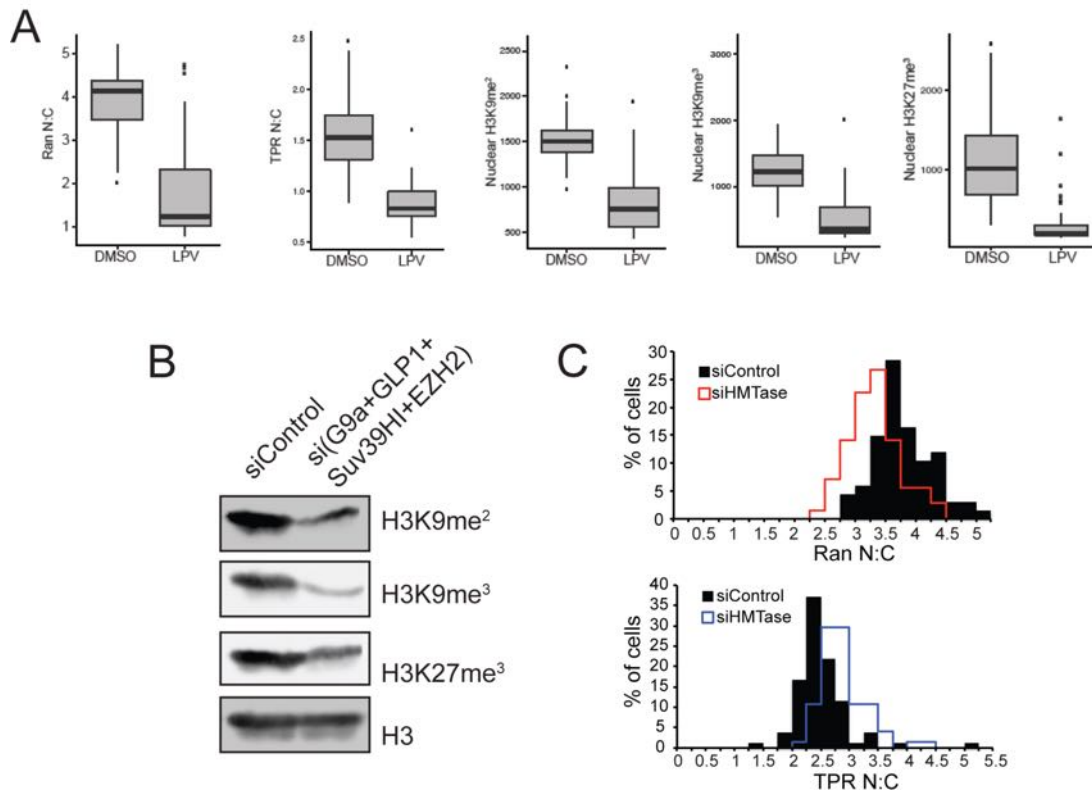


Loss of heterochromatin partially contributes to the Ran gradient disruption

Next, we went on to compare the extent of Ran gradient disruption by affecting the heterochromatin alone and that caused by constitutive attachment of Prelamin A by Lopinavir treatment. Although reduced methylation of histone H3 alters the Ran distribution in cells, as shown in Fig. 3.1, its effects on the Ran system is not as robust as seen in Progerin-expressing cells or Lopinavir-treated cells. We treated human fibroblasts with 40 μ M Lopinavir for 3 days, and by immunofluorescence we observed that there was a two- to three-fold difference in the nuclear : cytoplasmic ratio of Ran and TPR (Ran N:C and TPR N:C) in addition to significant reduction in heterochromatin marks (H3K9me², H3K9me³ and H3K27me³) ($p < 0.001$) (Fig. 3.5 A). However, knocking down four of the histone methyltransferases (HMTases)- G9a, GLP1, Suv39HI and EZH2, in HeLa cells only had a modest effect on the Ran N:C ratio, which was not enough to cause TPR mislocalization (Fig. 3.5 C), despite a decrease in the heterochromatin marks (Fig. 3.5 B). This posits that Progerin-induced loss of heterochromatin might be one of the factors that results in Ran gradient disruption, but Progerin expression involves other mechanisms as well to transduce its effects on the Ran system.

Fig. 3.5: Loss of heterochromatin-induced Ran gradient disruption is much less severe compared to that caused by constitutive attachment of Prelamin A. A. Box plots showing Ran N:C, TPR N:C, and nuclear intensities of H3K9me², H3K9me³ and H3K27me³ in control (DMSO) and Lopinavir (LPV)-treated human fibroblasts. B. Western blot showing the levels of heterochromatin marks (H3K9me², H3K9me³ and H3K27me³) and total histone H3 in control and histone methyltransferase (HMTase-G9a, GLP1, Suv39HI & EZH2) knock-down HeLa cells. C. Histograms showing Ran N:C and TPR N:C in control and HMTase-knock down HeLa cells.

Fig. 3.5



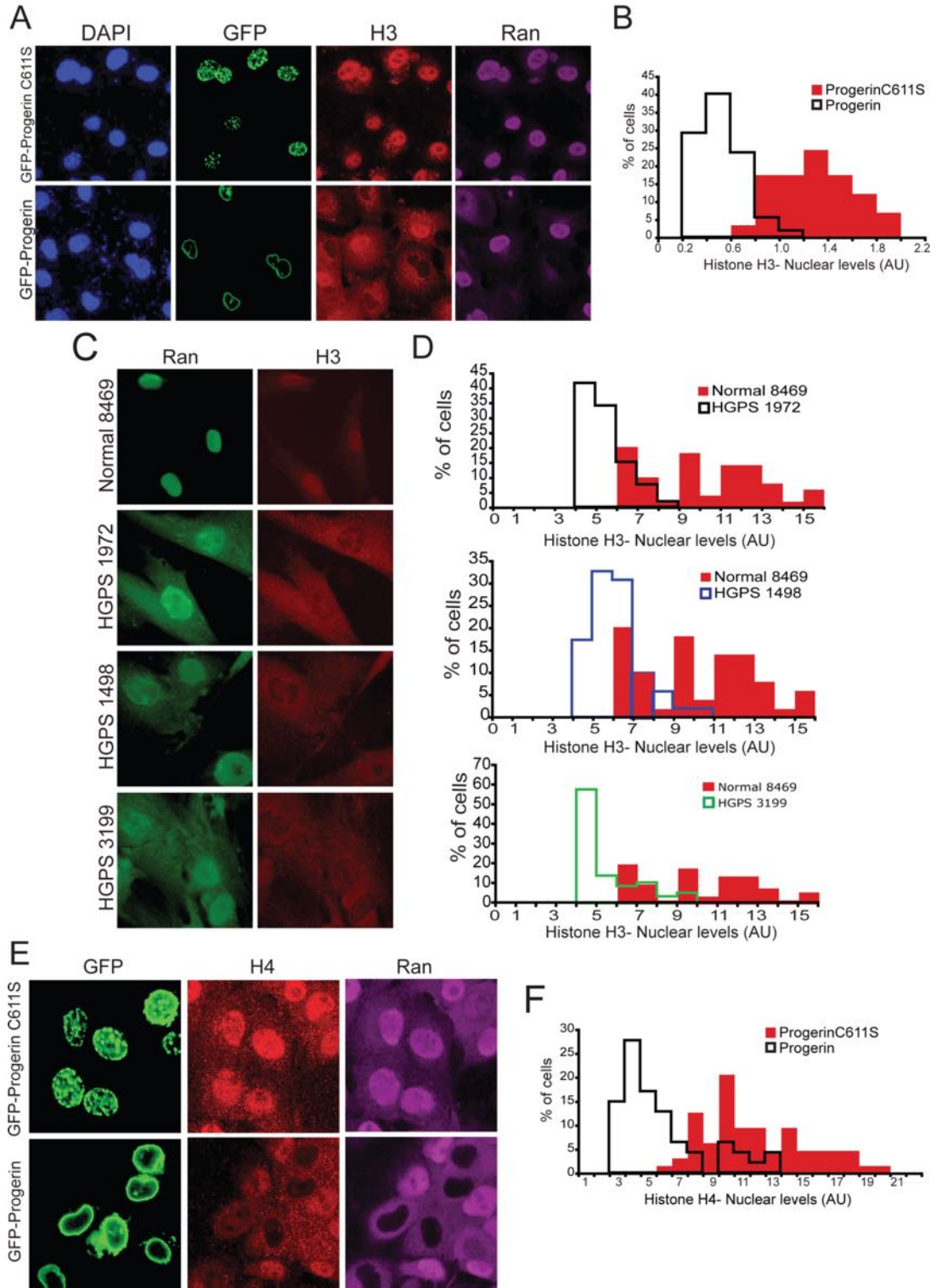
Progerin expression causes import defect of histones H3 and H4

To assess any contribution of the histones towards the alterations in chromatin organization in HGPS, we examined the nuclear level of histone H3 in HGPS patient fibroblasts. In three of the patient cell lines tested, the nuclear intensity of histone H3 was significantly reduced (Fig. 3.6 A & B). Confocal imaging of a very thin slice of the nucleus might cause it to appear as a complete loss of histone H3 from the nucleus, but in reality, we think that there is still enough histone H3 left in the nucleus for the viability of the cells despite its significant reduction.

Histones H3 and H4 are imported into the nucleus as a dimer (Keck and Pemberton, 2012). Therefore, we looked at the localization of both histones H3 and H4 in Progerin-transfected HeLa cells. Since Progerin remains constitutively farnesylated and attached to the nuclear membrane (Eriksson et al., 2003), we used a farnesylation-deficient mutant of Progerin (Progerin C611S) as the control. In contrast to the Progerin C611S- transfected COS cells, Progerin expression significantly reduced nuclear localization of both histones H3 and H4 (Fig. 3.6 C-F). This suggests that the constitutive membrane attachment of Progerin is responsible for the reduction in the nuclear localization of histones H3 and H4.

Fig. 3.6: Histones H3 and H4 import defect in presence of Progerin. A. Levels of histone H3 in COS cells transfected with Cys mutant of Progerin (control) and Progerin. B. Histograms of nuclear levels of histone H3 in presence of Progerin C611S (red bars) and Progerin (black lines). C. Ran distribution and histone H3 levels in normal (8469) and HGPS patient (1972, 1498 & 3199) cells. D. Histograms of nuclear levels of histone H3 in normal (8469, red bars) and HGPS patient (1972, black lines; 1498, purple lines; 3199, green lines) cells. E. Ran distribution and histone H4 levels in COS cells transfected with Cys mutant of Progerin and Progerin. F. Histograms of nuclear levels of histone H4 in COS cells in presence of ProgerinC611S (red bars) or Progerin (black lines).

Fig. 3.6



Imp4, the import receptor of H3-H4 dimer is mislocalized in presence of Progerin

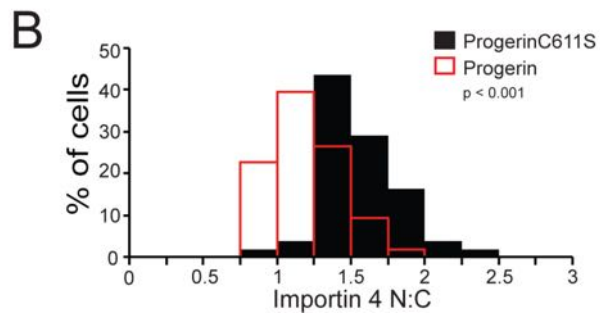
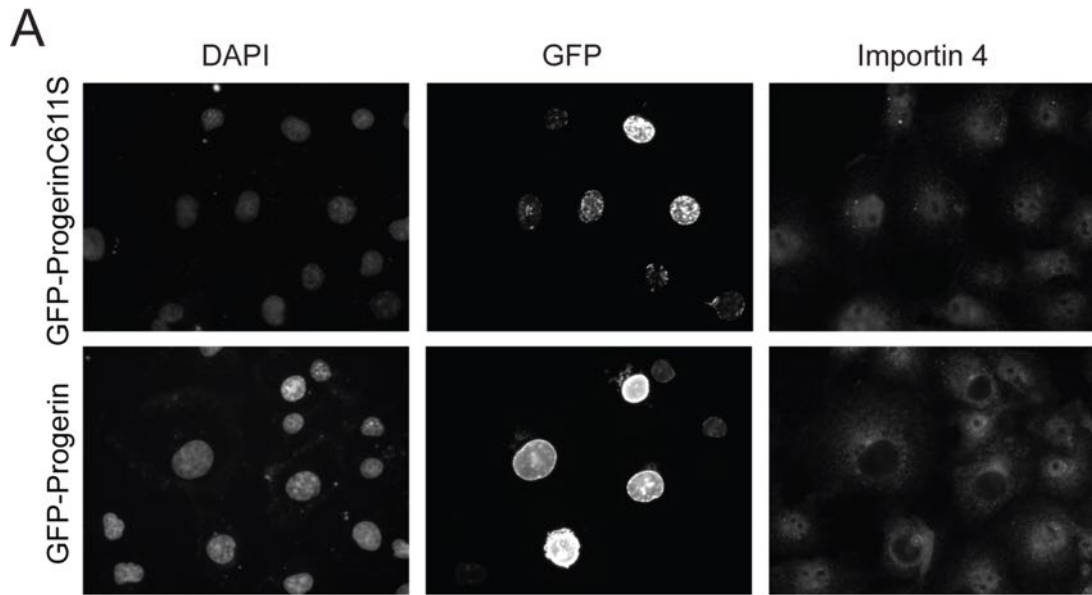
Newly-synthesized histones are incorporated in chromatin mainly during S-phase, when the cells double its chromatin content (Keck and Pemberton, 2012). Histones are below the diffusion limit of nuclear pore complexes. However, as soon as the histones are synthesized in the cytoplasm, several chaperones shield their positive charges to prevent non-specific interactions with DNA or other interacting partners and also to facilitate their transport into the nucleus (Elsässer and D'Arcy, 2012). Hence, histones are actively transported in the nucleus as part of a large transport complex, the size of which exceeds the ~40 kDa diffusion limit. The nuclear import of histones is a cell cycle-regulated process to ensure their efficient deposition on the newly replicated DNA. The incorporation of the newly synthesized histones to form nucleosomes occurs in a two-step process (Annunziato, 2012; Nakagawa et al., 2001; Smith and Stillman, 1991). H3-H4 dimer is deposited first on the DNA, followed by H2A-H2B. Therefore, lack of H3-H4 deposition on DNA might affect the incorporation of H2A-H2B as well, perturbing the chromatin assembly and organization.

Most histone chaperones have preference for binding to either H2A-H2B or H3-H4, with some exceptions where some chaperones bind both H2A-H2B and H3-H4 dimers. It has been shown in both yeast and mammalian cells that histones H3 and H4 together are transported into the nucleus with the help of the import receptor Importin 4 (Campos et al., 2010; Mosammaparast et al., 2002). Therefore, significant reduction in the nuclear pool of histone H3 and H4 led us to test the localization of Importin 4 (Imp4) in presence of Progerin in COS cells.

Imp4 localized mainly in the nucleus of the control cells, whereas Progerin expression resulted in its nuclear exclusion, and the mislocalization of Imp4 in presence of Progerin was significant ($p < 0.001$) (Fig. 3.7 A & B). This suggests that the nuclear exclusion of Imp4 in Progeria might affect the transport of newly synthesized histones H3 and H4 into the nucleus, which, in turn, affect the chromatin organization in cells. Together they indicate that there might be a feedback from the disrupted histone import in HGPS to the loss of chromatin organization.

Fig. 3.7: Importin 4, the import receptor of histones H3 and H4 is mislocalized in presence of Progerin. A. Localization of Importin 4 in presence of Cys mutant of Progerin (Progerin C611S) and Progerin in COS cells. B. Histograms showing the nuclear to cytoplasmic ratio of Importin 4 in presence of Progerin C611S (black bars) and Progerin (red lines) in COS cells.

Fig. 3.7



DISCUSSION

This study documents the role of heterochromatin in regulating the Ran gradient in cells. In two separate studies, it was elucidated that the Progeria patient cells show a decrease in the heterochromatin marks (Scaffidi and Misteli, 2006; Shumaker et al., 2006). These patient cells also exhibit disruption of Ran gradient-dependent nuclear transport (Datta et al., 2014; Kelley et al., 2011; Snow et al., 2013). Not only the Ran distribution is altered due to Progerin expression, it also resulted in the mislocalization of Ran-dependent cargoes, namely, TPR and Ubc9. Here, we showed that the reduction in heterochromatin marks in cells was directly responsible for the disruption of RanGTPase distribution, and also caused mislocalization of TPR (Fig. 3.1). This work also showed that the nuclear intensities of histone methyltransferases (HMTases), such as G9a and GLP1 are significantly reduced in Progeria cells (Fig. 3.2). This reduction can be attributed to the constitutive nuclear membrane attachment of Progerin, as depicted in Lopinavir-treated human fibroblasts (Fig. 3.3 A & B). In support of previously published data, our study also showed marked downregulation in the mRNA level of at least two of HMTases tested, namely EZH2 and Suv39HI (Fig. 3.3 C). Together, they suggest that the depletion of the HMTases in the nucleus might cause disruption of Ran distribution.

Progerin-induced loss of heterochromatin ensuing gene expression changes is thought as an early event in Progeria that leads to a series of alterations in the cellular phenotypes. However, our data indicates that the degree of Ran gradient disruption by altering the heterochromatin alone was not

severe enough that the changes in cellular phenotypes could be attributed to the loss of heterochromatin. Moreover, knocking-down histone methyltransferases, G9a, GLP1, Suv39HI and EZH2, in HeLa cells yielded a modest change in the Ran distribution without any significant alteration in TPR localization. In the study published by Scaffidi & Misteli, HGPS patient cells exhibited a 3-fold decrease in the nuclear level of H3K9 trimethylation (H3K9me³) (Scaffidi and Misteli, 2006). Frequency of H3K27me³-positive HGPS cells was found to be significantly lower than the control cells (only 36%, compared to 80% of the control cells) in late passage (Shumaker et al., 2006). With this level of reduction in heterochromatin marks, the nuclear : cytoplasmic ratio of Ran usually equals 1 or less than 1 (Ran N:C = 1 or <1) with a significant increase in the cytoplasmic intensity of Ran and very little Ran left in the nucleus (Kelley et al., 2011). In both BIX-treated human fibroblasts and HMTase-knock down HeLa cells, Ran N:C ratio always remained above 1 despite being significantly reduced compared to the control cells. Therefore, the effect of Progerin expression on the Ran gradient seems much more severe than that observed by affecting the heterochromatin alone (Fig. 3.8 Model 1). This led us to believe that loss of heterochromatin might be one of the several mechanisms by which Progerin executes its effect on the Ran gradient.

Our data do not explain any mechanism of Ran gradient disruption in response to the loss of heterochromatin. However, we speculate that RCC1 activity might be inhibited by the global alterations in heterochromatin landscape in Progeria, because RCC1 has been shown to preferentially bind heterochromatin in yeast (Casolari et al., 2004). And also, Progerin expression in

cells reduced RCC1 mobility on chromatin (Kelley et al., 2011). Posttranslational modifications of histones also influence the interaction between RCC1 and chromatin, as shown in apoptotic cells, where H2BSer14 phosphorylation immobilized RCC1 on chromatin, which, in turn, reduced RanGTP level in the nucleus (Wong et al., 2008). Therefore, it is reasonable to conjecture that the loss of heterochromatin in Progeria might transduce its effects on RanGTPase via its chromatin-binding guanine nucleotide exchange factor, RCC1.

Along with its role in nucleocytoplasmic transport, spindle assembly and nuclear envelope assembly in cells, the Ran system has been implicated in the regulation of the heterochromatin organization of telomere and telomere silencing. The first evidence suggesting any role of the Ran system in chromatin organization came from the observation that mutation in RCC1 caused premature chromosome condensation in hamster tsBN2 cells (Uchida et al., 1990). Since then significant work has been done to find out the mechanism of regulation of heterochromatin assembly and telomere silencing by different components of the Ran system that occur in a nucleocytoplasmic transport-independent manner. Both Ran and RCC1 overexpression have been shown to cause severe derepression of telomere in yeast (Clément et al., 2006). Ran affected telomeric function through Sir4 protein, a crucial factor in telomere organization. Overexpression of Mog1, which has been found to release GTP from Ran and bind nucleotide-free Ran, caused loss of telomere silencing (Clément et al., 2006; Steggerda and Paschal, 2000). Later, Hayashi et al. showed that RanGAP promotes telomere silencing in a Sir3-dependent manner

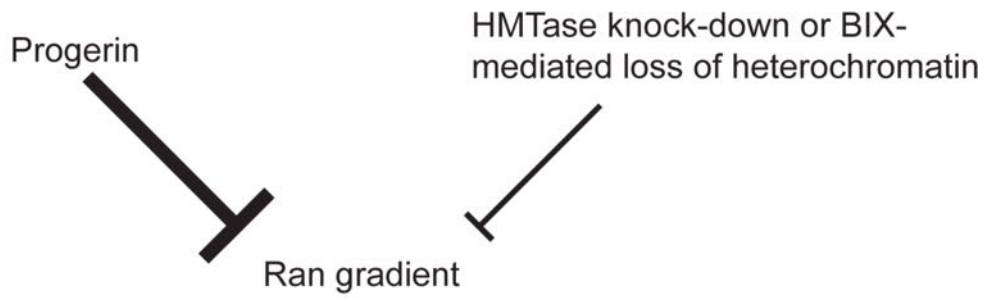
(Hayashi et al., 2007)(Hayashi et al, 2005). Furthermore, RanGAP mutant phenotypes in fission yeast are suppressed by the overexpression of chromatin remodeling factor Snf2 homolog (Kusano et al., 2004), which suggests that RanGAP regulates telomere silencing via the Swi/Snf complex, important for this process (Dror and Winston, 2004; Nishijima, 2006).

Although considerable effort has been made in determining a mechanism of regulating telomere silencing by the Ran system, any direct link between the loss of heterochromatin in Progeria and Ran gradient disruption was yet to be shown. Here, in this study we showed for the first time that the loss of heterochromatin disrupted the Ran distribution and mislocalized TPR. This implies that in this pathway chromatin organization lies upstream of Ran gradient in cells (Fig. 3.8 Model 2). And we think, unlike telomere silencing, the link between the loss of heterochromatin and Ran gradient disruption in Progeria is not completely independent of Ran-dependent nuclear transport. We also showed here that Progerin expression resulted in the disruption of the nuclear import of histones H3 and H4, that might send a feedback and amplify the effect on heterochromatin in HGPS, which, in turn, results in severe Ran gradient disruption. Therefore, we conclude that the lack of heterochromatin in HGPS might be a combined effect of the downregulation of the histone methyltransferases and disruption of histone import in cells, which eventually contributes to the changes in Ran system.

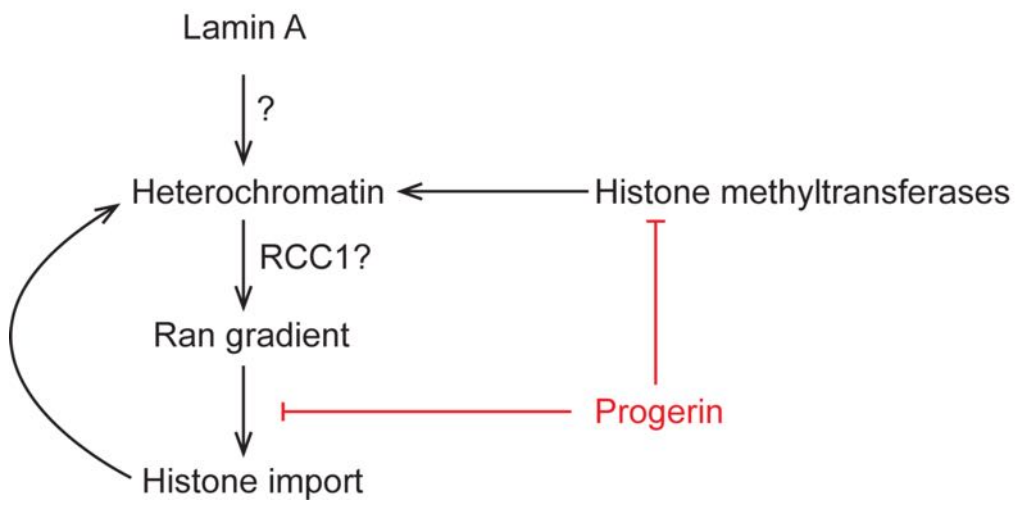
Fig. 3.8: Model 1. Effect of Progerin on Ran gradient is more severe than that observed by loss of heterochromatin alone.

Model 2. Model showing how Progerin-induced loss of heterochromatin affects Ran gradient. Progerin expression downregulates histone methyltransferases leading to loss of heterochromatin and affects chromatin organization that partially contributes to Ran gradient disruption and histone import defect in Progeria. Disruption of histone import might also amplify the effect on chromatin organization. Moreover, Progerin expression is likely to involve multiple mechanisms to transduce its effect on Ran gradient.

Model 1



Model 2



MATERIALS & METHODS

Cell culture and drug treatment

HeLa and COS-7 cells were grown at 37°C in 5% CO₂ in Dulbecco's modified Eagle's medium (DMEM) (Gibco/Invitrogen, Carlsbad, CA) containing 10% fetal bovine serum (Atlanta Biologicals, Lawrenceville, GA). Human fibroblasts were grown at 37°C in 5% CO₂ in minimum essential media (MEM) (Gibco/Invitrogen, Carlsbad, CA) containing 15% fetal bovine serum (HyClone), 1% L-glutamine (Gibco/Invitrogen), 1% MEM vitamin solution (HyClone) and 1% antibiotic- Penicillin/Streptomycin (Gibco/Invitrogen). Human fibroblasts were treated with 40 μM Lopinavir (Selleck Chemicals, Catalog No. S1380) for 2-3 days at 37°C, with 2 μM BIX01294 (Sigma-Aldrich, B9311) for 2days at 37°C, and with 3 μM FTI-277 (Sigma-Aldrich, F9803) for 4 days at 37°C.

Plasmids and siRNAs

pEGFP-Progerin was constructed by standard cloning procedure where Progerin coding sequence was amplified by PCR and inserted in the pEGFP cloning vector. A point mutation was introduced to pEGFP-Progerin to generate pEGFP-Progerin C611S by QuikChange II site directed mutagenesis (Agilent-Stratgene, La Jolla, CA). Cys611 site of Progerin is the farnesylation site, mutating which resulted in inhibition of its attachment to the nuclear envelope and abrogated its effects on the Ran system. That is why C611S mutant of Progerin has been used as a control for any non-specific effects of Progerin overexpression.

Small interfering RNAs (siRNAs) for G9a, GLP1, Suv39HI and EZH2 were obtained from Invitrogen (Carlsbad, CA). The siRNA sequences are as follows:

G9a (sense 5'-CCAUGAACAUUCGACCGCAA-3', and antisense 5'-UUGCGGUCGAUGUUCAUGG-3'); GLP1 (sense 5'-AGCUCAUACUUGACCACGC-3', and antisense 5'-GCGUGGUCAAGUAUGAGCU-3'); Suv39HI (sense 5'-ACCUCUUUGACCUGGACUA-3', and antisense 5'-UAGUCCAGGUCAAAGAGGU-3') and EZH2 (sense 5'-AAGACUCUGAAUGCAGUUGCU-3', and antisense 5'-AGCAACUGCAUUCAGAGUCUU-3').

Transfection and knock-down

24 hours after plating COS cells, they were transfected with pEGFP-Progerin C611S and pEGFP-Progerin using transfection reagent Fugene 6 (Promega) following the manufacturer's guide. 24 hours post-transfection, the cells were harvested and fixed for immunofluorescence.

HeLa cells were plated and after 24 hours they were transfected with control (20 nM) and four siRNAs (5 nM each) using Lipofectamine RNAiMax (Invitrogen) following manufacturer's instruction (reverse transfection protocol). 4 days after transfection they were fixed for immunofluorescence experiment.

RT-PCR

The forward and reverse primers for RT-PCR are as follows:

G9a (5'-GAGGTCACCTTTCCCAGTGA-3' and 5'-
CCAAACCAGGAAATGGACAG-3'); GLP1 (5'-TTGTCTGCGAGTATGTTGGG-3'
and 5'-GATGCAGTAAACCTCCCCG-3'); Suv39HI (5'-
CTGACGGTCGTAGATCTGCC-3' and 5'-ATTCGCAAGAACAGCTTCGT-3');
EZH2 (5'-GAGACTGGCGAAGAGCTGTTT-3' and 5'-
GGCATCAGCCTGGCTGTATC-3').

RT-PCR was performed using standard methods. Biological duplicates were included in the experiment. Error bars shown are the standard deviation of triplicate wells.

IF and microscopy

IF microscopy was performed using standard methods as previously described (Kelley et al., 2011). Cells were grown on glass coverslips, washed with PBS, and fixed for 20 min with 3.75% formaldehyde, followed by permeabilization in 0.2% Triton X-100 for 5 min. Cells were blocked for 1 hr in blocking buffer (2% FBS and 2% BSA in PBS). Primary antibody was diluted in blocking buffer, and incubation was performed for 2 hrs at room temperature or overnight at 4°C. The primary antibodies used for IF were Ran mAb (catalog number 610341; BD), rabbit polyclonal TPR antibody (Snow et al, 2013), rabbit polyclonal histone H3 (tri-methyl K9) antibody (abcam, ab8898), mouse monoclonal histone H3 (di-methyl K9) antibody (abcam, ab1220), rabbit polyclonal G9a (Cell Signaling Technology, #3306), rabbit polyclonal GLP1/EHMT1 (Millipore, Cat# 09-078), mouse monoclonal EZH2 (Cell Signaling

Technology, #3147), rabbit polyclonal histone H3 (Activ Motif, 39163), rabbit polyclonal histone H4 (Activ Motif, 39212), and rabbit polyclonal Importin 4 (abcam, ab28387). Secondary antibodies were diluted in blocking buffer, and incubation was performed at room temperature for 1 hr. Secondary antibodies used were FITC-labeled donkey anti-mouse, Cy3-labeled donkey anti-rabbit and far red-labeled donkey anti-mouse IgG (Jackson ImmunoResearch Laboratories, Inc.). Slides were mounted for imaging.

Images were acquired using wide-field and confocal microscopes. Most of the fixed-cell imaging was performed using an upright microscope (Eclipse E800; Nikon) using a 40x, 1.0 NA oil immersion objective and were captured with a charge-coupled device camera (C4742-95; Hamamatsu Photonics) with OpenLab software (PerkinElmer). The images of Fig. 3.6 A & E were acquired on a microscope (LSM 700; Carl Zeiss) equipped with a 40x, 1.3 NA oil immersion objective and ZEN software (Carl Zeiss). All imaging was performed at room temperature (~24°C).

Quantitative analysis of IF images (ratios of the nuclear intensity to the cytoplasmic intensity, N:C ratios of Ran and TPR) were measured as described previously (Kelley and Paschal, 2007; Kelley et al., 2011) using ImageJ (National Institutes of Health). Both nuclear and cytoplasmic regions of each cell were selected, and the mean IF was determined by ImageJ software. n:c ratios = (mean fluorescence of nucleus)/(mean fluorescence of cytoplasm). For heterochromatin marks, HMTases and histones, only the nuclear intensities were measured. All histograms were made and statistical tests (Student's t test) were

performed using Microsoft Excel. All IF images shown were processed in Photoshop (Adobe). Adjustments to brightness and contrast were performed using the levels function and images of all conditions in an experiment were treated equally.

Immunoblotting

SDS-PAGE and immunoblotting were performed by standard methods. The primary antibodies used for immunoblotting were a rabbit polyclonal histone H3 (tri-methyl K9) antibody (abcam, ab8898), mouse monoclonal histone H3 (di-methyl K9) antibody (abcam, ab1220), rabbit polyclonal histone H3 (tri-methyl K27) antibody (Millipore, Cat # 07-449) and mouse monoclonal histone H3 (abcam, ab10799). The IR dye-conjugated secondary antibodies- Alexa Fluor 800-conjugated donkey anti-mouse IgG and Alexa Fluor 680-conjugated donkey anti-rabbit IgG, were used and the Odyssey system was used for detection and analysis.

Chapter 4

Discussion and Future Directions

Significance

Ever since the discovery of lamin A mutation causing Hutchinson-Gilford Progeria Syndrome (HGPS), most of the studies focused on the downstream effects of the mutation in cells. The observations ranged from alterations in the nuclear morphology to chromatin organization and gene expression, mainly affecting vascular smooth muscle cells, adipocytes and osteocytes at the tissue level. A pathway describing how mutated lamin A yields such a diverse phenotype is still obscure. Although there are gene expression changes in Progeria cells, what causes these changes are not known. Our data suggest that disruption of the nuclear transport might be an early event in Progeria, which might even affect the nuclear transport of transcription factors leading to the changes in gene expression. We showed that Ran gradient and Ran gradient-dependent nuclear transport are disrupted in HGPS cells (Kelley et al., 2011; Snow et al., 2013). Nucleocytoplasmic transport, being a fundamental cellular process, might potentially lie upstream of all the phenotypes, including alteration in gene expression in HGPS. The objective of this thesis is to determine a mechanism by which nuclear transport is affected in Progeria. We focused on the guanine-nucleotide exchange factor for Ran GTPase (RanGEF), RCC1, in particular, as the target of Progerin to transduce its effects on the Ran gradient. In Chapter 2, we showed that high oxidative stress inhibited RCC1 activity to disrupt the Ran gradient and cause nuclear transport defect, while Chapter 3 dealt with the role of loss of heterochromatin in Ran gradient disruption in HGPS

cells. A possibility of the existence of one or more feedback loops cannot be ignored, which might make this study a complicated, yet an interesting one.

RCC1 has long been known as an important factor for cell cycle progression. When tsBN2 cells (cell line with temperature-sensitive mutation in RCC1 gene), arrested in S-phase, were shifted to non-permissive temperature, the cells entered mitosis with prematurely condensed, but incompletely replicated DNA (Nishimoto et al., 1978). Therefore, RCC1 turned out to be a factor required for proper chromosome condensation during G2/M transition in the cell cycle. Later, it was demonstrated that RCC1 degradation at non-permissive temperature in tsBN2 cells led to the activation of p34^{cdc2}/ histone H1 kinase in the cells those were in either S or G2 phase (Nishitani et al., 1991). However, the cells that were in G1 did not enter mitosis upon RCC1 degradation, and remained arrested in G1, probably because the mitosis-inducing factors are not synthesized until the cells pass G1/S transition (Moreno and Nurse, 1990). The replication cessation in cells at S phase could still be attributed to the premature entry into mitosis. However, inhibition of transcription and translation in tsBN2 cells at non-permissive temperature, even in the cells arrested in G1, suggested a role of RCC1 in G1 phase, which seemed distinct from that in mitosis (Dasso, 1993). Much of the work to explain the role of RCC1 in cells was aimed at demonstrating its function in cell cycle progression. However, it was not clear whether the pleiotropic phenotype observed in RCC1-deficient conditions was directly affected by the loss of RCC1 or was a consequence of mitotic defect in those cells. Although nucleotide exchange activity of RCC1 towards Ran, and the

necessity of Ran GTPase in nuclear transport machinery were described in the early '90s (Bischoff and Ponstingl, 1991; Moore and Blobel, 1993), the pivotal role played by the Ran system in nucleocytoplasmic transport was not understood until a decade later (Görllich and Kutay, 1999). It is possible that the diverse phenotypes observed in RCC1-deficient cells, for example, defects in mitosis, inhibition of transcription and translation (Dasso, 1993; Moreno and Nurse, 1990; Nishitani et al., 1991), are all due to the disruption of the nuclear transport machinery in these cells.

Since the role of the Ran system in nuclear transport was described, significant progress has been made in the field of RCC1 and Ran. The crystal structures of RCC1 alone and in combination with Ran GTPase and chromatin have been solved (England et al., 2010; Makde et al., 2010; Renault et al., 2001; 1998). The role of chromatin in RCC1 activity, and the importance of posttranslational modifications of RCC1 and chromatin in generating RanGTP in cells were demonstrated (Chen et al., 2007; Hutchins et al., 2004; Nemergut et al., 2001; Wong et al., 2008). It was shown that the posttranslational modifications of RCC1, such as phosphorylation and methylation, were required for its proper interaction with chromatin in mitotic cells (Chen et al., 2007; Hutchins et al., 2004). The evidence showing the requirement of these factors in regulating RCC1 activity in interphase cells was lacking. In this study, we showed that oxidative posttranslational modifications of RCC1 impacted its activity in interphase cells. Mass spectrometry revealed that several cysteine residues of RCC1 were oxidized in cells, which inhibited its activity.

The Ran system and RanGTPase-dependent nuclear transport are affected by several different cellular stresses. Ran distribution, and the localization of transport receptors and nucleoporins upon induction of stress have been reported (Crampton et al., 2009; Czubryt et al., 2000; Kelley and Paschal, 2007; Kodiha et al., 2004; 2008; Miyamoto et al., 2004; Stochaj et al., 2000; Yasuda et al., 2006). Activation of the MAPK signaling pathway and posttranslational modification of nucleoporins have been shown to be involved in exerting the effects of cellular stress on the Ran system (Czubryt et al., 2000; Kodiha et al., 2009b; Kosako et al., 2009). However, no specific mechanism of how cellular stress alters the distribution of Ran GTPase was suggested. In one of the studies here, we proposed a mechanism for this, and introduced a new mediator, RCC1, for oxidative stress-induced Ran gradient disruption. We identified the Cysteine residues of RCC1 that are modified by oxidation and showed that oxidative stress reversibly modified these Cys residues to inhibit RCC1 activity. Cys93 was found to be the major residue through which oxidative stress affected Ran-RCC1 binding. Oxidative stress also altered RCC1-chromatin interaction in cells. Therefore, oxidative stress-mediated alterations in Ran- and chromatin-binding by RCC1 was suggested to inhibit RCC1 activity, leading to Ran gradient disruption and nuclear transport defect. This mechanism explains how the Ran gradient might be disrupted in HGPS cells that have high oxidative stress (Kelley et al., 2011; Viteri et al., 2010). There is evidence showing an induction of ROS production in cells upon Progerin expression (Viteri et al., 2010), but it is still not clear how oxidative stress is induced in Progerin-

expressing cells. Previous work suggested that oxidative stress lies upstream of the Ran gradient disruption in HGPS cells (Datta et al., 2014; Yasuda et al., 2006). Here, we determined a mechanism of how oxidative stress might affect the Ran distribution in cells.

Ran gradient disruption in Progerin-expressing cells results in nuclear transport defects of Ubc9, TPR and several other large cargoes (Kelley et al., 2011; Snow et al., 2013). In addition to this, HGPS cells exhibit a plethora of nuclear defects, including global loss of heterochromatin reflected by the reduction in heterochromatin marks, such as H3K9me³ and H3K27me³ (Scaffidi and Misteli, 2006; Shumaker et al., 2006). Downregulation of the histone methyltransferase, EZH2, responsible for methylating histone H3 Lys27, has been implicated in the loss of H3K27me³ in these cells (Shumaker et al., 2006). Here in Chapter 3, we demonstrated that loss of heterochromatin resulted in Ran gradient disruption. Cells were treated with a small molecule inhibitor BIX02194, which specifically inhibits the histone methyltransferase G9a that methylates histone H3 Lys9 (Kubicek et al., 2007). This treatment induced a reduction in H3K9 di- and tri-methylation, and caused Ran gradient disruption. This data suggested that the loss of heterochromatin in HGPS cells might be the causal factor for Ran gradient disruption. We further showed that inhibiting mature lamin A formation by treating the cells with protease inhibitor Lopinavir that mimicked HGPS-like condition, down-regulated mRNA expression of the methyltransferase Suv39H1, in addition to EZH2. In HGPS fibroblasts the nuclear levels of the methyltransferases G9a and GLP1 were significantly reduced, which were

rescued by farnesyltransferase inhibitor FTI-277. This suggested that the constitutive membrane attachment of Progerin resulted in the downregulation of the methyltransferases and global loss of heterochromatin that caused Ran gradient disruption. Since RCC1 exhibits some preference for heterochromatin binding over euchromatin (Casolari et al., 2004), it is reasonable to hypothesize that global loss of heterochromatin might alter RCC1-chromatin interaction and affect RCC1 activity. However, it is possible that loss of heterochromatin and Progerin-induced oxidative stress together inhibit RCC1 activity in Progeria, leading to Ran gradient disruption. Progerin expression also resulted in a significant reduction in nuclear levels of histones H3 and H4. We speculate that disruption of Ran gradient might affect histone import in HGPS cells, which in turn, alters the chromatin organization and epigenetic landscape via a negative feedback loop.

Relevance in normal aging

Genomic instability is considered as one of the hallmarks of aging (Lopez-Otin et al., 2013), and defects in nuclear lamina can also cause genomic instability (Dechat et al., 2008). This connection made researchers look into the expression of Progerin in cells from old individuals, in which low levels of Progerin was detected (McClintock et al., 2007; Scaffidi and Misteli, 2006). Prelamin A accumulation in the vascular smooth muscle cells (VSMCs) of elderly individual was also observed (Ragnauth et al., 2010), and Progerin expression was found in non-HGPS coronary arteries with many similarities between HGPS

vascular pathology and age-related atherosclerosis (Olive et al., 2010). Progerin expression reduces the stem-ness of human mesenchymal stem cells, yet another hallmark of aging (Lopez-Otin et al., 2013; Scaffidi and Misteli, 2006). Telomere attrition is also linked to physiological aging (Lopez-Otin et al., 2013). Progerin expression has been shown to cause shortening of telomeric length and telomere damage (Benson et al., 2010; Cao et al., 2011a). Induction of telomere damage upregulates Progerin expression by changes in alternative splicing (Cao et al., 2011a). All these observations together suggest that Progerin expression in non-HGPS old individuals might induce changes in telomere length and stem cell population leading to senescence. Progerin has even been called a “biomarker” of aging (McClintock et al., 2007).

Future directions

In the Chapter 2 of this thesis I showed that oxidative stress inhibits RCC1 activity and disrupts the Ran gradient in cells. I also proposed a mechanism by which oxidative stress inhibits RCC1 activity. Oxidative stress reversibly modifies Cys residues in RCC1 to impair Ran binding and also alter RCC1-chromatin interactions, leading to a reduced level of activity. It would also be interesting to test if Progerin expression in patient cells disrupts the Ran gradient by inhibiting RCC1. Although the nucleotide exchange activity of RCC1 from HGPS patient cells should address this, the heterogeneity of these primary fibroblasts could complicate interpretation of the data. The HGPS patient cell population consists of cells that show a range of HGPS phenotypes owing to the fact that they

express different levels of Progerin. This non-uniformity of the population could mask the effect of oxidative stress on RCC1 activity in a biochemical assay. This difficulty can potentially be overcome by treating normal fibroblasts with the protease-inhibitor Lopinavir, which induces Progeria-like phenotypes by constitutive attachment of prelamin A to the nuclear envelope. However, whether or not the amount of ROS generated by Lopinavir treatment is comparable with that of Progeria patient cells is an open question. In addition to measuring RCC1 activity in Lopinavir-treated cells, a parallel estimation of ROS production by Lopinavir might address this to some extent.

In this chapter, an effect of oxidative stress on the RCC1-chromatin interaction has been shown. I also mentioned that diamide modified two Cys residues, Cys228 and Cys280, which are present in the chromatin-binding surface of RCC1. It would be interesting to formally prove that these Cys residues are required for diamide-mediated alterations in RCC1-chromatin interaction. A FRAP experiment on diamide-treated cells, transfected with fluorescently-tagged mutants of these Cys residues (individually and in combination) would be ideal to test the role of these amino acids in RCC1-chromatin interaction in the presence of oxidative stress. It is worth-mentioning that oxidative stress can also modify chromatin itself to alter RCC1-chromatin interaction. Therefore, its effects on the activity of RCC1 might be a combination of both RCC1 and chromatin modifications.

In Chapter 3 of this thesis, I studied interplay between the heterochromatin marks and the Ran gradient in HGPS cells, and I showed that the reduction of

the heterochromatin-related methylation marks in HGPS lies upstream of the Ran gradient disruption in these cells. It is yet to be shown carefully whether the reduction of the methyl-marks- H3K9me² and H3K9me³, by inhibiting the methyltransferase G9a is sufficient to cause similar degree of Ran gradient disruption as observed in Progeria. In our experience, Progerin-induced Ran gradient disruption is more severe than that in BIX01294-treated cells. This prompts us to compare the Ran gradient disruption in fibroblasts, treated with Lopinavir and knocking down histone methyltransferases.

Since Progerin expression causes histone import defects in cells, it is possible that the reduction in heterochromatin marks in Progeria patient cells is observed due to the reduced amount of histones present in the nuclei of these cells. This is supported by the fact that the reduction of other histone marks, such as histone H3 Ser10 phosphorylation (H3S10p) and histone H3 Lys14 acetylation (H3K14Ac), which are not associated with heterochromatin, have also been noticed in Progerin-expressing cells (data not shown). Studying the changes in histone localization and post-translational modifications in a time-course of Lopinavir treatment on fibroblasts might shed some light on the order of events occurring in the pathway. Normalizing the fluorescence intensity of the histone marks (H3Ser10p and H3K14Ac) to the total histone H3 signal in the nucleus would be an ideal addition in the time-course experiment to depict whether or not the changes in the histone marks in Progeria are due to the defects in histone import. To test whether reduction in heterochromatin marks precedes histone import, we could also study histone localization in BIX-treated fibroblasts.

Finally, it is not known whether Progerin-induced reduction in heterochromatin marks and oxidative stress are two different pathways or parts of the same pathway. Since the changes in the heterochromatin marks are likely to alter the expression of several genes including that of the antioxidant enzymes, it is possible that the reduction in heterochromatin marks in Progeria might contribute to the elevated levels of ROS. Measuring the levels of ROS by DCF-DA fluorescence in BIX-treated fibroblasts can test this.

Role of nuclear transport in cardiac hypertrophy

Cardiac hypertrophy is a condition where the ventricular wall thickens in order to decrease ventricular wall stress (Maillet et al., 2013). Hypertrophy is either physiological, caused by physical exercise or pregnancy, or pathological resulting from cardiomyopathy. There is evidence showing that nuclear import is inhibited in cardiac hypertrophy (Perez-Terzic et al., 2001). It is thought that cardiac cells undergo a phase of adaptation during hypertrophy, where the GTP:GDP ratio in cells increases with a dramatic accumulation of Ran in the nucleus, disrupting the nuclear import of histone H1. Moreover, during cardiac differentiation of embryonic stem cells, a distinct gene expression pattern of the components of nuclear transport machinery was observed (Perez-Terzic et al., 2007). Cellular compartmentalization of different cardiac transcription factors is thought to be regulated by the differential gene expression during lineage commitment. Even the nuclear pore complex undergoes a structural adaptation in stem cell-derived cardiomyocytes (Perez-Terzic et al., 2007; 2003). All these

observations suggest that the nucleocytoplasmic transport in cardiomyocytes is highly regulated and is important in cardiac development and regeneration.

Human heart is known to consume approx. 8-15 ml O₂/ min/ 100 g tissue at a resting pulse (Giordano, 2005). Constant oxygen supply is indispensable for the function of the heart and myocardial gene expression. On the other hand, the effect of ROS generated during aerobic respiration can be deleterious. In a number of studies, ROS has been implicated in coronary artery disease. ROS activity in the vessel wall causes oxidation of low-density lipid, a major contributor of atherosclerosis (Witztum and Steinberg, 1991). ROS-induced activation of vascular membrane metalloproteinase results in coronary thrombosis (Rajagopalan et al., 1996). ROS also activates various signaling pathways, including MAPK p38, PKC, JNK, ERK1/2 etc. and cardiomyocyte apoptosis that lead to cardiac hypertrophy and heart failure (Giordano, 2005). The role of ROS and nuclear transport in cardiac tissue development and pathology is of special interest to us, because the majority of the mortality in HGPS is caused due to myocardial infarction and heart failure. The mechanism suggested in our study showing the effect of oxidative stress on nuclear transport by targeting RCC1 might be relevant in studying cardiovascular diseases. Given the crucial role played by nucleocytoplasmic transport in cardiac development and regeneration, it is reasonable to speculate that oxidative stress-mediated disruption of nuclear transport of transcription factors might affect the gene expression pattern in cardiac cells.

Role of nuclear transport in epigenetic changes in stem cell aging

A section of this thesis is dedicated to examine the role of heterochromatin in Ran gradient disruption. It was already shown in different studies that HGPS cells exhibit a global loss of heterochromatin (Scaffidi and Misteli, 2006; Shumaker et al., 2006), and have disruption of Ran gradient and nuclear transport (Kelley et al., 2011). In this thesis, we show that loss of heterochromatin is sufficient to cause Ran gradient disruption in cells. However, the degree of Ran gradient disruption in these cells was not as robust as the Progerin-expressing cells. This can be explained by the multitude of phenotypes caused due to Progerin expression, not just the loss of heterochromatin.

Exhaustion of the stem cell population has also been observed in HGPS patients with expression of lineage-specific differentiation markers and enhanced differentiation in Progerin-expressing mesenchymal stem cells compared to control cells (Halaschek-Wiener and Brooks-Wilson, 2007; Scaffidi and Misteli, 2008a). Based on the observations in this thesis, a comparison between epigenetic changes during differentiation in normal and HGPS cells seems interesting and might shed some light on the interplay between heterochromatin and the stem cell population in HGPS. Reports of high levels of open chromatin marks, such as H3K4me² and H3K4me³ in old hematopoietic stem cells (HSC) already exist (Beerman and Rossi, 2014). But these cells showed a decrease in H4K16Ac, a transcriptional activation mark. Age-regulated expression of several histone lysine demethylases has also been observed (Beerman and Rossi, 2014). This might be correlated with the observation that the histone methyltransferases

are downregulated in HGPS cells (Chapter 3; Shumaker et al, 2006). These epigenetic changes most likely either entail alterations in gene expression directly, or inhibit RCC1 activity to disrupt Ran gradient and nuclear transport of transcription factors in these cells. This, in turn, might induce age-related phenotypes.

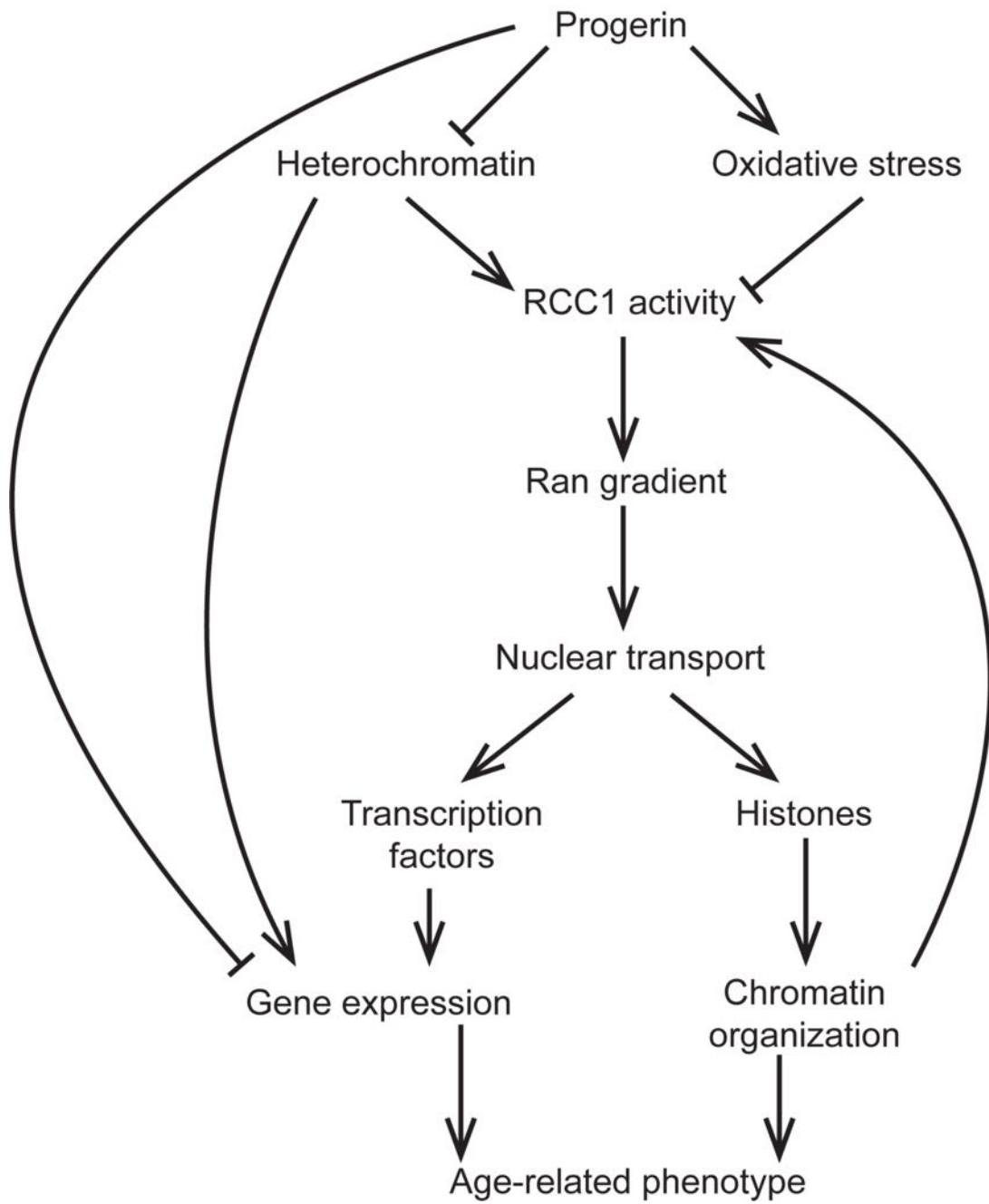
Conclusion

Alterations in nuclear transport and RCC1 activity are proposed to play important roles in transducing the effects of Progerin to the cell (Fig. 4.1). RCC1 forms the integrating point in the pathway where Progerin expression-induced loss of heterochromatin and ROS generation meet. Both can potentially inhibit RCC1 activity in cells, decreasing RanGTP production in the nucleus, which disrupts the Ran gradient and causes nuclear import defects of macromolecules, such as histones and transcription factors. The histone import defect has a direct impact on chromatin organization, which might, in turn, affect RCC1 activity by a negative feedback loop. An import defect of transcription factors might negatively impact gene expression in cells. Progerin-induced loss of heterochromatin might directly affect gene expression in cells. Also, since peripheral chromatin and several transcription factors directly interact with the nuclear lamina, changes in nuclear architecture due to Progerin expression might alter transcription. All these together eventually lead to cellular senescence and organismal aging. The complex crosstalk between each of the components in the network makes the experimental observations difficult to interpret. However, our data suggest that

alterations in the Ran GTPase system is one of the early events in Progeria that results in the nuclear transport defect of proteins, including histones and transcription factors, leading to the changes in chromatin organization, including reduction in heterochromatin marks, and gene expression pattern.

Fig. 4.1: Model integrating different pathways engaged by Progerin in order to cause age-associated phenotypes. Progerin disrupts Ran gradient by directly affecting heterochromatin and increasing oxidative stress. Ran gradient disruption might, in turn, results into nuclear transport defect of histones and transcription factors leading to alterations in chromatin organization and gene expression, commonly observed in aging.

Fig. 4.1



REFERENCES

- Alleman, R.J., Katunga, L.A., Nelson, M.A.M., Brown, D.A., and Anderson, E.J. (2014). The “Goldilocks Zone” from a redox perspective-Adaptive vs. deleterious responses to oxidative stress in striated muscle. *Front Physiol* 5, 358.
- Andrulis, E.D.E., Neiman, A.M.A., Zappulla, D.C.D., and Sternglanz, R.R. (1998). Perinuclear localization of chromatin facilitates transcriptional silencing. *Nature* 394, 592–595.
- Annunziato, A.T. (2012). Assembling chromatin: The long and winding road. *Biochimica Et Biophysica Acta (BBA)* 1819, 196–210.
- Azuma, Y., Renault, L., Garcia-Ranea, J.A., Valencia, A., Nishimoto, T., and Wittinghofer, A. (1999). Model of the Ran-RCC1 interaction using biochemical and docking experiments. *J Mol Biol* 289, 1119–1130.
- Bayliss, R., Corbett, A.H., and Stewart, M. (2000). The molecular mechanism of transport of macromolecules through nuclear pore complexes. *Traffic* 1, 448–456.
- Beerman, I., and Rossi, D.J. (2014). Epigenetic regulation of hematopoietic stem cell aging. *Experimental Cell Research* 329, 192–199.
- Benavente, R., Krohne, G., and Franke, W.W. (1985). Cell type-specific expression of nuclear lamina proteins during development of *Xenopus laevis*. *Cell* 41, 177–190.
- Benson, E.K., Lee, S.W., and Aaronson, S.A. (2010). Role of progerin-induced telomere dysfunction in HGPS premature cellular senescence. *J Cell Sci* 123, 2605–2612.
- Bione, S.S., Maestrini, E.E., Rivella, S.S., Mancini, M.M., Regis, S.S., Romeo, G.G., and Toniolo, D.D. (1994). Identification of a novel X-linked gene responsible for Emery-Dreifuss muscular dystrophy. *Nat Genet* 8, 323–327.
- Bischoff, F.R., Klebe, C., Kretschmer, J., Wittinghofer, A., and Ponstingl, H. (1994). RanGAP1 induces GTPase activity of nuclear Ras-related Ran. *Proc Natl Acad Sci USA* 91, 2587–2591.
- Bischoff, F.R., and Ponstingl, H. (1991). Catalysis of guanine nucleotide exchange factor on Ran by the mitotic regulator RCC1. *Nature* 354, 80–82.
- Bonne, G., Di Barletta, M.R., Varnous, S., Bécane, H.M., Hammouda, E.H., Merlini, L., Muntoni, F., Greenberg, C.R., Gary, F., Urtizbera, J.A., et al.

- (1999). Mutations in the gene encoding lamin A/C cause autosomal dominant Emery-Dreifuss muscular dystrophy. *Nat Genet* 21, 285–288.
- Bos, J.L., Rehmann, H., and Wittinghofer, A. (2007). GEFs and GAPs: critical elements in the control of small G proteins. *Cell* 129, 865–877.
- Bourne, H.R., Sanders, D.A., and McCormick, F. (1991). The GTPase superfamily: conserved structure and molecular mechanism. *Nature* 349, 117–127.
- Boyle, S., Gilchrist, S., Bridger, J.M., Mahy, N.L., Ellis, J.A., and Bickmore, W.A. (2001). The spatial organization of human chromosomes within the nuclei of normal and emerin-mutant cells. *Hum. Mol. Genet.* 10, 211–219.
- Cai, H. (2005). Hydrogen peroxide regulation of endothelial function: Origins, mechanisms, and consequences. *Cardiovascular Research* 68, 26–36.
- Campos, E.I., Fillingham, J., Li, G., Zheng, H., Voigt, P., Kuo, W.-H.W., Seepany, H., Gao, Z., Day, L.A., Greenblatt, J.F., et al. (2010). The program for processing newly synthesized histones H3.1 and H4. *Nat Struct Mol Biol* 17, 1343–1351.
- Cao, H., and Hegele, R.A. (2000). Nuclear lamin A/C R482Q mutation in canadian kindreds with Dunnigan-type familial partial lipodystrophy. *Hum. Mol. Genet.* 9, 109–112.
- Cao, H., and Hegele, R.A. (2003). LMNA is mutated in Hutchinson-Gilford progeria (MIM 176670) but not in Wiedemann-Rautenstrauch progeroid syndrome (MIM 264090). *J Hum Genet* 48, 271–274.
- Cao, K., Blair, C.D., Faddah, D.A., Kieckhafer, J.E., Olive, M., Erdos, M.R., Nabel, E.G., and Collins, F.S. (2011a). Progerin and telomere dysfunction collaborate to trigger cellular senescence in normal human fibroblasts. *The Journal of Clinical Investigation* 121, 2833–2844.
- Cao, K., Capell, B.C., Erdos, M.R., Djabali, K., and Collins, F.S. (2007). A lamin A protein isoform overexpressed in Hutchinson-Gilford progeria syndrome interferes with mitosis in progeria and normal cells. *Proc Natl Acad Sci USA* 104, 4949–4954.
- Cao, K., Graziotto, J.J., Blair, C.D., Mazzulli, J.R., Erdos, M.R., Krainc, D., and Collins, F.S. (2011b). Rapamycin reverses cellular phenotypes and enhances mutant protein clearance in Hutchinson-Gilford progeria syndrome cells. *Sci Transl Med* 3, 89ra58.
- Capell, B.C., Erdos, M.R., Madigan, J.P., Fiordalisi, J.J., Varga, R., Conneely, K.N., Gordon, L.B., Der, C.J., Cox, A.D., and Collins, F.S. (2005). Inhibiting farnesylation of progerin prevents the characteristic nuclear

- blebbing of HGPS. *Proc Natl Acad Sci USA* *102*, 12879–12884.
- Casolari, J.M., Brown, C.R., Komili, S., West, J., Hieronymus, H., and Silver, P.A. (2004). Genome-wide localization of the nuclear transport machinery couples transcriptional status and nuclear organization. *Cell* *117*, 427–439.
- Chen, D., Toone, W.M., Mata, J., Lyne, R., Burns, G., Kivinen, K., Brazma, A., Jones, N., and Bähler, J. (2003). Global transcriptional responses of fission yeast to environmental stress. *Mol Biol Cell* *14*, 214–229.
- Chen, T., Muratore, T.L., Schaner-Tooley, C.E., Shabanowitz, J., Hunt, D.F., and Macara, I.G. (2007). N-terminal alpha-methylation of RCC1 is necessary for stable chromatin association and normal mitosis. *Nat Cell Biol* *9*, 596–603.
- Ckless, K., Reynaert, N.L., Taatjes, D.J., and Lounsbury, K.M. (2004). In situ detection and visualization of S-nitrosylated proteins following chemical derivatization: identification of Ran GTPase as a target for S-nitrosylation. *Nitric Oxide* *11*, 216–227.
- Clarkson, W., Corbett, A.H., Paschal, B.M., Kent, H.M., McCoy, A.J., Gerace, L., Silver, P.A., and Stewart, M. (1997). Nuclear protein import is decreased by engineered mutants of nuclear transport factor 2 (NTF2) that do not bind GDP-Ran. *J Mol Biol* *272*, 716–730.
- Clements, L., Manilal, S., Love, D.R., and Morris, G.E. (2000). Direct Interaction between Emerin and Lamin A. *Biochemical and Biophysical Research Communications* *267*, 709–714.
- Clément, M., Deshaies, F., de Repentigny, L., and Belhumeur, P. (2006). The nuclear GTPase Gsp1p can affect proper telomeric function through the Sir4 protein in *Saccharomyces cerevisiae*. *Mol Microbiol* *62*, 453–468.
- Coffinier, C., Hudon, S.E., Farber, E.A., Chang, S.Y., Hrycyna, C.A., Young, S.G., and Fong, L.G. (2007). HIV protease inhibitors block the zinc metalloproteinase ZMPSTE24 and lead to an accumulation of prelamin A in cells. *Proc Natl Acad Sci USA* *104*, 13432–13437.
- Conti, E., Uy, M., Leighton, L., Blobel, G., and Kuriyan, J. (1998). Crystallographic analysis of the recognition of a nuclear localization signal by the nuclear import factor Karyopherin α . *Cell* *94*, 193–204.
- Crampton, N., Kodiha, M., Shrivastava, S., Umar, R., and Stochaj, U. (2009). Oxidative stress inhibits nuclear protein export by multiple mechanisms that target FG nucleoporins and Crm1. *Mol Biol Cell* *20*, 5106–5116.
- Cushman, I., Stenoien, D., and Moore, M.S. (2003). The dynamic association of RCC1 with chromatin is modulated by Ran-dependent nuclear transport.

- Mol Biol Cell 15, 245–255.
- Czubryt, M.P., Austria, J.A., and Pierce, G.N. (2000). Hydrogen peroxide inhibition of nuclear protein import is mediated by the mitogen-activated protein kinase, ERK2. *J Cell Biol* 148, 7–16.
- D'Angelo, M.A., Raices, M., Panowski, S.H., and Hetzer, M.W. (2009). Age-dependent deterioration of nuclear pore complexes causes a loss of nuclear integrity in postmitotic cells. *Cell* 136, 284–295.
- Dahl, K.N., Scaffidi, P., Islam, M.F., Yodh, A.G., Wilson, K.L., and Misteli, T. (2006). Distinct structural and mechanical properties of the nuclear lamina in Hutchinson-Gilford progeria syndrome. *Proc Natl Acad Sci USA* 103, 10271–10276.
- Dasso, M. (1993). RCC1 in the cell cycle: the regulator of chromosome condensation takes on new roles. *Trends Biochem Sci* 18, 96–101.
- Datta, S., Snow, C.J., and Paschal, B.M. (2014). A pathway linking oxidative stress and the Ran GTPase system in progeria. *Mol Biol Cell* 25, 1202–1215.
- De Sandre-Giovannoli, A., Bernard, R., Cau, P., Navarro, C., Amiel, J., Boccaccio, I., Lyonnet, S., Stewart, C.L., Munnich, A., Le Merrer, M., et al. (2003). Lamin A truncation in Hutchinson-Gilford progeria. *Science* 300, 2055–2055.
- De Sandre-Giovannoli, A., Chaouch, M., Kozlov, S., Vallat, J.-M., Tazir, M., Kassouri, N., Szepietowski, P., Hammadouche, T., Vandenberghe, A., Stewart, C.L., et al. (2002). Homozygous defects in LMNA, encoding lamin A/C nuclear-envelope proteins, cause autosomal recessive axonal neuropathy in human (Charcot-Marie-Tooth disorder type 2) and mouse. *Am J Hum Genet* 70, 726–736.
- Dechat, T., Adam, S.A., and Goldman, R.D. (2009). Nuclear lamins and chromatin: when structure meets function. *Adv Enzyme Regul* 49, 157–166.
- Dechat, T., Pflieger, K., Sengupta, K., Shimi, T., Shumaker, D.K., Solimando, L., and Goldman, R.D. (2008). Nuclear lamins: major factors in the structural organization and function of the nucleus and chromatin. *Genes Dev* 22, 832–853.
- Dechat, T., Shimi, T., Adam, S.A., Rusinol, A.E., Andres, D.A., Spielmann, H.P., Sinensky, M.S., and Goldman, R.D. (2007). Alterations in mitosis and cell cycle progression caused by a mutant lamin A known to accelerate human aging. *Proc Natl Acad Sci USA* 104, 4955–4960.

- Dingwall, C., and Laskey, R.A. (1991). Nuclear targeting sequences-a consensus? *Trends Biochem Sci* 16, 478–481.
- Dror, V., and Winston, F. (2004). The Swi/Snf chromatin remodeling complex is required for ribosomal DNA and telomeric silencing in *Saccharomyces cerevisiae*. *Mol Cell Biol* 24, 8227–8235.
- Eisinger-Mathason, T.K., Andrade, J., Groehler, A.L., Clark, D.E., Muratore-Schroeder, T.L., Pasic, L., Smith, J.A., Shabanowitz, J., Hunt, D.F., Macara, I.G., et al. (2008). Co-dependent functions of RSK2 and the apoptosis promoting factor TIA-1 in stress granule assembly and cell survival. *Mol Cell* 31, 722–736.
- Elsässer, S.J., and D'Arcy, S. (2012). Towards a mechanism for histone chaperones. *Biochim Biophys Acta* 1819, 211–221.
- England, J.R., Huang, J., Jennings, M.J., Makde, R.D., and Tan, S. (2010). RCC1 uses a conformationally diverse loop region to interact with the nucleosome: a model for the RCC1–nucleosome complex. *J Mol Biol* 398, 518–529.
- Eriksson, M., Brown, W.T., Gordon, L.B., Glynn, M.W., Singer, J., Scott, L., Erdos, M.R., Robbins, C.M., Moses, T.Y., Berglund, P., et al. (2003). Recurrent de novo point mutations in lamin A cause Hutchinson-Gilford progeria syndrome. *Nature* 423, 293–298.
- Espada, J., Varela, I., Flores, I., Ugalde, A.P., Cadiñanos, J., Pendas, A.M., Stewart, C.L., Tryggvason, K., Blasco, M.A., Freije, J.M.P., et al. (2008). Nuclear envelope defects cause stem cell dysfunction in premature-aging mice. *J Cell Biol* 181, 27–35.
- Fahrenkrog, B., and Aebi, U. (2003). The nuclear pore complex: nucleocytoplasmic transport and beyond. *Nat Rev Mol Cell Biol* 4, 757–766.
- Finkel, T., and Holbrook, N.J. (2000). Oxidants, oxidative stress and the biology of ageing. *Nature* 408, 239–247.
- Fong, L.G., Frost, D., Meta, M., Qiao, X., Yang, S.H., Coffinier, C., and Young, S.G. (2006). A protein farnesyltransferase inhibitor ameliorates disease in a mouse model of progeria. *Science* 311, 1621–1623.
- Fontes, M.R., Teh, T., and Kobe, B. (2000). Structural basis of recognition of monopartite and bipartite nuclear localization sequences by mammalian importin-alpha. *J Mol Biol* 297, 1183–1194.
- Gasch, A.P., Spellman, P.T., Kao, C.M., Carmel-Harel, O., Eisen, M.B., Storz, G., Botstein, D., and Brown, P.O. (2000). Genomic expression programs in

- the response of yeast cells to environmental changes. *Mol Biol Cell* *11*, 4241–4257.
- Geiszt, M., and Leto, T.L. (2004). The Nox family of NAD(P)H oxidases: host defense and beyond. *J Biol Chem* *279*, 51715–51718.
- Gerace, L., and Blobel, G. (1980). The nuclear envelope lamina is reversibly depolymerized during mitosis. *Cell* *19*, 277–287.
- Gilford, H. (1897). On a condition of mixed premature and immature development. *Med.-Chir. Trans.* *80*, 17–46.25.
- Giordano, F.J. (2005). Oxygen, oxidative stress, hypoxia, and heart failure. *J Clin Invest* *115*, 500–508.
- Glynn, M.W., and Glover, T.W. (2005). Incomplete processing of mutant lamin A in Hutchinson-Gilford progeria leads to nuclear abnormalities, which are reversed by farnesyltransferase inhibition. *Hum. Mol. Genet.* *14*, 2959–2969.
- Go, Y.-M., and Jones, D.P. (2013). The redox proteome. *J Biol Chem* *288*, 26512–26520.
- Goldberg, M., Jenkins, H., Allen, T., Whitfield, W.G., and Hutchison, C.J. (1995). *Xenopus* lamin B3 has a direct role in the assembly of a replication competent nucleus: evidence from cell-free egg extracts. *J Cell Sci* *108* (Pt 11), 3451–3461.
- Goldman, A.E., Maul, G., Steinert, P.M., Yang, H.-Y., and Goldman, R.D. (1986). Keratin-like proteins that coisolate with intermediate filaments of BHK-21 cells are nuclear lamins. *Proc Natl Acad Sci USA* *83*, 3839–3843.
- Goldman, R.D., Gruenbaum, Y., Moir, R.D., Shumaker, D.K., and Spann, T.P. (2002). Nuclear lamins: building blocks of nuclear architecture. *Genes & Development* *16*, 533–547.
- Goldman, R.D., Shumaker, D.K., Erdos, M.R., Eriksson, M., Goldman, A.E., Gordon, L.B., Gruenbaum, Y., Khuon, S., Mendez, M., Varga, R., et al. (2004). Accumulation of mutant lamin A causes progressive changes in nuclear architecture in Hutchinson-Gilford progeria syndrome. *Proc Natl Acad Sci USA* *101*, 8963–8968.
- Gordon, L.B., Kleinman, M.E., Miller, D.T., Neuberg, D.S., Giobbie-Hurder, A., Gerhard-Herman, M., Smoot, L.B., Gordon, C.M., Cleveland, R., Snyder, B.D., et al. (2012). Clinical trial of a farnesyltransferase inhibitor in children with Hutchinson-Gilford progeria syndrome. *Proc Natl Acad Sci USA* *109*, 16666–16671.

- Görlich, D.D., and Kutay, U.U. (1999). Transport between the cell nucleus and the cytoplasm. *Annu Rev Cell Dev Biol* 15, 607–660.
- Görlich, D., Seewald, M.J., and Ribbeck, K. (2003). Characterization of Ran-driven cargo transport and the RanGTPase system by kinetic measurements and computer simulation. *Embo J* 22, 1088–1100.
- Gruenbaum, Y., Goldman, R.D., Meyuhas, R., and Mills, E. (2003). The nuclear lamina and its functions in the nucleus. *Int Rev Cytol* 226, 1–62.
- Hadjebi, O., Casas-Terradellas, E., Garcia-Gonzalo, F.R., and Rosa, J.L. (2008). The RCC1 superfamily: From genes, to function, to disease. *Biochim Biophys Acta* 1783, 1467–1479.
- Halaschek-Wiener, J., and Brooks-Wilson, A. (2007). Progeria of stem cells: stem cell exhaustion in Hutchinson-Gilford progeria syndrome. *J. Gerontol. a Biol. Sci. Med. Sci.* 62, 3–8.
- Hancock, J.T. (2009). The role of redox mechanisms in cell signalling. *Mol Biotechnol* 43, 162–166.
- Hao, Y., and Macara, I.G. (2008). Regulation of chromatin binding by a conformational switch in the tail of the Ran exchange factor RCC1. *J Cell Biol* 182, 827–836.
- Harreman, M.T., Cohen, P.E., Hodel, M.R., Truscott, G.J., Corbett, A.H., and Hodel, A.E. (2003). Characterization of the auto-inhibitory sequence within the N-terminal domain of importin alpha. *J Biol Chem* 278, 21361–21369.
- Hayashi, N., Kobayashi, M., Shimizu, H., Yamamoto, K.-I., Murakami, S., and Nishimoto, T. (2007). Mutations in Ran system affected telomere silencing in *Saccharomyces cerevisiae*. *Biochem Biophys Res Commun* 363, 788–794.
- Hernandez, L., Roux, K.J., Wong, E.S.M., Mounkes, L.C., Mutalif, R., Navasankari, R., Rai, B., Cool, S., Jeong, J.-W., Wang, H., et al. (2010). Functional coupling between the extracellular matrix and nuclear lamina by Wnt signaling in progeria. *Dev Cell* 19, 413–425.
- Holbrook, N.J., Martin, G.R., and Lockshin, R.A. (1996). *Cellular Aging and Cell Death* (John Wiley & Sons).
- Hood, F.E., and Clarke, P.R. (2007). RCC1 isoforms differ in their affinity for chromatin, molecular interactions and regulation by phosphorylation. *J Cell Sci* 120, 3436–3445.
- Houben, F., Ramaekers, F.C.S., Snoeckx, L.H.E.H., and Broers, J.L.V. (2007). Role of nuclear lamina-cytoskeleton interactions in the maintenance of

- cellular strength. *Biochim Biophys Acta* 1773, 675–686.
- Huang, S., Chen, L., Libina, N., Janes, J., Martin, G.M., Campisi, J., and Oshima, J. (2005). Correction of cellular phenotypes of Hutchinson-Gilford Progeria cells by RNA interference. *Hum Genet* 118, 444–450.
- Hutchins, J., Moore, W.J., Hood, F.E., Wilson, J., Andrews, P.D., Swedlow, J.R., and Clarke, P.R. (2004). Phosphorylation regulates the dynamic interaction of RCC1 with chromosomes during mitosis. *Curr Biol* 14, 1099–1104.
- Hutchinson, J. (1886). Congenital absence of hair and mammary glands. *Med.-Chir. Trans.* 69, 473–477.
- Hutchison, C.J., and Worman, H.J. (2004). A-type lamins: guardians of the soma? *Nat Cell Biol* 6, 1062–1067.
- Hutchison, C.J. (2002). Lamins: building blocks or regulators of gene expression? *Nat Rev Mol Cell Biol* 3, 848–858.
- Ibrahim, M.X., Sayin, V.I., Akula, M.K., Liu, M., Fong, L.G., Young, S.G., and Bergo, M.O. (2013). Targeting isoprenylcysteine methylation ameliorates disease in a mouse model of progeria. *Science* 340, 1330–1333.
- Imai, S., Nishibayashi, S., Takao, K., Tomifuji, M., Fujino, T., Hasegawa, M., and Takano, T. (1997). Dissociation of Oct-1 from the nuclear peripheral structure induces the cellular aging-associated collagenase gene expression. *Mol Biol Cell* 8, 2407–2419.
- Izaurralde, E., Kutay, U., vonKobbe, C., Mattaj, I.W., and Gorlich, D. (1997). The asymmetric distribution of the constituents of the Ran system is essential for transport into and out of the nucleus. *Embo J* 16, 6535–6547.
- Keck, K.M., and Pemberton, L.F. (2012). Histone chaperones link histone nuclear import and chromatin assembly. *Biochim Biophys Acta* 1819, 277–289.
- Kelley, J.B., and Paschal, B.M. (2007). Hyperosmotic stress signaling to the nucleus disrupts the Ran gradient and the production of RanGTP. *Mol Biol Cell* 18, 4365–4376.
- Kelley, J.B., Datta, S., Snow, C.J., Chatterjee, M., Ni, L., Spencer, A., Yang, C.-S., Cubeñas-Potts, C., Matunis, M.J., and Paschal, B.M. (2011). The defective nuclear lamina in Hutchinson-gilford progeria syndrome disrupts the nucleocytoplasmic Ran gradient and inhibits nuclear localization of Ubc9. *Mol Cell Biol* 31, 3378–3395.
- Klebe, C., Bischoff, F.R., Ponstingl, H., and Wittinghofer, A. (1995). Interaction of the nuclear GTP-binding protein Ran with its regulatory proteins RCC1

- and RanGAP1. *Biochemistry* **34**, 639–647.
- Kobe, B. (1999). Autoinhibition by an internal nuclear localization signal revealed by the crystal structure of mammalian importin alpha. *Nat Struct Biol* **6**, 388–397.
- Kodiha, M., Chu, A., Matusiewicz, N., and Stochaj, U. (2004). Multiple mechanisms promote the inhibition of classical nuclear import upon exposure to severe oxidative stress. *Cell Death Differ* **11**, 862–874.
- Kodiha, M., Bański, P., and Stochaj, U. (2009a). Interplay between MEK and PI3 kinase signaling regulates the subcellular localization of protein kinases ERK1/2 and Akt upon oxidative stress. *FEBS Lett* **583**, 1987–1993.
- Kodiha, M., Rassi, J.G., Brown, C.M., and Stochaj, U. (2007). Localization of AMP kinase is regulated by stress, cell density, and signaling through the MEK→ERK1/2 pathway. *Am J Physiol Cell Physiol* **293**, C1427–C1436.
- Kodiha, M., Tran, D., Morogan, A., Qian, C., and Stochaj, U. (2009b). Dissecting the signaling events that impact classical nuclear import and target nuclear transport factors. *PLoS ONE* **4**, e8420.
- Kodiha, M., Tran, D., Qian, C., Morogan, A., Presley, J.F., Brown, C.M., and Stochaj, U. (2008). Oxidative stress mislocalizes and retains transport factor importin-alpha and nucleoporins Nup153 and Nup88 in nuclei where they generate high molecular mass complexes. *Biochim Biophys Acta* **1783**, 405–418.
- Kosako, H., Yamaguchi, N., Aranami, C., Ushiyama, M., Kose, S., Imamoto, N., Taniguchi, H., Nishida, E., and Hattori, S. (2009). Phosphoproteomics reveals new ERK MAP kinase targets and links ERK to nucleoporin-mediated nuclear transport. *Nat Struct Mol Biol* **16**, 1026–1035.
- Kosower, N.S., and Kosower, E.M. (1995). [11] Diamide: An oxidant probe for thiols. In *Methods in Enzymology*, (Elsevier), pp. 123–133.
- Kubicek, S., O'Sullivan, R.J., August, E.M., Hickey, E.R., Zhang, Q., Teodoro, M.L., Rea, S., Mechtler, K., Kowalski, J.A., Homon, C.A., et al. (2007). Reversal of H3K9me2 by a small-molecule inhibitor for the G9a histone methyltransferase. *Mol Cell* **25**, 473–481.
- Kusano, A., Yoshioka, T., Nishijima, H., Nishitani, H., and Nishimoto, T. (2004). *Schizosaccharomyces pombe* RanGAP homolog, SpRna1, is required for centromeric silencing and chromosome segregation. *Mol Biol Cell* **15**, 4960–4970.
- Lammerding, J., Schulze, P.C., Takahashi, T., Kozlov, S., Sullivan, T., Kamm, R.D., Stewart, C.L., and Lee, R.T. (2004). Lamin A/C deficiency causes

- defective nuclear mechanics and mechanotransduction. *J Clin Invest* **113**, 370–378.
- Lee, S.J., Matsuura, Y., Liu, S.M., and Stewart, M. (2005). Structural basis for nuclear import complex dissociation by RanGTP. *Nature* **435**, 693–696.
- Lehner, C.F., Stick, R., Eppenberger, H.M., and Nigg, E.A. (1987). Differential expression of nuclear lamin proteins during chicken development. *J Cell Biol* **105**, 577–587.
- Lenz-Böhme, B., Wismar, J., Fuchs, S., Reifegerste, R., Buchner, E., Betz, H., and Schmitt, B. (1997). Insertional mutation of the *Drosophila* nuclear lamin Dm0 gene results in defective nuclear envelopes, clustering of nuclear pore complexes, and accumulation of annulate lamellae. *J Cell Biol* **137**, 1001–1016.
- Li, H.-Y., and Zheng, Y. (2004). Phosphorylation of RCC1 in mitosis is essential for producing a high RanGTP concentration on chromosomes and for spindle assembly in mammalian cells. *Genes Dev* **18**, 512–527.
- Li, H.-Y., Wirtz, D., and Zheng, Y. (2003). A mechanism of coupling RCC1 mobility to RanGTP production on the chromatin in vivo. *J Cell Biol* **160**, 635–644.
- Li, J., Stouffs, M., Serrander, L., Banfi, B., Bettioli, E., Charnay, Y., Steger, K., Krause, K.-H., and Jaconi, M.E. (2006). The NADPH oxidase NOX4 drives cardiac differentiation: Role in regulating cardiac transcription factors and MAP kinase activation. *Mol Biol Cell* **17**, 3978–3988.
- Lin, F., and Worman, H.J. (1993). Structural organization of the human gene encoding nuclear lamin A and nuclear lamin C. *J Biol Chem* **268**, 16321–16326.
- Liu, B., Wang, J., Chan, K.M., Tjia, W.M., Deng, W., Guan, X., Huang, J.-D., Li, K.M., Chau, P.Y., Chen, D.J., et al. (2005). Genomic instability in laminopathy-based premature aging. *Nat Med* **11**, 780–785.
- Liu, G.-H., Barkho, B.Z., Ruiz, S., Diep, D., Qu, J., Yang, S.-L., Panopoulos, A.D., Suzuki, K., Kurian, L., Walsh, C., et al. (2011). Recapitulation of premature ageing with iPSCs from Hutchinson-Gilford progeria syndrome. *Nature* **472**, 221–225.
- Lloyd, D.J., Trembath, R.C., and Shackleton, S. (2002). A novel interaction between lamin A and SREBP1: implications for partial lipodystrophy and other laminopathies. *Hum. Mol. Genet.* **11**, 769–777.
- Loewinger, L., and McKeon, F. (1988). Mutations in the nuclear lamin proteins resulting in their aberrant assembly in the cytoplasm. *Embo J* **7**, 2301–

2309.

- Lopez-Otin, C., Blasco, M.A., Partridge, L., Serrano, M., and Kroemer, G. (2013). The hallmarks of aging. *Cell* *153*, 1194–1217.
- Macara, I.G. (2001). Transport into and out of the nucleus. *Microbiol Mol Biol Rev* *65*, 570–594.
- Maillet, M., van Berlo, J.H., and Molkentin, J.D. (2013). Molecular basis of physiological heart growth: fundamental concepts and new players. *Nat Rev Mol Cell Biol* *14*, 38–48.
- Makde, R.D., England, J.R., Yennawar, H.P., and Tan, S. (2010). Structure of RCC1 chromatin factor bound to the nucleosome core particle. *Nature* *467*, 562–566.
- Mancini, M.A., Shan, B., Nickerson, J.A., Penman, S., and Lee, W.H. (1994). The retinoblastoma gene product is a cell cycle-dependent, nuclear matrix-associated protein. *Proc Natl Acad Sci USA* *91*, 418–422.
- McClintock, D., Ratner, D., Lokuge, M., Owens, D.M., Gordon, L.B., Collins, F.S., and Djabali, K. (2007). The mutant form of lamin A that causes Hutchinson-Gilford progeria is a biomarker of cellular aging in human skin. *PLoS ONE* *2*, e1269.
- Meier, J., Campbell, K.H., Ford, C.C., Stick, R., and Hutchison, C.J. (1991). The role of lamin LIII in nuclear assembly and DNA replication, in cell-free extracts of *Xenopus* eggs. *J Cell Sci* *98* (Pt 3), 271–279.
- Misteli, T., and Scaffidi, P. (2005). Genome instability in progeria: when repair gets old. *Nat Med* *11*, 718–719.
- Miyamoto, Y., Saiwaki, T., Yamashita, J., Yasuda, Y., Kotera, I., Shibata, S., Shigeta, M., Hiraoka, Y., Haraguchi, T., and Yoneda, Y. (2004). Cellular stresses induce the nuclear accumulation of importin alpha and cause a conventional nuclear import block. *J Cell Biol* *165*, 617–623.
- Moir, R.D., Spann, T.P., Herrmann, H., and Goldman, R.D. (2000). Disruption of nuclear lamin organization blocks the elongation phase of DNA replication. *J Cell Biol* *149*, 1179–1192.
- Moore, M.S., and Blobel, G. (1993). The GTP-binding protein Ran/TC4 is required for protein import into the nucleus. *Nature* *365*, 661–663.
- Moore, W.J., Zhang, C., and Clarke, P.R. (2002). Targeting of RCC1 to chromosomes is required for proper mitotic spindle assembly in human cells. *Curr Biol* *12*, 1442–1447.

- Moreno, S., and Nurse, P. (1990). Substrates for p34cdc2: In vivo veritas? *Cell* 61, 549–551.
- Mosammaparast, N., Guo, Y., Shabanowitz, J., Hunt, D.F., and Pemberton, L.F. (2002). Pathways mediating the nuclear import of histones H3 and H4 in yeast. *J Biol Chem* 277, 862–868.
- Muchir, A., van Engelen, B.G., and Lammens, M. (2003). Nuclear envelope alterations in fibroblasts from LGMD1B patients carrying nonsense Y259X heterozygous or homozygous mutation in lamin A/C gene. *Exp Cell Res* 291, 352–362.
- Nakagawa, T., Bulger, M., Muramatsu, M., and Ito, T. (2001). Multistep chromatin assembly on supercoiled plasmid DNA by nucleosome assembly protein-1 and ATP-utilizing chromatin assembly and remodeling factor. *J Biol Chem* 276, 27384–27391.
- Navarro, C.L., Cadiñanos, J., De Sandre-Giovannoli, A., Bernard, R., Courrier, S., Boccaccio, I., Boyer, A., Kleijer, W.J., Wagner, A., Giuliano, F., et al. (2005). Loss of ZMPSTE24 (FACE-1) causes autosomal recessive restrictive dermopathy and accumulation of Lamin A precursors. *Hum. Mol. Genet.* 14, 1503–1513.
- Nemergut, M.E., Mizzen, C.A., Stukenberg, T., Allis, C.D., and Macara, I.G. (2001). Chromatin docking and exchange activity enhancement of RCC1 by histones H2A and H2B. *Science* 292, 1540–1543.
- Nemergut, M.E., Lindsay, M.E., Brownawell, A.M., and Macara, I.G. (2002). Ran-binding protein 3 links Crm1 to the Ran guanine nucleotide exchange factor. *J Biol Chem* 277, 17385–17388.
- Nishijima, H. (2006). Nuclear RanGAP Is Required for the Heterochromatin Assembly and Is Reciprocally Regulated by Histone H3 and Ctr4 Histone Methyltransferase in *Schizosaccharomyces pombe*. *Mol Biol Cell* 17, 2524–2536.
- Nishimoto, T., Eilen, E., and Basilico, C. (1978). Premature chromosome condensation in a ts DNA-mutant of BHK cells. *Cell* 15, 475–483.
- Nishimoto, T., Uzawa, S., and Schlegel, R. (1992). Mitotic checkpoints. *Curr Opin Cell Biol* 4, 174–179.
- Nishitani, H., Kobayashi, H., Ohtsubo, M., and Nishimoto, T. (2008). Cloning of *Xenopus* RCC1 cDNA, a homolog of the human RCC1 gene: complementation of tsBN2 mutation and identification of the product. *J. Biochem.* 107, 228–235.
- Nishitani, H., Ohtsubo, M., Yamashita, K., Iida, H., Pines, J., Yasudo, H., Shibata,

- Y., Hunter, T., and Nishimoto, T. (1991). Loss of RCC1, a nuclear DNA-binding protein, uncouples the completion of DNA replication from the activation of cdc2 protein kinase and mitosis. *Embo J* 10, 1555–1564.
- Ohtsubo, M., Kai, R., Furuno, N., Sekiguchi, T., Sekiguchi, M., Hayashida, H., Kuma, K., Miyata, T., Fukushige, S., and Murotsu, T. (1987). Isolation and characterization of the active cDNA of the human cell cycle gene (RCC1) involved in the regulation of onset of chromosome condensation. *Genes Dev* 1, 585–593.
- Ohtsubo, M., Okazaki, H., and Nishimoto, T. (1989). The RCC1 protein, a regulator for the onset of chromosome condensation locates in the nucleus and binds to DNA. *J Cell Biol* 109, 1389–1397.
- Okusaga, O.O. (2014). Accelerated aging in schizophrenia patients: the potential role of oxidative stress. *Aging Dis* 5, 256–262.
- Olive, M., Harten, I., Mitchell, R., Beers, J.K., Djabali, K., Cao, K., Erdos, M.R., Blair, C., Funke, B., Smoot, L., et al. (2010). Cardiovascular pathology in Hutchinson-Gilford progeria: correlation with the vascular pathology of aging. *Arterioscler Thromb Vasc Biol* 30, 2301–2309.
- Osorio, F.G., Navarro, C.L., Cadiñanos, J., Lopez-Mejia, I.C., Quirós, P.M., Bartoli, C., Rivera, J., Tazi, J., Guzmán, G., Varela, I., et al. (2011). Splicing-directed therapy in a new mouse model of human accelerated aging. *Sci Transl Med* 3, 106ra107.
- Palladino, F., Laroche, T., Gilson, E., Axelrod, A., Pillus, L., and Gasser, S.M. (1993). SIR3 and SIR4 proteins are required for the positioning and integrity of yeast telomeres. *Cell* 75, 543–555.
- Paschal, B.M., and Gerace, L. (1995). Identification of NTF2, a cytosolic factor for nuclear import that interacts with nuclear pore complex protein p62. *J Cell Biol* 129, 925–937.
- Paschal, B.M., Delphin, C., and Gerace, L. (1996). Nucleotide-specific interaction of Ran/TC4 with nuclear transport factors NTF2 and p97. *Proc Natl Acad Sci USA* 93, 7679–7683.
- Pemberton, L.F., and Paschal, B.M. (2005). Mechanisms of receptor-mediated nuclear import and nuclear export. *Traffic* 6, 187–198.
- Perez-Terzic, C., Gacy, A.M., Bortolon, R., Dzeja, P.P., Puceat, M., Jaconi, M., Prendergast, F.G., and Terzic, A. (2001). Directed inhibition of nuclear import in cellular hypertrophy. *J Biol Chem* 276, 20566–20571.
- Perez-Terzic, C., Behfar, A., Méry, A., van Deursen, J.M.A., Terzic, A., and Puceat, M. (2003). Structural adaptation of the nuclear pore complex in

- stem cell-derived cardiomyocytes. *Circ Res* 92, 444–452.
- Perez-Terzic, C., Faustino, R.S., Boorsma, B.J., Arrell, D.K., Niederländer, N.J., Behfar, A., and Terzic, A. (2007). Stem cells transform into a cardiac phenotype with remodeling of the nuclear transport machinery. *Nat Clin Pract Cardiovasc Med* 4 *Suppl 1*, S68–S76.
- Peter, M., Kitten, G.T., Lehner, C.F., Vorburger, K., Bailer, S.M., Maridor, G., and Nigg, E.A. (1989). Cloning and sequencing of cDNA clones encoding chicken lamins A and B1 and comparison of the primary structures of vertebrate A- and B-type lamins. *J Mol Biol* 208, 393–404.
- Poole, L.B., and Nelson, K.J. (2008). Discovering mechanisms of signaling-mediated cysteine oxidation. *Curr Opin Chem Biol* 12, 18–24.
- Ragnauth, C.D., Warren, D.T., Liu, Y., McNair, R., Tajsic, T., Figg, N., Shroff, R., Skepper, J., and Shanahan, C.M. (2010). Prelamin A acts to accelerate smooth muscle cell senescence and is a novel biomarker of human vascular aging. *Circulation* 121, 2200–2210.
- Rajagopalan, S., Meng, X.P., Ramasamy, S., Harrison, D.G., and Galis, Z.S. (1996). Reactive oxygen species produced by macrophage-derived foam cells regulate the activity of vascular matrix metalloproteinases in vitro. Implications for atherosclerotic plaque stability. *J Clin Invest* 98, 2572–2579.
- Reddie, K.G., and Carroll, K.S. (2008). Expanding the functional diversity of proteins through cysteine oxidation. *Curr Opin Chem Biol* 12, 746–754.
- Ren, M., Drivas, G., D'Eustachio, P., and Rush, M.G. (1993). Ran/TC4: a small nuclear GTP-binding protein that regulates DNA synthesis. *J Cell Biol* 120, 313–323.
- Renault, L., Kuhlmann, J., Henkel, A., and Wittinghofer, A. (2001). Structural basis for guanine nucleotide exchange on Ran by the regulator of chromosome condensation (RCC1). *Cell* 105, 245–255.
- Renault, L., Nassar, N., Vetter, I., Becker, J., Klebe, C., Roth, M., and Wittinghofer, A. (1998). The 1.7 Å crystal structure of the regulator of chromosome condensation (RCC1) reveals a seven-bladed propeller. *Nature* 392, 97–101.
- Ribbeck, K., and Gorlich, D. (2001). Kinetic analysis of translocation through nuclear pore complexes. *Embo J* 20, 1320–1330.
- Ribbeck, K.K., Lipowsky, G.G., Kent, H.M.H., Stewart, M.M., and Görlich, D.D. (1998). NTF2 mediates nuclear import of Ran. *Embo J* 17, 6587–6598.

- Richards, S.A.S., Muter, J.J., Ritchie, P.P., Lattanzi, G.G., and Hutchison, C.J.C. (2011). The accumulation of un-repairable DNA damage in laminopathy progeria fibroblasts is caused by ROS generation and is prevented by treatment with N-acetyl cysteine. *Hum. Mol. Genet.* *20*, 3997–4004.
- Rodriguez, S., Coppede, F., Sagelius, H., and Eriksson, M. (2009). Increased expression of the Hutchinson-Gilford progeria syndrome truncated lamin A transcript during cell aging. *Eur J Hum Genet* *17*, 928–937.
- Rosengardten, Y., McKenna, T., Grochova, D., and Eriksson, M. (2011). Stem cell depletion in Hutchinson-Gilford progeria syndrome. *Aging Cell* *10*, 1011–1020.
- Rout, M.P., Aitchison, J.D., Suprpto, A., Hjertaas, K., Zhao, Y., and Chait, B.T. (2000). The yeast nuclear pore complex: composition, architecture, and transport mechanism. *J Cell Biol* *148*, 635–651.
- Royall, J.A., and Ischiropoulos, H. (1993). Evaluation of 2',7'-dichlorofluorescein and dihydrorhodamine 123 as fluorescent probes for intracellular H₂O₂ in cultured endothelial cells. *Arch Biochem Biophys* *302*, 348–355.
- Sauer, H., Rahimi, C., Hescheler, J., and Wartenberg, M. (2000). Role of reactive oxygen species and phosphatidylinositol 3-kinase in cardiomyocyte differentiation of embryonic stem cells. *FEBS Lett* *476*, 218–223.
- Scaffidi, P., and Misteli, T. (2006). Lamin A-dependent nuclear defects in human aging. *Science* *312*, 1059–1063.
- Scaffidi, P., and Misteli, T. (2008a). Lamin A-dependent misregulation of adult stem cells associated with accelerated ageing. *Nat Cell Biol* *10*, 452–459.
- Scaffidi, P., and Misteli, T. (2008b). Reversal of the cellular phenotype in the premature aging disease Hutchinson-Gilford progeria syndrome. *Nat Med* *11*, 440–445.
- Schatten, G., Maul, G.G., Schatten, H., Chaly, N., Simerly, C., Balczon, R., and Brown, D.L. (1985). Nuclear lamins and peripheral nuclear antigens during fertilization and embryogenesis in mice and sea urchins. *Proc Natl Acad Sci USA* *82*, 4727–4731.
- Schwoebel, E.D. (1998). Ran-dependent signal-mediated nuclear import does not require GTP hydrolysis by Ran. *J Biol Chem* *273*, 35170–35175.
- Seino, H., Hisamoto, N., Uzawa, S., Sekiguchi, T., and Nishimoto, T. (1992). DNA-binding domain of RCC1 protein is not essential for coupling mitosis with DNA replication. *J Cell Sci* *102 (Pt 3)*, 393–400.
- Seki, T., Hayashi, N., and Nishimoto, T. (1996). RCC1 in the Ran pathway. *J.*

Biochem. 120, 207–214.

- Shackleton, S., Lloyd, D.J., Jackson, S.N.J., Evans, R., Niermeijer, M.F., Singh, B.M., Schmidt, H., Brabant, G., Kumar, S., Durrington, P.N., et al. (2000). LMNA, encoding lamin A/C, is mutated in partial lipodystrophy. *Nat Genet* 24, 153–156.
- Shimi, T., Pflieger, K., Kojima, S.-I., Pack, C.-G., Solovei, I., Goldman, A.E., Adam, S.A., Shumaker, D.K., Kinjo, M., Cremer, T., et al. (2008). The A- and B-type nuclear lamin networks: microdomains involved in chromatin organization and transcription. *Genes Dev* 22, 3409–3421.
- Shinkai, Y., and Tachibana, M. (2011). H3K9 methyltransferase G9a and the related molecule GLP. *Genes Dev* 25, 781–788.
- Shumaker, D.K., Dechat, T., Kohlmaier, A., Adam, S.A., Bozovsky, M.R., Erdos, M.R., Eriksson, M., Goldman, A.E., Khuon, S., Collins, F.S., et al. (2006). Mutant nuclear lamin A leads to progressive alterations of epigenetic control in premature aging. *Proc Natl Acad Sci USA* 103, 8703–8708.
- Shumaker, D.K., Solimando, L., Sengupta, K., Shimi, T., Adam, S.A., Grunwald, A., Strelkov, S.V., Aebi, U., Cardoso, M.C., and Goldman, R.D. (2008). The highly conserved nuclear lamin Ig-fold binds to PCNA: its role in DNA replication. *J Cell Biol* 181, 269–280.
- Smith, A., Brownawell, A., and Macara, I.G. (1998). Nuclear import of Ran is mediated by the transport factor NTF2. *Curr Biol* 8, 1403–1406.
- Smith, J.S., and Boeke, J.D. (1997). An unusual form of transcriptional silencing in yeast ribosomal DNA. *Genes & Development* 11, 241–254.
- Smith, S., and Stillman, B. (1991). Stepwise assembly of chromatin during DNA replication in vitro. *Embo J* 10, 971–980.
- Snow, C.J., Dar, A., Dutta, A., Kehlenbach, R.H., and Paschal, B.M. (2013). Defective nuclear import of Tpr in Progeria reflects the Ran sensitivity of large cargo transport. *J Cell Biol* 201, 541–557.
- Spann, T.P., Moir, R.D., Goldman, A.E., Stick, R., and Goldman, R.D. (1997). Disruption of nuclear lamin organization alters the distribution of replication factors and inhibits DNA synthesis. *J Cell Biol* 136, 1201–1212.
- Spann, T.P., Goldman, A.E., Wang, C., Huang, S., and Goldman, R.D. (2002). Alteration of nuclear lamin organization inhibits RNA polymerase II-dependent transcription. *J Cell Biol* 156, 603–608.
- Steggerda, S.M., and Paschal, B.M. (2000). The mammalian Mog1 protein is a guanine nucleotide release factor for Ran. *J Biol Chem* 275, 23175–23180.

- Stewart, M. (2007). Molecular mechanism of the nuclear protein import cycle. *Nat Rev Mol Cell Biol* 8, 195–208.
- Stierlé, V., Couprie, J., Ostlund, C., Krimm, I., Zinn-Justin, S., Hossenlopp, P., Worman, H.J., Courvalin, J.-C., and Duband-Goulet, I. (2003). The carboxyl-terminal region common to lamins A and C contains a DNA binding domain. *Biochemistry* 42, 4819–4828.
- Stochaj, U., Rassadi, R., and Chiu, J. (2000). Stress-mediated inhibition of the classical nuclear protein import pathway and nuclear accumulation of the small GTPase Gsp1p. *Faseb J* 14, 2130–2132.
- Stuurman, N., Heins, S., and Aebi, U. (1998). Nuclear lamins: their structure, assembly, and interactions. *J Struct Biol* 122, 42–66.
- Tachibana, M., Sugimoto, K., Nozaki, M., Ueda, J., Ohta, T., Ohki, M., Fukuda, M., Takeda, N., Niida, H., Kato, H., et al. (2002). G9a histone methyltransferase plays a dominant role in euchromatic histone H3 lysine 9 methylation and is essential for early embryogenesis. *Genes Dev* 16, 1779–1791.
- Tachibana, M., Ueda, J., Fukuda, M., Takeda, N., Ohta, T., Iwanari, H., Sakihama, T., Kodama, T., Hamakubo, T., and Shinkai, Y. (2005). Histone methyltransferases G9a and GLP form heteromeric complexes and are both crucial for methylation of euchromatin at H3-K9. *Genes Dev* 19, 815–826.
- Tachibana, T., Imamoto, N., Seino, H., Nishimoto, T., and Yoneda, Y. (1994). Loss of Rcc1 Leads to Suppression of Nuclear-Protein Import in Living Cells. *J Biol Chem* 269, 24542–24545.
- Tao, G.-Z., Zhou, Q., Strnad, P., Salemi, M.R., Lee, Y.M., and Omary, M.B. (2005). Human Ran Cysteine 112 oxidation by Pervanadate regulates its binding to Keratins. *J Biol Chem* 280, 12162–12167.
- Taub, J., Lau, J.F., Ma, C., Hahn, J.H., Hoque, R., Rothblatt, J., and Chalfie, M. (1999). A cytosolic catalase is needed to extend adult lifespan in *C. elegans* daf-C and clk-1 mutants. *Nature* 399, 162–166.
- Toledano, M.B., and Leonard, W.J. (1991). Modulation of transcription factor NF-kappa B binding activity by oxidation-reduction in vitro. *Proc Natl Acad Sci USA* 88, 4328–4332.
- Toone, W.M., Kuge, S., Samuels, M., Morgan, B.A., Toda, T., and Jones, N. (1998). Regulation of the fission yeast transcription factor Pap1 by oxidative stress: requirement for the nuclear export factor Crm1 (Exportin) and the stress-activated MAP kinase Sty1/Spc1. *Genes Dev* 12, 1453–1463.

- Toth, J.I., Yang, S.H., Qiao, X., Beigneux, A.P., Gelb, M.H., Moulson, C.L., Miner, J.H., Young, S.G., and Fong, L.G. (2005). Blocking protein farnesyltransferase improves nuclear shape in fibroblasts from humans with progeroid syndromes. *Proc Natl Acad Sci USA* *102*, 12873–12878.
- Uchida, S., Sekiguchi, T., Nishitani, H., Miyauchi, K., Ohtsubo, M., and Nishimoto, T. (1990). Premature chromosome condensation is induced by a point mutation in the hamster RCC1 gene. *Mol Cell Biol* *10*, 577–584.
- van Montfort, R.L., Congreve, M., Tisl, D., Carr, R., and Jhoti, H. (2003). Oxidation state of the active-site cysteine in protein tyrosine phosphatase1B. *Nature* *423*, 773–777.
- Veal, E.A., Day, A.M., and Morgan, B.A. (2007). Hydrogen peroxide sensing and signaling. *Mol Cell* *26*, 1–14.
- Vetter, I.R., and Wittinghofer, A. (2001). The guanine nucleotide-binding switch in three dimensions. *Science* *294*, 1299–1304.
- Villa-Bellocosta, R., Rivera-Torres, J., Osorio, F.G., Acín-Perez, R., Enriquez, J.A., Lopez-Otin, C., and Andrés, V. (2013). Defective extracellular pyrophosphate metabolism promotes vascular calcification in a mouse model of Hutchinson-Gilford progeria syndrome that is ameliorated on pyrophosphate treatment. *Circulation* *127*, 2442–2451.
- Viteri, G., Chung, Y.W., and Stadtman, E.R. (2010). Effect of progerin on the accumulation of oxidized proteins in fibroblasts from Hutchinson Gilford progeria patients. *Mech Ageing Dev* *131*, 2–8.
- Vorburger, K., Lehner, C.F., Kitten, G.T., Eppenberger, H.M., and Nigg, E.A. (1989). A second higher vertebrate B-type lamin:cDNA sequence determination and in vitro processing of chicken lamin B 2. *J Mol Biol* *208*, 405–415.
- Watson, W.H., Pohl, J., Montfort, W.R., Stuchlik, O., Reed, M.S., Powis, G., and Jones, D.P. (2003). Redox potential of human thioredoxin 1 and identification of a second dithiol/disulfide motif. *J Biol Chem* *278*, 33408–33415.
- Witztum, J.L., and Steinberg, D. (1991). Role of oxidized low density lipoprotein in atherogenesis. *J Clin Invest* *88*, 1785–1792.
- Wong, C.-H., Chan, H., Ho, C.-Y., Lai, S.-K., Chan, K.-S., Koh, C.-G., and Li, H.-Y. (2008). Apoptotic histone modification inhibits nuclear transport by regulating RCC1. *Nat Cell Biol* *11*, 36–45.
- Yang, S.H., Meta, M., Qiao, X., Frost, D., Bauch, J., Coffinier, C., Majumdar, S., Bergo, M.O., Young, S.G., and Fong, L.G. (2006). A farnesyltransferase

- inhibitor improves disease phenotypes in mice with a Hutchinson-Gilford progeria syndrome mutation. *J Clin Invest* 116, 2115–2121.
- Yang, W., and Musser, S.M. (2006). Nuclear import time and transport efficiency depend on importin beta concentration. *J Cell Biol* 174, 951–961.
- Yasuda, Y., Miyamoto, Y., Saiwaki, T., and Yoneda, Y. (2006). Mechanism of the stress-induced collapse of the Ran distribution. *Exp Cell Res* 312, 512–520.
- Yasuda, Y., Miyamoto, Y., Yamashiro, T., Asally, M., Masui, A., Wong, C., Loveland, K.L., and Yoneda, Y. (2012). Nuclear retention of importin alpha coordinates cell fate through changes in gene expression. *Embo J* 31, 83–94.
- Zglinicki, von, T., Saretzki, G., Döcke, W., and Lotze, C. (1995). Mild Hyperoxia Shortens Telomeres and Inhibits Proliferation of Fibroblasts: A Model for Senescence? *Exp Cell Res* 220, 186–193.
- Zhang, J., Lian, Q., Zhu, G., Zhou, F., Sui, L., Tan, C., Mutalif, R.A., Navasankari, R., Zhang, Y., Tse, H.-F., et al. (2011). A Human iPSC Model of Hutchinson Gilford Progeria Reveals Vascular Smooth Muscled and Mesenchymal Stem Cell Defects. *Stem Cell* 8, 31–45.